Acquired Resistance to Targeted Therapy in EGFR-Mutant Lung Adenocarcinoma

By

Caroline Amalia Nebhan

Dissertation

Submitted to the Faculty of the

Graduate School of Vanderbilt University

in partial fulfillment of the requirements

for the degree of

DOCTOR OF PHILOSOPHY

in

Cancer Biology

December, 2014

Nashville, Tennessee

Approved:

Albert Reynolds, Ph.D.

Carlos Arteaga, M.D

Pierre Massion, M.D.

Jennifer Pietenpol, Ph.D.

William Pao, M.D., Ph.D.

To my mother, who taught me to love learning

ACKNOWLEDGEMENTS

I would like to thank my advisor, William Pao, M.D., Ph.D., for his superb mentorship. Despite the many demands on his schedule, Dr. Pao has always made time for me and all of his students. He has taught me to think critically, ask questions, and design experiments to answer them in an efficient and thorough manner. Some of the most important lessons I learned from Dr. Pao were those in which he taught by example. He exemplifies efficiency while still maintaining a high standard for thoroughness in all projects, seamlessly manages his roles as clinician, primary investigator, and administrator, remains positive and encouraging even in stressful situations, and always put his patients first. Even after Dr. Pao's departure from Vanderbilt, he has remained committed to his students through conference calls and prompt email responses. As an M.D./Ph.D student, I cannot imagine a better lab in which to have completed my graduate training.

I am extremely appreciative of my committee members: my chair Al Reynolds, Ph.D., Carlos Arteaga, M.D., Pierre Massion, M.D., and Jennifer Peitenpol, Ph.D. My committee meetings were always very inspiring to me, as I have such incredible scientific leaders to guide me. I thoroughly enjoyed the discussions that occurred. Dr. Arteaga is very encouraging and thoughtful physician-scientist who brought a keen eye to the nuances of cancer signaling to my project. I am also very grateful to him for opening his lab to me to share reagents and equipment. Dr. Massion is a true expert in the field of lung cancer and brought an important clinical perspective to my project. I am very thankful for his coordination of our lung cancer works-in-progress seminar series, a valuable institutional forum to engage with colleagues. Dr. Pietenpol is a gifted scientist

and leader who serves as a tremendous role model to me and all of our next generation of female science leaders. As my committee chair, Dr. Reynolds has been especially important to my graduate training. He and I have met regularly since Dr. Pao's departure, and I am very grateful to have his guidance as I finished up my projects. While I spend much of my time in the world of translational and clinical medicine, Dr. Reynolds has reminded me that all medicine is founded in basic science. I know that I will carry the wisdom of my mentors with me throughout my career.

The Pao lab has become like a second family to me, and every member has been helpful to me through many experiments over the past three years. I would like to first thank Dr. Eiki Ichihara, M.D., Ph.D., my PRB 660 roommate. Eiki is always positive and encouraging, even when my data is not. He is always happy to discuss my project, ask provocative questions, and share papers with me. Previous Pao lab post-doctoral fellows Dr. Kadoaki Ohashi, M.D., Ph.D., and Dr. Monica Red Brewer, Ph.D., were also invaluable to my graduate school experience. During my first months in lab, Kadoaki was tremendously patient with me as he helped me learn my way around the lab. He also provided many colorful soundtracks of techno dance music during our many hours working in the tissue culture room together. Monica has always been happy to stop whatever she is doing to help me with a new protocol or reagent. I am thankful that after completing her tenure in the Pao lab, she moved just down the hall to the Arteaga lab, where she has continued to be very supportive of me. I am also very grateful to the wonderful technicians who have helped with my projects over the past three years, including Paula Spitzler for her work with our mouse models, Helen Pan for her assistance in running the SNaPshot assay on numerous samples, and Hailing Jin for

her hand in numerous experiments (and helpful life advice!). The Pao Lab would not run without the coordination of our fearless manager, Abudi Nashabi. I feel so lucky to work in a lab where, thanks to Abudi's close monitoring, I never had to worry about running out of any needed reagents. Additionally, Abudi has helped fuel the Pao Lab with a bounty delicious organic produce grown in his backyard, and he is always happy to provide both a listening ear and sage advice when necessary. I am tremendously grateful to have fellow graduate students Katie Hutchinson and Catherine Meador in the lab. Through late nights and early mornings, coffee runs and ice cream trips, we have kept each other sane. I am so thankful to call both of these brilliant women my dear friends.

In addition to the Pao lab, I am very grateful to Dr. Christine Lovly, M.D., Ph.D., and her growing lab. Christine, then a fellow in the Pao lab, was a fantastic mentor to me during my rotation during the summer of 2010. She was one of the major motivators in my decision to join the Pao Lab. As a female physician-scientist, it has been absolutely invaluable and very inspiring to observe her career evolve as she transitioned from her role as a fellow into a Vanderbilt faculty member and primary investigator with a strong lab of her own. Following Dr. Pao's departure from Vanderbilt in May 2014, Christine has seamlessly assimilated the Pao Lab with her own and ensures that all lab members feel fully supported during and after the transition. Christine works harder than anyone I know, but always remains positive and selfless. She is one of the best role models I could ask hope to have. Additionally, Lovly lab members Dr. Huan Qiao, Yingjun Yan, J-N Gallant, and Merrida Childress have all be delightful coworkers.

Nearly every day for the last three years, I have walked under a quotation by Margarat Mead inscribed over the entrance to the Vanderbilt-Ingram Cancer Center that reads “Never doubt that a small group of thoughtful, committed people can change the world.” The many scientists that I have worked with during graduate school have very much embodied this message. I would like to thank Dr. Kim Dahlman and her lab members, Dr. Zhongming Zhao and his team, Dr. Katerina Politi and Dr. Valentina Pirazzoli at the Yale Cancer Center, and our many collaborators at Memorial-Sloan Kettering. I am also very grateful to Katisha Moton and Roddy Smith for their organization in submitting and administering grant funding. Dr. Donna Webb, Ph.D., was my PI during my undergraduate research experience; her fantastic mentorship and encouragement is the reason I have pursued this career. I am also very thankful to Dr. Terry Dermody, M.D., and the entire MSTP Leadership Team have also been tremendously supportive to me for the last five years.

I am very grateful to the funding sources that have made my work possible. These projects have been supported by individual support from both the NIH F30 CA180353-01 and by the Melly Family Scholarship Award. Additional support came from the Vanderbilt MSTP.

I would like to thank my family for always believing in me and instilling the values that have made me who I am today. My father has been my rock and I am grateful his many stoic pep talks encouraging me to “man up,” which were always followed by shipments of chocolate, Lebanese teas and snacks, and other care package treats to my door.

TABLE OF CONTENTS

Page

LIST OF TABLES

LIST OF FIGURES

Figure **Page**

LIST OF PUBLICATIONS

Cross DA, Ashton SE, Ghiorghiu S, Eberlein C, **Nebhan CA**, Spitzler PJ, Orme JP, Finlay MR, Ward RA, Mellor MJ, Hughes G, Rahi A, Jacobs VN, Red Brewer M, Ichihara E, Sun J, Jin H, Ballard P, Al-Kadhimi K, Rowlinson R, Klinowska T, Richmond GH, Cantarini M, Kim DW, Ranson MR, Pao W. (2014) "AZD9291, an irreversible EGFR TKI, overcomes T790M-mediated resistance to EGFR inhibitors in lung cancer." *Cancer Discov.* CD-14-0337

Pirazzoli V*, **Nebhan CA***, Song X, Wurtz A, Walther Z, Cai G, Zhao Z, Jia P, de Stanchina E, Shapiro EM, Gale M, Yin R, Horn L, Carbone DP, Stephens PJ, Miller V, Gettinger S, Pao W, Politi K. (2014) "Acquired resistance of EGFR-mutant lung adenocarcinomas to afatinib plus cetuximab is associated with activation of mTORC1." *Cell Rep.*7(4):999-1008 *co-first author

Nebhan CA, Pao W. (2013) "Further advances in genetically informed lung cancer medicine." J. Thorac. Oncol. 8(5):521-2

Takezawa K, Pirazzoli V, Arcila ME, **Nebhan CA**, Song X, de Stanchina E, Ohashi K, Janjigian YY, Spitzler PJ, Melnick MA, Riely GJ, Kris MG, Miller VA, Ladanyi M, Politi K, Pao W. (2012) "HER2 amplification: a potential mechanism of acquired resistance to EGFR inhibition in EGFR-mutant lung cancers that lack the second-site EGFRT790M mutation." *Cancer Discov*., 5(10):922-33

CHAPTER I

Introduction

EGFR-mutant lung cancer

Lung cancer is the leading cause of cancer-related death in the United States and worldwide (Molina, Yang et al. 2008). Adenocarcinoma of the lung accounts for approximately half of all diagnosed lung cancer cases, making it the most commonly diagnosed histological subtype of lung cancer (Travis, Brambilla et al. 2011). Over the past decade, advances in genotyping technologies have enabled the identification of specific 'driver mutations' in lung adenocarcinoma. Such mutations are causally implicated in oncogenesis and positively selected for throughout tumor generation (Weinstein 2002; Stratton, Campbell et al. 2009). Since then, lung adenocarcinomas have been increasingly stratified based on their molecular driver, some of which encode druggable therapeutic targets. Currently, genes with known driver mutations in lung adenocarcinoma include but are not limited to *EGFR*, *HER2*, *KRAS*, *BRAF*, *PIK3CA*, *AKT1*, *NRAS*, and *MAP2K1*. Gene fusions implicated in lung adenocarcinoma include *ALK* (most commonly fused to *EML4*), *ROS1* (commonly fused to *SLC34A2* or *CD74)*, *FGFR1/2/3* (commonly fused to *BAG4* or *TACC3*) and *RET* (commonly fused to *KIF5B* or *CCDC6)* (Pao and Hutchinson 2012), (Takeuchi, Soda et al. 2012), (Majewski, Mittempergher et al. 2013). While many of these identified mutations do not yet have an

effective targeted inhibitor identified, activating mutations in *EGFR, ALK* and *ROS1* are bona fide therapeutic targets (Sakashita, Sakashita et al. 2014).

Between 18-33% of lung adenocarcinomas harbor activating *EGFR* mutations, making this set of alterations the most commonly mutated druggable target among all genetic subtypes of lung adenocarcinomas. EGFR-driven lung adenocarcinoma occurs most frequently in specific patient groups, including patients of Asian descent, women, and never-smokers (Pao and Chmielecki 2010). Approximately 28% of never-smokers diagnosed with lung cancer in the United States have tumors harboring EGFR mutations (Lee, Cho et al. 2010), (Sun, Ren et al. 2010).

Biology of the wild-type epidermal growth factor receptor

First discovered in 1978 by Graham Carpenter and Stanley Cohen at Vanderbilt University and cloned in 1984 by Julian Downward, Epidermal Growth Factor Receptor (EGFR) is the founding member of the ErbB receptor tyrosine kinase (TK) family, which also includes HER2/ErbB2, HER3/ErbB3, and HER4/ErbB4 (Carpenter, Lembach et al. 1975) (Carpenter, King et al. 1978) (Downward, Yarden et al. 1984). All family members are transmembrane cell surface receptor tyrosine kinases. The architecture of EGFR, an 1186- amino acid/170kDa glycoprotein, includes an extracellular ligand-binding ectodomain, a transmembrane lipophilic domain, an intracellular kinase domain, and an intracellular regulatory domain (**Figure 1, left panel**). The extracellular domain consists of four subdomains (I-IV) which can bind 11 different peptide ligands, though epidermal growth factor (EGF), transforming growth factor alpha (TGFα), epiregulin and

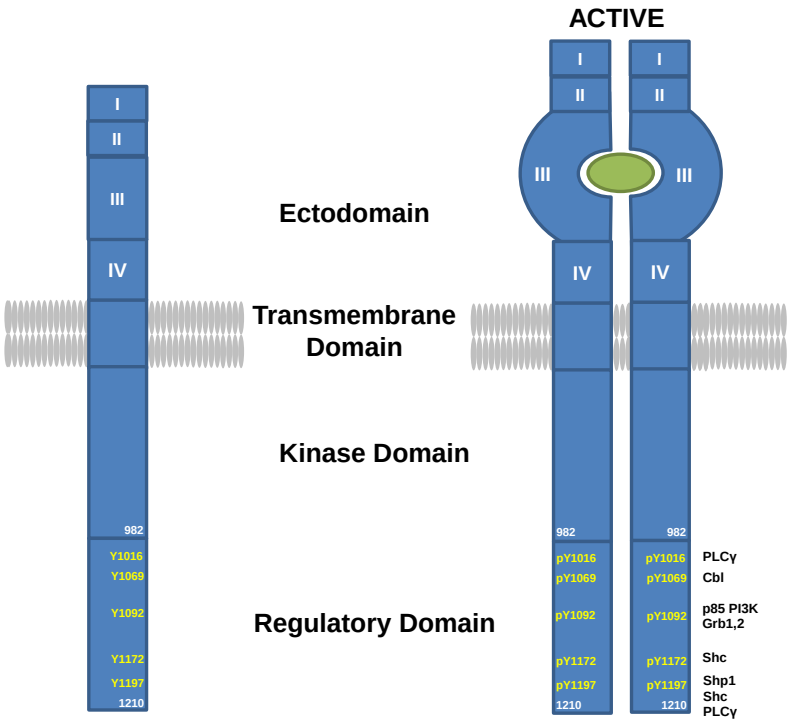

Figure 1. Canonical Structure and Activation of the Epidermal Growth Factor Receptor

EGFR is composed of an ectodomain, a transmembrane domain, a kinase domain and a regulatory domain. The extracellular ectodomain consists four subdomains (I-IV). Subdomain III may bind to ligand, which induces a conformational change in subdomains I and II, allowing dimerization. Once dimerized, the intracellular kinase domain is enzymatically activated to phosphorylates tyrosine residues within the regulatory domain, which serve as docking sites for numerous downstream signaling cascade proteins.

amphiregulin are thought to be most prevalent in EGFR signaling (Piepkorn, Pittelkow et al. 1998) (Mitsudomi and Yatabe 2010).The kinase domain of EGFR exists in either a minimally active “off” state or a maximally active “on” state; the switch to an active state catalyzes the transfer of a γ-phosphate of ATP to the hydroxyl group of tyrosine (Huse and Kuriyan 2002).

In normal, wild-type cells, EGFR is activated upon ligand to subdomain III of the ectocellular domain **(Figure 1, right panel)**. This induces a conformational change in ectocellular subdomains I and II, which exposes the protein’s dimerization domain. EGFR may form homo- or heterodimers with itself or TK family members HER2, HER3 or HER4 (Mitsudomi and Yatabe 2010). HER2 is the preferred heterodimerization partner for EGFR (Graus-Porta, Beerli et al. 1997). This dimerization frees the intracellular kinase domains to form enzymatically active dimers, resulting in regulatory domain tyrosine autophosphorylation at tyrosine resides Y1016, Y1069, Y1092, Y1172 and Y1197 (Downward, Parker et al. 1984) (Ono and Kuwano 2006). The phosphotyrosine residues generated by autophosphorylation constitute docking sites for several downstream signaling proteins containing *src* homology 2 (SH2) and phosphotyrosine binding (PTB) domains (Oda, Matsuoka et al. 2005), including protein lipase C gamma (PLCγ) at Y1016, Cbl at Y1069, the p85 subunit of the phosphoinositide 3-kinase (PI3K), the PI3K regulatory subunit α (Grb1), and growth factor receptor bound protein 2 (Grb2) and at Y1092, Src-transforming protein (Shc) at Y1172, Src homology region 2 domain-containing phosphatase-1 (Shp1), Shc, and PLCγ at Y1197 (Ono and Kuwano 2006). Through these downstream signaling molecules, EGFR activates a number of signaling pathways critical to cell survival,

including the phosphatidylinositol-4,5-bisphosphate 3-kinase/AKT (PI3K/AKT) signaling cascade and the mitogen activated protein kinase (MAPK) signaling cascade. These pathways are responsible for apoptosis evasion, cell cycle progression, differentiation, development and transcription (Arkhipov, Shan et al. 2013), (Roskoski 2014), (Roskoski 2014).

Pathobiology of mutant EGFR

In 2004, activating mutations in the EGFR were identified as the first targetable mutation in lung adenocarcinoma (Lynch, Bell et al. 2004; Pao, Miller et al. 2004) (Paez, Janne et al. 2004). Since then, over 60 unique *EGFR* mutations have been reported in lung adenocarcinoma patients. In the vast majority of tumors sampled, the existence of a specific *EGFR* mutation usually precludes the existence of a second TKI-sensitizing mutation (Pao, Miller et al. 2004; Kancha, von Bubnoff et al. 2009).

Of note, the field of EGFR biology uses two different numbering systems to localize amino acid residues. One system, most commonly used in genomic and translational research applications, reflects the inclusion of a 24-amino acid peptide that is part of the *EGFR* gene, but absent from the mature protein. Another system, most commonly used in biochemical and structural analyses, does not include this 24-amino acid sequence. The former numbering system is used throughout this manuscript.

A 2014 study of 774 lung cancer samples to evaluate the use of cytologic samples for detection of *EGFR* mutation in lung cancer identified 164 mutations within exons 18-21 of the *EGFR* gene (Rossi, Gerhard et al. 2014). Of these 164 identified *EGFR* mutations, 53.7% of samples harbored various exon 19 multinucleotide in-frame

deletion mutations (exon19del), 34.1% of samples harbored mutations substituting an arginine reside for a leucine reside at position 858 (L858R) within exon 21, 3.7% of samples harbored mutations substituting an alanine reside for a glycine reside at position 719 (G719A) within exon 18, and the remaining 8.5% of samples harbored various other substitution, duplications and insertions within exons 18-21 **(Figure 2)**.

Exon19del mutations occur adjacent to K745, a site shown to be critical for ATP binding (Honegger, Dull et al. 1987). L858R occurs in the activation loop of the kinase (Huse and Kuriyan 2002D). Interestingly, recent studies have demonstrated variability of tyrosine kinase inhibitors efficacy in cells harboring different EGFR mutations, but the most common *EGFR* mutations in lung adenocarcinoma (L858R and exon19del) both showed strong sensitivity to first-generation tyrosine kinase inhibitors (Kancha, von Bubnoff et al. 2009), (Yeh, Chen et al. 2013).

First-generation EGFR tyrosine kinase inhibitors in lung cancer

First-generation tyrosine kinase inhibitors used in lung cancer include gefitinib (Iressa®; AstraZeneca, London, UK) and erlotinib (Tarceva®; Genentech, San Francisco, USA) (**Table 1**). These compounds are both reversible aniline-quinazolines, a class of compounds built upon a fused benzene ring and pyrimidine ring core (Hidalgo, Siu et al. 2001) (Wakeling, Guy et al. 2002). Long before the discovery of EGFR-driven lung adenocarcinomas, these drugs were identified as having good potency against wild-type tyrosine kinases though structure-based searching without requiring the synthesis of new compounds (Ward, Cook et al. 1994). The potency of gefitinib *in vitro* and *in vivo* was evaluated in the 1990s, when it was demonstrated that

gefitinib had strong selectivity for EGFR over other receptor tyrosine kinases as well as a suitable pharmacokinetic/pharmacodynamics profile (Wakeling, Guy et al. 2002), (Barker, Gibson et al. 2001).

Gefitinib was first used in lung cancer patients in 1998 prior to its approval by the FDA in 2003 (Lynch, Bell et al. 2004). At this time, the drug was used in an unselected patient population; it took nearly more than decade to produce sufficient evidence supporting *EGFR* mutation as a biomarker for response to gefitinib. The first phase II clinical trials of gefitinib, published in 2003 and 2004, demonstrated a 12-18% objective tumor response rate among an general (non-EGFR enriched) population of patients with non-small cell lung cancer who had received one or two chemotherapy regimens (Fukuoka, Yano et al. 2003), (Kris, Natale et al. 2003). Gefitinib gained FDA approval in May 2003 for use in patients with locally advanced or metastatic non-small-cell lung cancer after failure of at least one prior chemotherapy regimen. A clinical trial evaluating erlotinib demonstrated a 12% objective response rate among a similarly general non-small-cell lung cancer patient population (Perez-Soler, Chachoua et al. 2004). Erlotinib gained FDA approval in November 2004; like gefitinib, it was also evaluated in a general group of non-small-cell lung cancer patients not stratified based on genotype (Shepherd, Rodrigues Pereira et al. 2005). It was not until 2009 that the superior efficacy of gefitinib and erlotinib in molecularly-stratified, EGFR-mutant subset of lung cancer patients became widely recognized. A phase III open-label study (called the Iressa Pan Asian Study or IPASS) published in 2009 definitively showed that first-line treatment with gefitinib is superior to standard chemotherapy (carboplatin+paclitaxel) in

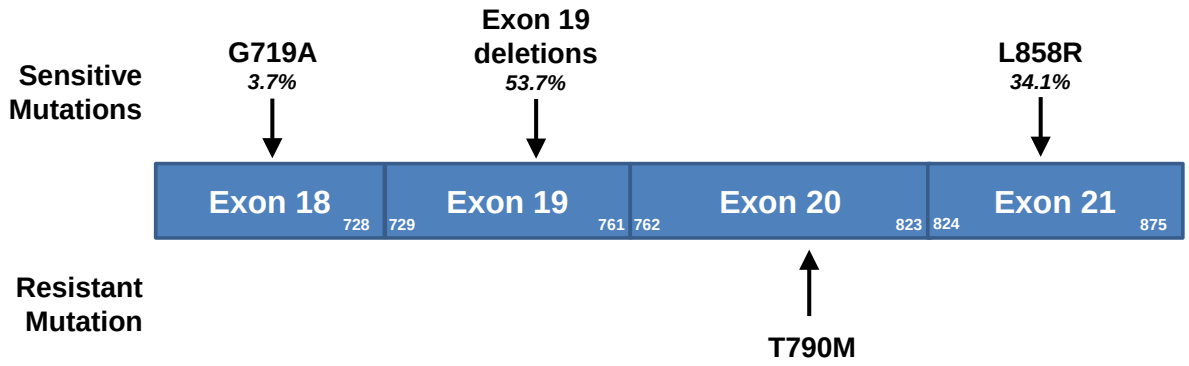

Figure 2. Identified TKI-sensitive and TKI-resistant mutations in EGFR kinase domain

Location of kinase domain EGFR mutations in lung adenocarcinoma. Upper panel; indicated sensitive mutations account for over 90% of all known; various other substitutions, insertions, and deletions in exon 18-21 constitute the remaining mutations. Lower panel; the gatekeeper residue mutation T790M is responsible for over 50% of primary acquired resistance.

never- or light-former-smokers of East Asian descent, and that the presence of *EGFR* mutation is a strong predictor of gefitinib response (hazard ratio for progression or death upon gefitinib treatment with EGFR mutation, 0.48; without EGFR mutation, 2.85) (Mok, Wu et al. 2009). In 2013, the FDA formally updated the indication of use for erlotinib to include first-line use in patients with EGFR-mutant lung cancer.

The effects of combination targeted therapy plus general cytotoxic chemotherapy in a molecularly stratified, EGFR-mutant cohort of patients has also been evaluated. A 2012 study demonstrated that erlotinib + chemotherapy (cisplatin+paclitaxel) dual treatment was no better than erlotinib monotherapy in EGFR-mutant lung cancer patients with never- or light-former-smoker histories. Patients in the erlotinib + chemotherapy cohort experienced significantly higher incidence of both hematologic and non-hematologic toxicity than was observed in the erlotinib-only cohort (Janne, Wang et al. 2012).

Acquired resistance to anti-EGFR therapies in lung cancer

Primary acquired resistance to erlotinib/gefitinib

All patients with metastatic disease who respond to first-line EGFR tyrosine kinase inhibition will eventually experience progressive disease within a median of 9-16 months of continuous treatment, meeting the criterion for primary acquired resistance (Mok, Wu et al. 2009; Jackman, Pao et al. 2010) (Rosell, Carcereny et al. 2012) (Janne, Wang et al. 2012) **(Figure 3)**. Numerous studies have evaluated the mechanisms of primary acquired resistance by conducting tumor rebiopsy and resequencing of *EGFR* in

		Drug	Structure	TK Target
Anilino-quinazolines Reversible inhibitors	1st generation	Gefitinib	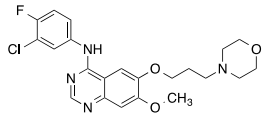	EGFR
		Erlotinib	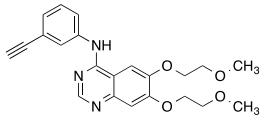	EGFR
		Lapatinib	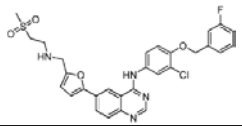	EGFR HER2
Anilino-quinazolines Irreversible inhibitors	2nd generation	Afatinib	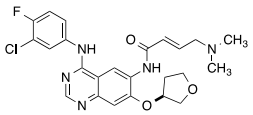	EGFR HER2
		Neratinib	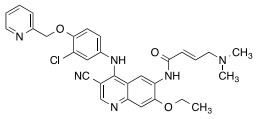	HER2 EGFR
		Dacomitinib	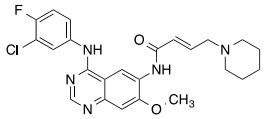	EGFR HER2 HER4
		Canertinib	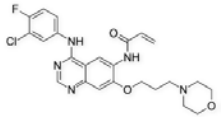	EGFR HER2 HER4
		Pelitinib	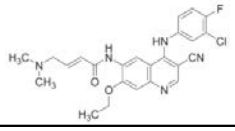	EGFR
Anilino-pyrimidines Irreversible inhibitors	3rd generation	WZ-4002	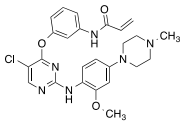	EGFR T790M
		CO-1686	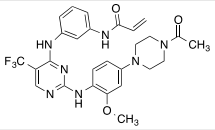	EGFR T790M
		AZD9291	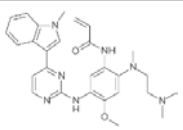	EGFR T790M

Table 1. EGFR Tyrosine Kinase Inhibitors Evaluated in Lung Adenocarcinoma

patients with progressive disease after initial response to erlotinib or gefitinib, as well as preclinical modeling using cell lines and animal models. The most common mechanism, identified in 2005, leads to the substitution of methionine for threonine at residue 790 of the receptor's kinase domain (Pao, Miller et al. 2005),(Kobayashi, Boggon et al. 2005) **(Figure 2).** The crystal structure of the EGFR kinase domain identifies threonine 790 as located in the hydrophobic ATP-binding pocket of the catalytic region, where a critical hydrogen bond between receptor and drug is formed. Thus, it is predicted that substitution of threonine with the larger methionine at this position would sterically hinder drug but not ATP binding (Stamos, Sliwkowski et al. 2002), ensuring that the catalytic activity of EGFR remains intact while also protecting the protein from interference by first-generation EGFR tyrosine kinase inhibitor (Stamos, Sliwkowski et al. 2002). Alternatively, other groups report that the T790M mutation functions to increase the affinity of ATP over drug to the binding pocket (Yun, Mengwasser et al. 2008).

The T790M mutation in EGFR occurs in the protein's gatekeeper residue. This residue is highly conserved residue within all kinase domains. First described in 1998 in the non-receptor tyrosine kinase Src, the "gatekeeper residue" was so named because it functions as a molecular "gate" to partially or fully restrict access hydrophobic region deep in the ATP binding pocket (Liu, Shah et al. 1998). Many small molecule inhibitors have exploited this conserved residue for binding specificity, but as seen with the EGFR gatekeeper residue mutation, substitution of the wild-type gatekeeper with a bulkier residue can lead to drug resistance. Analogous mutations in the gatekeeper residue that induce resistance to the small molecular inhibitor imatinib occur in the ABL kinase (of

BCR-ABL fusion protein drivers) of CML, KIT of gastrointestinal stromal tumor, and PDGFRA of hypereosinophilic syndrome (Shah, Nicoll et al. 2002) (Tamborini, Bonadiman et al. 2004) (Cools, Stover et al. 2003).

Since the discovery of the T790M mutation, additional (albeit less frequent) mechanisms of acquired resistance to first-generation EGFR tyrosine kinase inhibitors have been identified (Oxnard, Arcila et al. 2011). Importantly, mutations conferring resistance to erlotinib or gefitinib appear to be mutually exclusive, supporting the supreme selective advantage these mutations provide to *EGFR*-driven tumor cells. Focal amplification of hepatocyte growth factor receptor (MET) was identified in both cell lines and patient samples as a mechanism of acquired resistance in 2007 (Engelman, Zejnullahu et al. 2007), (Bean, Brennan et al. 2007). This mutation drives downstream PI3K signaling via the HER3 receptor, which is not targeted by erlotinib or gefitinib. Though lower in frequency than initially thought, MET amplification is thought to account for 4% of primary acquired resistance (Arcila, Oxnard et al. 2011), (Sequist, Waltman et al. 2011). A third identified mechanism of acquired resistance to erlotinib or gefitinib involves the histological transformation of tumor initially confirmed as adenocarcinoma to a small cell histologic phenotype (Arcila, Oxnard et al. 2011), (Sequist, Waltman et al. 2011), (Zakowski, Ladanyi et al. 2006), (Alam, Gustafson et al. 2010). Small cell transformation accounts for approximately 6% of all cases of primary acquired resistance in lung adenocarcinoma. More recently, amplification of *HER2* was identified as a mechanism primary acquired resistance in cell lines, mouse models, and patient samples (Takezawa, Pirazzoli et al. 2012). HER2 amplification may account for

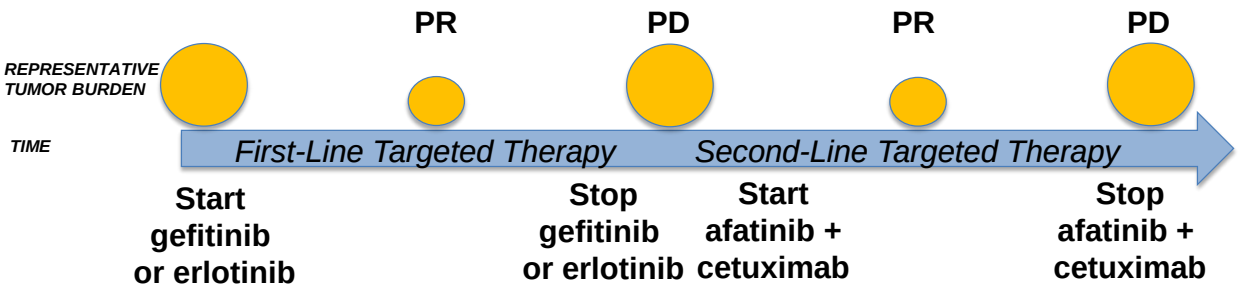

Figure 3. Representative Course of Treatment for EGFR-mutant lung adenocarcinoma

Many comprehensive cancer centers now routinely evaluate the tumors of lung adenocarcinoma patients by molecular profiling to evaluate for targetable mutations. If the tumor is found to harbor mutation in *EGFR,* first-line treatment includes a first-generation tyrosine kinase inhibitor, erlotinib or gefitinib. Approximately 70% of patients may expect to experience a partial response (PR) with median duration of 8-12 months. However, all patients who initially respond to first-line targeted therapy will invariably develop primary acquired resistance and experience progressive disease (PD). To overcome primary acquired resistance, a patient may be treated with second-line anti-EGFR combination therapy, afatinib+cetuximab. Approximately 29% of patients may expect to experience a partial response with a median duration of response of 5-6 months. Unfortunately, all patients who show an initial response will go on to develop secondary acquired resistance to afatinib+cetuximab and experience progressive disease.

up to 12% of primary acquired resistance. A study of 195 patient tumor samples with primary acquired resistance to erlotinib or gefitinib identified second-site activating mutations in *BRAF*; such mutations were confirmed to induce resistance in model systems and may account for 1% of primary acquired resistance (Ohashi, Sequist et al. 2012). Acquired mutations in *PIK3CA* have also been observed to induce resistance, accounting for approximately 5% of primary acquired resistance (Sequist, Waltman et al. 2011). Most recently, reduced expression of neurofibrin, the protein product of the *NF1* gene, was found to induce resistance to EGFR tyrosine kinase inhibitors (de Bruin, Cowell et al. 2014). Rare activating mutations and amplifications in the receptor tyrosine kinase *AXL* have been identified in patients with acquired resistance to EGFR tyrosine kinase inhibitors; they are hypothesized to occur in the setting of epithelial-to-mesenchymal histologic transition (EMT) (Zhang, Lee et al. 2012) Rarer still, amplification of *CRKL* gene is predicted to induce resistance to first-generation EGFR tyrosine kinase inhibitors (Suda, Mizuuchi et al. 2014). In total, approximately 20% of primary acquired resistance in EGFR-mutant lung adenocarcinoma has no identified mechanism of acquired resistance, emphasizing the need for continued study in this area.

Of note, primary acquired resistance and primary resistance have different definitions that should be used with distinction (Lovly and Shaw 2014) (Jackman, Pao et al. 2010). Primary acquired resistance is defined as disease progression after initial response to therapy; indeed, in lung adenocarcinoma, an initial radiographic response is required to meet the definition of primary acquired resistance. Primary resistance is defined as a de novo lack of treatment response despite the existence of the mutational

target. Approximately 30% of EGFR-mutant lung adenocarcinomas meet the definition for primary resistance (Mok, Wu et al. 2009), (Janne, Wang et al. 2012). Mechanisms of primary resistance are a worthy but separate topic of study in the era of targeted therapies.

Overcoming primary acquired resistance: second-generation TKIs and drug combinations

Because disease invariably progresses despite initial response to erlotinib or gefitinib, much research effort has been expended in attempt to devise novel therapeutic methods to overcome primary acquired resistance. Early studies indicated that second-generation irreversible EGFR tyrosine kinase inhibitors, which form an irreversible covalent bond with EGFR, may be successful in overcoming primary acquired resistance to the reversible inhibitors erlotinib and gefitinib. Second-generation EGFR tyrosine kinase inhibitors neratinib (HKI-272; Puma Biotechnology; Los Angeles, USA), canertinib (CI-1033, Pharmaprojects database), pelitinib (EKB-569, Pharmaprojects database), dacomitinib (PF00299804; Pfizer; New York City, USA) and afatinib (BIBW-2992; Boehringer Ingelheim; Ingelheim, Germany) all initially showed good efficacy in L858R/T790M tumor cells *in vitro* studies (Kwak, Sordella et al. 2005), (Carter, Wodicka et al. 2005),(Engelman, Zejnullahu et al. 2007), (Li, Ambrogio et al. 2008) (**Table 1**). While preclinical data evaluating second-generation tyrosine kinase inhibitors predicted good response to primary acquired resistance in patients, it is thought that the concentration of drug necessary to overcome T790M in humans is not achievable without dose-limiting toxicity (Ohashi, Sequist et al. 2012).

To date, afatinib is the only second-generation tyrosine kinase inhibitor to receive FDA approval. In preclinical studies, afatinib was shown to have activity against wild type EGFR and HER2 as well as the EGFR L858R mutant isoform and the EGFR L858R/T790M isoform in cell line and xenograft models, and afatinib alone was effective in EGFR L858R/T790M transgenic mouse models (Li, Ambrogio et al. 2008). However, various clinical trials have evaluated afatinib in EGFR-mutant lung cancer patients, with mixed results. Patients lacking primary acquired resistance generally saw improved progression-free survival (PFS) and higher response rates when compared to standard chemotherapy (cisplatin/pemetrexed or cisplatin/gemcitabine). However, patients with EGFR-mutant lung cancer and primary acquired resistance experienced low or no survival benefit when treated with afatinib alone (Yu and Pao 2013). Afatinib received FDA approval in July 2013 with indicated use in only previously TKI-naïve patients.

Many clinical trials have evaluated the ability of second-generation EGFR tyrosine kinase inhibitors and targeted combination therapy to overcome primary acquired resistance, but most have seen little success. Monotherapy with neratinib resulted in in response rates between 0-3% among patients with primary acquired resistance to erlotinib or gefitinib (Sequist, Besse et al. 2010). Though combination therapy of mTOR inhibitor everolimus plus erlotinib seemed promising, a low ($\leq$15%) response rate and high grade 3/4 toxicity profile did not warrant further trials in primary acquired resistance patients (Milton, Riely et al. 2007), (Besse, Leighl et al. 2014). Combination targeted therapy with EGFR tyrosine kinase inhibitors of both first-generation, erlotinib, and second-generation, dasatinib, was shown to have no activity in patients with primary acquired resistance (Johnson, Riely et al. 2011). Other EGFR-

dependent therapeutic strategies to overcome primary acquired resistance evaluated cetuximab (Erbitux; Bristol-MyersSquibb; New York, USA and Eli Lilly; Indianapolis, USA), a monoclonal anti-EGFR antibody, in cell line and mouse models, and showed promising preclinical results (Doody, Wang et al. 2007).

However, when compared to monotherapy with either drug, the combination of second-generation EGFR tyrosine kinase inhibitor afatinib administered with the anti-EGFR monoclonal antibody cetuximab showed a surprising response in transgenic mouse models of L858R/T790M driven lung adenocarcinomas (Regales, Gong et al. 2009). Co-treatment with afatinib+cetuximab resulted in simultaneous depletion of phospho- and total EGFR. This study provided preclinical rationale for a phase Ib clinical trial of afatinib+cetuximab in patients with primary acquired resistance to erlotinib or gefitinib. Results from the clinical trial showed a 29% response rate among 129 enrolled patients with primary acquired resistance, with a median progression-free survival of 4.7 months. A manageable toxicity profile was reported, with grade 3/4 responses occurring in 44%/2% of patients (Janjigian et al, Can Disc 2014, in press). Interestingly, the response rate was comparable in primary acquired resistance tumors regardless of T790M status, implying that combination therapy with afatinib + cetuximab exploits an EGFR-dependent but T790M-independent mechanism of action.

Secondary acquired resistance to afatinib plus cetuximab

Unfortunately, as observed with first-line EGFR tyrosine kinase inhibition, acquired resistance to afatinib+cetuximab invariably develops. A representative course of treatment for an EGFR-mutant lung adenocarcinoma patient under current treatment

plans would include first-line erlotinib or gefitinib treatment with expected partial response but invariable primary acquired resistance. At the point of disease progression, such a patient may be treated with second-line anti-EGFR combination treatment afatinib+cetuximab, though again, all patients who show an initial response will go on to develop secondary acquired resistance **(Figure 3).**

As targeted therapy regimens become increasingly complex in effort to overcome acquired resistance, strictly defined terminology is essential for expansion of this field of study. Secondary acquired resistance, as such, is used to define resistance to second-line targeted therapy which occurs after treatment with first-line targeted therapy and subsequent primary acquired resistance **(Figure 3)**. Evaluation of ideal treatment regimens will study the effectiveness of existing targeted therapies in the setting of first- vs. second-line (and beyond) treatment (Meador et al, manuscript in preparation). In addition, further study is needed to understand potentially targetable mutations that confer secondary acquired resistance.

Third-generation EGFR TKIs in lung cancer

In contrast to early tyrosine kinase inhibitors identified through structure-based searching of existing compound libraries, TKIs under development today are the result of rationally-designed structural alterations. To date, three such compounds have been described in the literature (**Table 1**). Evaluation of the first, WZ4006, showed excellent specificity for the T790M-containing mutant EGFR over wild-type EGFR, but has not gone on to clinical trials (Zhou, Ercan et al. 2009). Another third-generation EGFR tyrosine kinase inhibitor, CO-1686 (Clovis Oncology; Boulder, Colorado USA) is

currently undergoing phase II trials (Walter, Sjin et al. 2013). The third such compound under development is AZD9291 (AstraZeneca, London, UK). This drug is a mono-anilino-pyrimidine that is structurally and pharmacologically distinct from other third-generation tyrosine kinase inhibitors currently under development, which bear considerable structural similarity to each other (Cross, Ashton et al. 2014). AZD9291 was rationally designed to covalently bind the cysteine-797 residue within the ATP binding site of EGFR while maintaining optimal drug-like properties. Impressively, AZD9291 exhibits close to 200 times greater potency for L858R/T790M as compared to L858R alone, confirming the designed purpose of the mutant-specific drug.

Our studies also included the evaluation of pan-HER inhibitor AZD8931. Further studies of AZD9291 also identified a metabolite, AZ5104, which exhibited the same profile but greater potency against mutant and wild-type EGFR forms. Both the parent compound AZD8931 and the metabolite compound AZ5104 serve as important comparison compounds in the study of AZD9291. Additionally, future studies may evaluate AZD8931 as a primary compound for treatment of HER2-mutant tumors.

Merlin and EGFR

The work described herein explores a novel potential mechanism of acquired resistance to anti-EGFR targeted therapy in lung cancer involving inactivating mutation of the *NF2* gene (Chapters III, V). Merlin, named as the *m*oesin-*e*zrin-*r*adixin-*li*ke protein, is the protein product of the *NF2* gene. Along with closely related proteins moesin, ezrin, and radixin, merlin makes up part of the Band 4.1 superfamily of proteins,

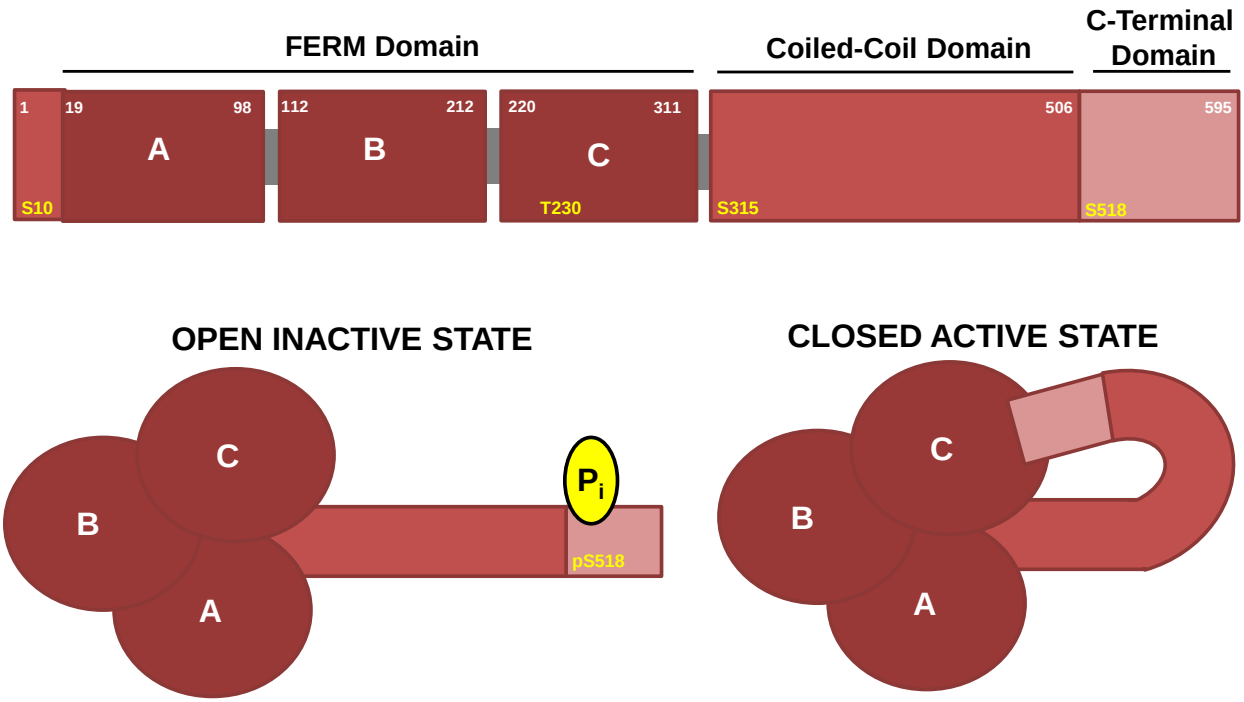

Figure 4. Structure and conformation of merlin
Upper Panel, Primary structure of *NF2* gene product containing FERM domain with three subdomains, coiled-coil domain, and C-terminal domain. Phosphorylation sites include serine 10, threonine 230, serine 325, and serine 518. Lower Panels, Representative schema of merlin's tertiary structure. Three subdomains of the FERM domain form globular "three-leaf clover." In the linear inactive state (left), phospho-serine 518 prevents the intramolecular loop formed from connection of the C-terminal domain to the FERM domain (right).

all of which share a conserved four point one, ezrin, radixin, and moesin (FERM) domain at their N-terminus. This superfamily was so named from its founding member's identification as a specific band upon SDS electrophoresis of erythrocyte membranes). Band 4.1 proteins are ubiquitous membrane-associated proteins that function to regulate the structure and function of various domains of the cell cortex (Bretscher, Edwards et al. 2002). Importantly, merlin is the only protein of this family to have tumor suppressor activity.

Structure and function of merlin

Discovered in 1993, merlin is the last identified member of this protein superfamily (Trofatter, MacCollin et al. 1993), (Rouleau, Merel et al. 1993). Consisting of 595 amino acids encoded by 17 exons, merlin undergoes a unique splicing pattern to result in three isoforms (Pykett, Murphy et al. 1994). Isoforms I and II are ubiquitously expressed and constitute the vast majority of merlin in cells, while isoform III is expressed only at low levels in cardiac and skeletal muscle. (Haase, Trofatter et al. 1994), (Arakawa, Hayashi et al. 1994). Structurally, merlin consists of an N-terminal FERM domain (residues 19-314), a coiled-coil domain (residues 314-492), and a C-terminal hydrophobic tail (492-595) (Laulajainen, Melikova et al. 2012) (**Figure 4, upper panel**). The FERM domain is composed of three subdomains (A, B, and C), which each make up a globular lobe of the domain tertiary "three-leaf clover" formation (Shimizu, Seto et al. 2002), (Bretscher, Edwards et al. 2002). A 295-amino acid sequence, the FERM domain of merlin bears a 65% sequence identity with family members ezrin, radixin, and moesin (ERM proteins) (Johnson, Kissil et al. 2002). This domain is essential for the function and localization of merlin and the ERM proteins.

Merlin can exist in two states: a dormant “off” state localized to the cytoplasm or nucleus without tumor suppressor function, and an active “on” state localized to the cell membrane with tumor suppressor function (Sherman, Xu et al. 1997) (**Figure 5**). In the “on” state, merlin occupies a tertiary intramolecular autoinhibitory loop conformation in which the protein’s C-terminal tail interacts with its FERM domain, forming a closed loop and rendering the protein capable of its tumor suppressive function (**Figure 4, lower panel**) (Laulajainen, Melikova et al. 2012). The release of the autoinhibitory loop is catalyzed by phosphorylation of serine 315 by protein kinase A (PKA) or p21-activated kinase (PAK) (Alfthan, Heiska et al. 2004), (Kissil, Johnson et al. 2002), which weakens the protein’s self-association. In the dormant, linearized state, merlin is incapable of inhibiting cell proliferation (Shaw, Paez et al. 2001). Once in the dormant state, further phosphorylation of merlin by Akt at serine 10 targets the protein for proteasomal degradation. Merlin harbors two other phosphorylation sites, threonine 230 and serine 315, though the control and impact of their phosphorylation status is not well understood (Laulajainen, Muranen et al. 2011).

Merlin has an extensive list of known direct binding partners with a broad range of cellular functions. Membrane proteins and complexes with roles in sensing cell density known to directly bind merlin include paxillin, alpha-catenin, CD44, and layilin (Fernandez-Valle, Tang et al. 2002) (Lallemand, Curto et al. 2003), (Morrison, Sherman et al. 2001), (Bono, Cordero et al. 2005). Adaptor scaffolding proteins known to link merlin to other proteins include NHERF1, magicin, syntenin, and HRS (Rangwala, Banine et al. 2005), (Wiederhold, Lee et al. 2004), (Jannatipour, Dion et al. 2001), (Sun, Haipek et al. 2002). Filamentous actin binding proteins that also bind to merlin include

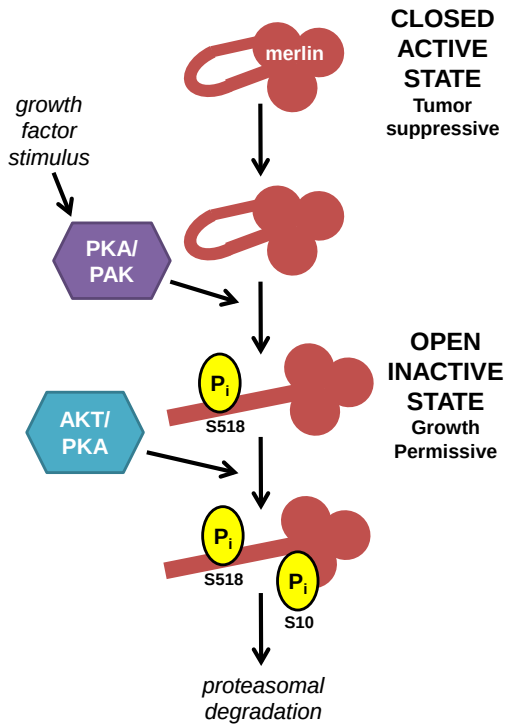

Figure 5. Activation states of merlin

The tumor suppressive function of merlin makes it unique from other FERM-domain containing proteins. When intramolecular interactions between the C-terminal tail and N-terminal FERM domain of merlin form a closed loop, merlin may localize the cell cortex and inhibit cell growth. Upon phopsphorylation at serine residue 518 by Protein Kinase A (PKA) or p21-Activated Kinase (PAK), merlin takes on its open, lineraized state and is incapable of tumor suppressive. Further phosphorylation at serine residue 10 by AKT or PKA targets merlin to proteasomal degradation.

β-II spectrin as well as fellow family members ezrin, radixin, and moesin (Scoles, Huynh et al. 1998), (Gronholm, Sainio et al. 1999). Merlin also directly binds a number of signaling molecules with diverse functions, including RalGDS, RhoGDI, Rak, MLK3, RIβ, PIKE-L, and N-WASP (Ryu, Kim et al. 2005), (Maeda, Matsui et al. 1999), (Kissil, Johnson et al. 2002), (Chadee, Xu et al. 2006), (Gronholm, Vossebein et al. 2003), (Rong, Tang et al. 2004), (Manchanda, Lyubimova et al. 2005).

Merlin mutations in cancer

Merlin was first characterized and is best studied in the nervous system tumors of its namesake disease, neurofibromatosis type II. Mutations in the *NF2* gene are known to be the most common genetic cause of familial NF2 syndrome, an autosomal dominant disease characterized by the appearance of spontaneous meningiomas, ependymomas, and the pathognomonic bilateral vestibular schwannomas (tumors of the nerve sheath of cranial nerve VIII) (Evans 2009) (Ahronowitz, Xin et al. 2007). Overall, *NF2* mutations occur in about 2% of all solid and liquid tumors (Yoo, Park et al. 2012), with somatic mutation occurring most frequently sporadic schwannomas, meningiomas, hepatocellular carcinoma, thyroid medullary carcinomas, and renal cell carcinomas (Stemmer-Rachamimov, Xu et al. 1997),(Ruttledge, Sarrazin et al. 1994),(Pineau, Marchio et al. 2003), (Sheikh, Tometsko et al. 2004), (Dalgliesh, Furge et al. 2010). In addition, loss of merlin at the post-translational level has been implicated in advanced breast cancer, and restoration of merlin expression decreased the invasive phenotype of breast cancer cells in xenograft models (Morrow, Das et al. 2011). Interestingly, inactivating somatic mutations in *NF2* are found in 35-40% of all malignant pleural mesotheliomas (Bianchi, Mitsunaga et al. 1995), (Sekido, Pass et al. 1995),

though the mechanism of tumor promotion in this setting is thought to rely on mutant merlin's inability to regulate cell cycle progression in the nucleus, unrelated to merlin's function at the cell cortex (Ladanyi, Zauderer et al. 2012).

Within the publically-available The Cancer Genome Atlas database (TCGA, NHRGI/NCI; cBio, MSKCC), only two of 129 human non-small-cell lung cancer samples are reported to harbor mutations in *NF2.* Both mutations are substitutions within the coiled-coil region of merlin. One mutation, A451T, occurs in a sample with squamous cell histology, while the other, Q470L, occurs in a sample with adenocarcinoma histology. Importantly, neither of these samples overlaps with the 24 samples harboring EGFR alterations. Similarly, the Cancer Cell Line Encyclopedia (CCLE; Broad Institute) identifies one human-derived lung adenocarcinoma cell line harboring *NF2* mutation (SW1573), but this cell line harbors mutant *KRAS* and has wild-type copies of *EGFR*. Mutations in *NF2* have not been studied in the context of the EGFR-driven cancer cell; indeed, the described publically available datasets show no samples or reagent in which this study would be possible. Of interest, a landmark study utilizing clustered regularly interspaced short palindromic repeat (CRISPR) technology identified *NF2* loss sufficient to confer resistance of human melanoma cell lines to the targeted inhibitor, vemurafinib (Zelboraf; Daiichi Sankyo; Tokyo, Japan) (Shalem, Sanjana et al. 2014). While the melanoma cell line used (A375) is driven by the V600E mutation in *BRAF* and harbors wild-type EGFR, this finding is one of the first to identify *NF2* loss in the setting of acquired resistance to targeted therapy.

Interaction of merlin, NHERF1, and EGFR

The structural interaction of merlin and EGFR has been studied only in non-cancer cell lines, including primary mouse embryonic fibroblasts, primary murine osteoblasts, murine liver-derived epithelial cells, and human embryonic kidney cells (Curto, Cole et al. 2007), (Lazar, Cresson et al. 2004). Importantly, the interaction of merlin and EGFR requires the adaptor protein Na+-H+ Exchange Regulatory Factor 1 (NHERF1). NHERF1, a 50kDa and 325 amino acid protein, was first identified in 1993 as a regulator of cAMP-mediated inhibition of the renal Na+/H+ exchanger isoform 3 (NHE3) (Weinman, Steplock et al. 1993). It has since been identified to play important roles in G-protein coupled receptor trafficking and conductance regulation of the cystic fibrosis transmembrane receptor (Cao, Deacon et al. 1999), (Hall, Ostedgaard et al. 1998). NHERF1 consists of two N-terminal PDZ domains and a C-terminal ERM domain (Donowitz, Cha et al. 2005).

NHERF1 was identified as a binding partner of merlin in a 1998 yeast two-hybrid screen, which further identified the C-terminal ERB domain of NHERF1 and the N-terminus of merlin as required for this interaction (Murthy, Gonzalez-Agosti et al. 1998) (**Figure 6**). In 2004, NHERF1 was identified as a binding partner of EGFR. This interaction occurs through the PDZ1 domain of NHERF1 binding to the DSFL motif at residues 1040-1043 of EGFR's regulatory domain (**Figure 6**). In human embryonic kidney cells, abrogation of NHERF1-EGFR binding enhances the rate of ligand-induced receptor endocytosis and downregulation of EGFR. Additional studies support the finding that NHERF1 functions as a stabilizer of EGFR at the cell surface. Furthermore, the presence of NHERF1 prolongs EGFR activation (Lazar, Cresson et al. 2004).

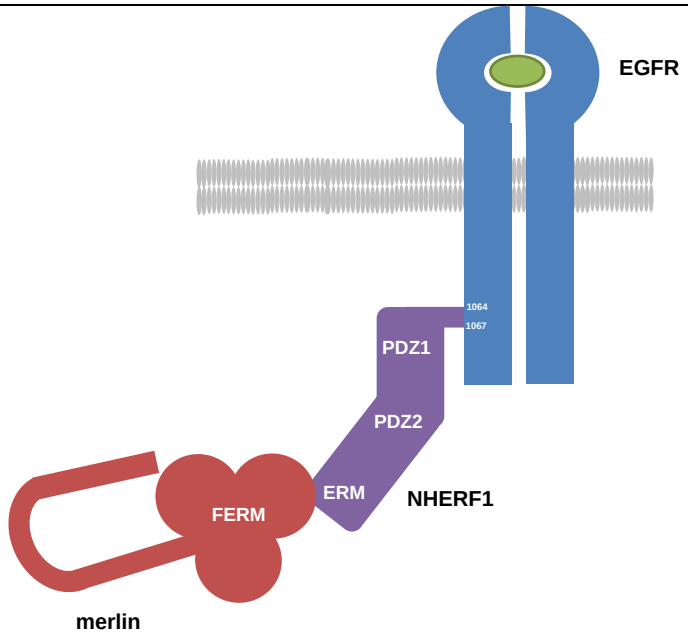

Figure 6. Interaction of merlin, NHERF1, and EGFR
Within the regulatory domain of EGFR, residues 1064-1067 (D-T-R-L) form a docking site for the N-terminal PDZ1 domain of NHERF1. The C-terminal ezrin, radixin, and moesin (ERM) binding domain of NHERF1 binds to the N-terminal FERM domain of merlin when merlin it in its closed conformation. Through physical interaction with NHERF1, merlin is thought to inhibit EGFR and function as a tumor suppressor by 1) preventing downstream signaling and 2) inhibiting receptor internalization and subsequent recycling.

Regulation of EGFR by merlin in non-cancer cells

As described above, all of the few currently published studies relating merlin and EGFR have been conducted in wild-type cells or cells genetically engineered to be driven by homozygous *NF2* loss(Curto, Cole et al. 2007), (Lazar, Cresson et al. 2004), (Morris and McClatchey 2009). Indeed, many of these studies take advantage of merlin's role as a tumor suppressor to elucidate normal mechanisms of cell proliferation control. These published studies suggest that merlin functions as a negative regulator of EGFR. Both cell line and xenograft models show an increase in total and phosphorylated EGFR in *NF2*-null cells (Curto, Cole et al. 2007), (Morris and McClatchey 2009). Specifically, it is proposed that merlin regulates contact-dependent inhibitor on EGFR signaling in cells through two mechanisms. In the setting of low cell density, merlin exists in the cytoplasmic compartment in its "off" state incapable of tumor suppressive functions. In the setting of high cell density and the formation of cell-cell contacts by cadherin-catenin complex proteins, merlin is recruited to nascent cell junctions (where is binds alpha-catenin) and activated (Gladden, Hebert et al. 2010). Once at the membrane, merlin stabilizes cadherin-catenin complexes and is localized such that it may bind EGFR-associated NHERF1. The physical interaction of merlin-NHERF1-EGFR serves to inhibit further EGFR signaling and prevent EGFR internalization and recycling (Curto, Cole et al. 2007). Indeed, overproliferation (defined in wild-type cell as the loss of contact-dependent inhibition) of NF2-/- cells both *in vitro* and *in vivo* is inhibited by pharmacologic inhibition of EGFR by erlotinib or gefitinib, providing further evidence that merlin regulates the contact-mediated inhibition of growth by EGFR (Curto, Cole et al. 2007), (Benhamouche, Curto et al. 2010).

Importantly, all existing studies evaluate merlin's effect on EGFR in cells harboring only mutations in *NF2;* other signaling circuitry exists in its wild-type state. As such, this work provides a springboard for further examination of merlin's role in cancer cells, but the highly perturbed signaling networks of cancer cells leave ample room for discovery.

Purpose of this study

While remarkable developments in genotyping technologies and drug development have dramatically advanced oncology treatment strategies in the current era of personalized cancer medicine, acquired resistance remains a major hurdle in improving patient outcomes. The application of drugs to highly-specific mutational targets has the unfortunate consequence of positively selecting out indolent clones of a heterogeneous tumor cell population. The studies described herein evaluate two unique therapeutic methods with the goal of overcoming acquired resistance: 1) identification of novel mutations in *NF2* with druggable consequences potentially responsible for secondary acquired resistance to afatinib+cetuximab, and 2) characterization of a novel, mutant-specific, third generation compound, AZD9291 (AstraZeneca, London UK).

First, these studies evaluate a novel potential mechanism of secondary acquired resistance in lung cancer. Following the identification of two mutations in the *NF2* gene that are incurred during treatment with afatinib+cetuximab, merlin loss is interrogated *in vitro* and *in vivo*. Resultant increase in mTOR activation in model systems is evaluated as a potential treatment mechanism to overcome secondary acquired resistance to afatinib+cetuximab. In combination with other studies identifying mTOR activation as a consequence of merlin loss, this work may provide solid preclinical rationale for the

evaluation of combination therapy including secondary anti-EGFR therapy with mTOR inhibition as a therapeutic strategy to prevent or overcome acquired resistance to afatinib+cetuximab. In addition, merlin is evaluated as a negative regulator of EGFR in the setting of EGFR-mutant lung cancer cells. While merlin has been evaluated as an EGFR regulator, all published studies to directly interrogate this relationship have been conducted in wild-type cells. The aberrant signaling environment of the cancer cell requires additional study to best understand the molecular function of merlin as a potential mechanism of secondary acquired resistance in EGFR-mutant lung cancer.

Furthermore, in collaboration with AstraZeneca (London, UK) the studies described herein evaluate a novel, mutant-specific, third-generation tyrosine kinase inhibitor, AZD9291. This drug is interrogated in numerous EGFR-mutant lung cancer cell lines for its potency compared to FDA-approved first- and second-line TKIs erlotinib and afatinib as well as parent and metabolized proprietary compounds AZD8931 and AZ5104. These studies test the hypothesis that AZD9291 has high potency against the cells harboring EGFR T790M, and will likely lead to efficacy in clinical trials as a novel drug with the express purpose of overcoming T790M-mediated acquired resistance to EGFR tyrosine kinase inhibitors. Further studies may also evaluate the potential of AZD9291 as a first-line treatment to prevent the development of acquired resistance, as well as the use of AZD9291 with other non-TKI agents as part of combination therapy regimens.

CHAPTER II

Materials and Methods

Adapted From: Pirazzoli V*, Nebhan C*, Song X, Wurtz A, Walther Z et al. (2014). "Acquired resistance of EGFR-mutant lung adenocarcinomas to afatinib plus cetuximab is associated with activation of mTORC1." *Cell Reports*. *co-first author

And: Cross DA, Ashton SE, Ghiorghiu S, Eberlein C, Nebhan CA et al (2014). “AZD9291, an irreversible EGFR TKI, overcomes T790M-mediated resistance to EGFR inhibitors in lung cancer.” *Cancer Discovery.*

Cell culture

Human lung adenocarcinoma cell lines were cultured in RPMI media (American Type Culture Collection) supplemented with 10% heat-inactivated fetal bovine serum (Gibco) and 1% penicillin/streptomycin (Corning). All described cell lines have been used as reagents in the Pao Lab since 2007 (**Table 2**)**.** Cells were re-genotyped multiple times to confirm the presence of known EGFR mutations by standard Sanger sequencing. Cells were grown in a humidified incubator with 5% CO 2 at 37°C.

Resistant cells derived *in vitro* have been previously described by our lab (Chmielecki, Foo et al. 2011). Briefly, parental cells were cultured with increasing concentrations of TKIs starting with the IC_{30}. Doses were increased in a stepwise pattern when normal cell proliferation patterns resumed. Fresh drug was added every

Parental Line	1° EGFR mutation	Isogenic Pair(s)	2° EGFR mutation
PC9par	exon 19 del	**PC9/ERc1**	T790M
		PC9/BRc1	T790M
HCC827par	exon 19 del	**HCC827/ER1**	T790M
		HCC827/ER1	MET amplification
HCC2279par	exon 19 del	**HCC2279/ER**	T790M
HCC2935par	exon 19 del	**HCC2935**	?
HCC4006par	exon 19 del	**HCC4006/ER**	EMT
VP-2	exon 19 del	---	T790M
11-18par	L858R	**11/18/ER**	NRAS Q61K
H3255par	L858R	**H3255/XLR**	T790M
HCC4011	L858R	**HCC4011/ER**	MET amplification
H1975	L858R	---	T790M
SW1573	--- (-/-*NF2*; mtKRAS)	---	---

Table 2. EGFR TKI-Sensitive and TKI-Resistant Cell Lines

72 to 96 hours. In some cell lines, clonal-resistant cells were isolated by limiting dilution. Resistant cell lines were maintained in the presence of drug as follows: erlotinib-resistant cells (/ER) were cultured in 1μM erlotinib, afatinib-resistant cells (/BR) were cultured in 250nM afatinib, afatinib+cetuximab-resistant xenograft-derived cell lines were cultured in 250nM afatinib plus 10μg/mL cetuximab, and AZD9291-resistant cells were cultured in 100nM AZD9291.

Immunoblotting

Cells were washed with cold PBS any lysed for 20minutes after scraping in with radioimmunoprecipitation assay (RIPA) buffer (150 mmol/L Tris-HCl, pH 7.5, 150 mmol/L NaCl, 1% NP-40 substitute, 0.1% SDS) supplemented with protease inhibitor cocktail (Roche), 40 mmol/L sodium fluoride, 1 mmol/L sodium orthovanadate, and 1 μmol/L okadaic acid. Protein levels were quantified with Bradford Reagent (Bio-Rad), and equal amounts were loaded for SDS-PAGE using 4% - 12% Bis-Tris precast gels (Invitrogen), followed by transfer by iBlot System to polyvinylidene difluoride membranes (Invitrogen).

Antibodies and reagents

Following transfer to PVDF membrane, membranes were blocked in 5% bovine serum albumin (Research Production International Co.) in tris buffered saline (Mediatech) plus 1% tween (Sigma) (5% BSA-TBST) for one hour at room temperature. Membranes were then blotted with antibodies diluted in 5% BSA-TBST at 4°C overnight at dilutions described (**Table 3**). Following three ten-minute washes in TBST,

Antibody	Catalog #/Company	Species	Dilution in 5% BSA-TBST
pEGFR (Y1068)	R&D Systems MAB3570	Mouse	1:1000
pEGFR (Y1173)	Santa Cruz sc-12351	Mouse	1:1000
Total EGFR	BD Transduction Labs 610017	Mouse	1:1000
merlin	Abcam ab889057	mouse	1:2000
	Santa Cruz sc-331	rabbit	1:1000
Pro-surfactant Protein C	Abcam ab90716	rabbit	1:1000
Actin	Sigma Aldrich A2066	rabbit	1:5000
phosphS6	Cell Signaling 2215	rabbit	1:2000
Total S6	Cell Signaling 2217	rabbit	1:2000
PhosphoAKT (S473)	Cell Signaling 9271	rabbit	1:500
Total AKT	Cell Signaling 9272	rabbit	1:1000
PhosphoERK (T202/Y204)	Cell Signaling 9101	Rabbit	1:2000
Total ERK	Cell Signaling 9102	rabbit	1:2000
α-catenin	Sigma C2081	rabbit	1:2000
	Invitrogen 139700	mouse	1:500
β-catenin	Sigma C2206	rabbit	1:10000
Plakoglobin	Novex 138500	mouse	1:1000
p120	BD Transduction Lab 610133	mouse	1:5000
E-cadherin	BD Transduction Lab 610181	mouse	1:5000
EBP50 (NHERF1)	Abcam ab3452	Rabbit	1:4000

Table 3. Antibodies used for immunoblot analysis

membranes were incubated in horseradish peroxidase (HRP)-conjugated secondary antibodies at 1:4000 dilution in 5% BSA-TBST (Cell Signaling, 7074 rabbit and 7076mouse). Signal was detected with Western Lightning Plus detection reagent (Perkin Elmer) as per manufacturer's protocol.

RNA interference and transfection

siRNAs specific for merlin (L-003917-00-0005), TSC1 (L-003028-00-0005) or scrambled control (D-001810-10-05) were obtained from Dharmacon, diluted in RNase/DNase-free H_2O to 20uM concentration, aliquoted to ensure minimal freeze-thaw cycles, and stored at -80°C. Transfection of RNAi was performed by the manufacturer's reverse transfection protocol using Lipofectamine RNAiMAX (Life Technologies).

Growth inhibition assays

Cellular growth inhibition was measured with CellTiter Blue Reagent (Promega, G8081) according to the manufacturer's instructions using cells plated in triplicate at a density of 2,000 cells per well. Fluorescence was measured on a SpectraMax fluorometer. Growth inhibition was calculated as percentage of vehicle-treated wells $\pm$ SD and Microsoft Excel software was use to IC_{50} values. Cellular Sytox proliferation assays were performed as described (Ward, Anderton et al. 2013) and Origin software used to interpolate IC_{50} values.

Soft agar assays

Colony-forming capacity of xenograft-derived cell lines was assessed using the CytoSelect 96-Well *In Vitro* Tumor Sensitivity Assay (Soft Agar Colony Formation) Kit

(Cell Biolabs Inc.), according to the manufacturer's protocol. Briefly, 50 μL of base agar matrix layer was dispensed into each well of a 96-well tissue culture plate. Cells ($5x10^3$) in 75 μl of cell suspension/agar matrix layer were dispensed into each well. The cells were treated with 50 μl of culture medium containing various drugs. After incubation for 8 days, 125μl of the 1x matrix solubilization buffer was added to solubilize the agar matrix completely, and MTT was added to each well. The absorbance was then recorded on a SpectraMax fluorometer at 570 nm.

Immunoprecipitation

When 100% confluent, cells were crosslinked with dithiobis(succinimidylpropionate) DSP (Pierce) by the optimized ReCLIP method (Smith, Friedman et al. 2011). Briefly, DSP was dissolved in DMSO to a concentration of 20mM immediately prior to treatment. Cells were moved to room temperature and washed twice in room-temperature PBS. 20mM DSP was then diluted in PBS on cells to a final concentration of 0.5mM. Cells were incubated for 30min at room temperature. After crosslinking, DSP was removed by aspiraton and the reaction was quenched by 10 minute incubation in 20mM Tris-HCl plus 5mM L-cysteine. Cells were then lysed in RIPA buffer and protein concentration was measured as described in immunoblotting procedure. Endogenous protein immunoprecipitation was conducted with agitation overnight at 4°C using 3μL antibody for either total EGFR R-1 (Santa Cruz, sc-101), merlin (Santa Cruz; sc-331), NHERF1 (Abcam, ab3254) or HA control in 3mg total protein lysate per reaction. 30μL Protein A (rabbit) or protein G (mouse) magnetic dynabeads (Life technologies) were then added to each reaction and incubated with

agitation for 4hr at 4°C. Beads were washed once in RIPA buffer, then resuspended in 2x Laemmli running buffer and boiled for 10min at 95°C before loading gel for SDS-PAGE electrophoresis.

Transgenic mice and xenografts

All animals were kept in pathogen-free housing under guidelines approved by the Memorial Sloan Kettering Cancer Center (MSKCC) and Yale institutional animal care and use committees, or under guidelines approved by the Vanderbilt University Medical Center Institutional Animal Care and Use Committee and conducted in accordance with UK Home Office legislation, the Animal Scientific Procedures Act 1986 (ASPA) and with Astrazeneca Global Bioethics policy. All experiments conducted in Chapter IV are outlined in project license 40/3483 which has gone through the AstraZeneca Ethical Review Process.

For studies outlined in Chapter III, TetO-EGFR$^{L858R+T790M}$ mice (Regales, Balak et al. 2007) and CCSP-rtTA mice have been previously described and used by our lab and others. For xenografts, 8-week-old nu/nu athymic nude mice (Harlan Labs) were injected subcutaneously with 10^3-10^6 PC-9/BRc1 cells together with Matrigel (BD Biosciences). Mice were randomized to receive either drug diluent alone (vehicle) or afatinib + cetuximab. Tumor size was measured twice a week using calipers. To further propagate afatinib+cetuximab-resistant tumors, these tumors were minced and immediately injected subcutaneously with Matrigen (tumor #16) or cultured for 2 weeks then reinjected subcutaneously into immunodeficient mice (tumor #24). Afatinib (produced by the Organic Synthesis Core Facility at MSKCC) was suspended in 0.5% (w/v) methylcellulose and administered orally (25 mg/kg/per day 5 days a week).

Cetuximab (Erbitux; Bristol-Myers Squibb and Eli Lilly Pharmaceuticals) was purchased and administered intraperitoneally (1mg twice a week). Rapamycin (LC Laboratories) was suspended in 0.5% carboxymethylcellulose and given orally (2mg/kg per day 5 days a week). The generation of $EGFR^{L858R}$ (45) and $EGFR^{L858R+T790M}$ mice (male and female) was previously described (46). Doxycycline was administered by feeding mice (aprox 3 week old) with doxycycline-impregnated food pellets (625 ppm; Harlan-Teklad), and treated for about 3 months during which time tumors developed. Afatinib and AZD9291 were suspended in 1% Polysorbate 80 and administered via oral gavage once daily at the doses of 7.5 mg/kg and 5 mg/kg, respectively. Mice were imaged weekly at the Vanderbilt University Institute of Imaging Science. For immunoblot analysis, mice were treated for eight hours with drug as described before dissection and flash freezing of the lungs. Lungs were pulverized in liquid nitrogen before lysis as described above.

For studies outlined in Chapter IV, 5×10^6 cells were implanted subcutaneously in a total volume of 0.1ml/mouse for PC-9 and H1975, and 1×10^7 cells implanted subcutaneously for A431. Both PC-9 and A431 cells were implanted in 50% Matrigel. PC-9 xenografts were established in female SCID mice and H1975 and A431 were established in female nude mice. All mice were greater than 6 weeks old at time of cell implant. Tumor growth was monitored twice weekly by bilateral caliper measurements, tumor volume calculated, and mice randomized into vehicle or treatment groups with approximate mean start size of 0.2-0.4cm^3. Randomization for animal studies is based on initial tumor volumes to ensure equal distribution across groups. A power analysis is performed whereby group sizes are calculated to enable statistically robust detection of

tumor growth inhibition. Mice were dosed once daily by oral gavage for duration of the treatment period. Tumor growth inhibition from start of treatment was assessed by comparison of the mean change in tumor volume for the control and treated groups. Statistical significance was evaluated using a one-tailed Students t test. For pharmacodynamic studies, mice were randomized at a mean tumor volume of approximately 0.5-0.8cm^3 using the same randomization criteria as the tumor growth inhibition studies. Mice were then treated orally with a single bolus dose of either vehicle or AZD9291. Tumors were excised at specific time points after dosing and fixed in 10% buffered formalin. Immunohistochemical analysis was performed on formalin fixed, paraffin embedded tissue sections staining for phosphorylated EGFR (Tyr1173) and phosphorylated ERK (p44/42 Thr202/Tyr204).

MRI

Mice were anesthetized via inhalation of 2%/98% isoflurane/oxygen and maintained under anesthesia throughout the course of the experiment. Animals were secured in a prone position in a 38-mm inner diameter radiofrequency (RF) coil and placed in a Varian 7T horizontal bore imaging system (Varian Inc, Palo Alto, CA) for data collection. A constant body temperature of 37°C was maintained using heated air flow. Prior to treatment, mice were scanned at least twice to confirm the presence of growing lung nodules and to avoid treating false-positive animals. Multi-slice T1-weighted gradient echo images were collected in all three imaging planes (axial, sagittal, and coronal) for localization of the lungs (repetition time (TR) =100ms, echo time (TE) = 5ms, slice thickness = 1mm, 40mm x 40mm field of view (FOV), approximately 15-20 slices). Following the initial scout imaging, respiratory triggered,

segmented fast low angle shot (FLASH) images were collected in both the axial and coronal planes with TR/TE = 850/2.8ms, flip angle = 15 degrees, number of slices = 22, slice thickness = 0.7mm with a 0.2mm gap between slices, and number of acquisitions = 16. For the axial images, the FOV = 23.04mm x 23.04mm, with a matrix size of 256x256, resulting in an in-plane resolution of 90 microns. For the coronal orientation, FOV = 30.72mm x 23.04mm, with a data matrix = 256x256, resulting in an in-plane resolution of 120x90 microns.

Following image acquisition, lung tumor volume measurements were performed using Matlab 2012a (The MathWorks, Inc, Natick, MA). A region of interest (ROI) was manually drawn around the lungs for each slice, excluding the heart, and a signal intensity threshold of 25 times the noise level (defined as the standard deviation of signal intensities in a region of the image background) was used to segment voxels within that ROI as positive for tumor. Total lung tumor volume was then calculated by multiplying the tumor area within the segmented region by 0.09 cm (the distance between each MRI slice).

Prior to treatment, mice were scanned at least twice to confirm the presence of growing lung nodules and to avoid treating false-positive animals. Multi-slice T1-weighted gradient echo images were collected in all three imaging planes (axial, sagittal, and coronal) for localization of the lungs (repetition time (TR) = 100ms, echo time (TE) = 5ms, slice thickness = 1mm, 40mm x 40mm field of view (FOV), approximately 15-20 slices). Following the initial scout imaging, respiratory triggered, segmented fast low angle shot (FLASH) images were collected in both the axial and coronal planes with TR/TE = 850/2.8ms, flip angle = 15 degrees, number of slices = 22,

slice thickness = 0.7mm with a 0.2mm gap between slices, and number of acquisitions = 16. For the axial images, the FOV = 23.04mm x 23.04mm, with a matrix size of 256x256, resulting in an in-plane resolution of 90 microns. For the coronal orientation, FOV = 30.72mm x 23.04mm, with a data matrix = 256x256, resulting in an in-plane resolution of 120x90 microns. Following image acquisition, lung tumor volume measurements were performed using Matlab 2012a (The MathWorks, Inc, Natick, MA). A region of interest (ROI) was manually drawn around the lungs for each slice, excluding the heart, and a signal intensity threshold of 25 times the noise level (defined as the standard deviation of signal intensities in a region of the image background) was used to segment voxels within that ROI as positive for tumor. Total lung tumor volume was then calculated by multiplying the tumor area within the segmented region by 0.09 cm (the distance between each MRI slice).

Modelling the binding mode of AZD9291

A published structure of the EGFR T790M mutant (pdb code 3IKA (Zhou, Ercan et al. 2009)) was used for the modelling of potential binding modes of AZD9291. Crystal structures were prepared using the protein preparation wizard in Maestro (Schrodinger Release 2013-1) which optimises hydrogen placements. The active site was defined by using the bound ligand, and the covalent docking protocol was used to model potential binding modes. These were ranked using the assigned scores and manually inspected for the retention of the key hinge interactions to the hinge region residue M793.

In vitro EGFR phosphorylation assays

Cells were treated for 2 h with a dose response of each drug. Wild-type cells were stimulated for 10 minutes with 25 ng/ml of EGF before lysis. Level of EGFR phosphorylation was quantified in cell extracts using a modified R&D Systems DuoSet Human phospho-EGFR ELISA (Ward, Anderton et al. 2013).

Expression vectors

The indicated EGFR cDNAs were cloned into the pcDNA3.1(-) expression vector and altered using site-directed mutagenesis as described (Pao, Miller et al. 2004). All cDNAs were re-sequenced to verify that no additional codon-changing mutations were present. pCDH-puro-EGFRvIII lacking exons 2-7 in EGFR (a kind gift from Dr. Jialiang Wang, Vanderbilt University) was constructed by subcloning the EGFRvIII fragment from MSCV-XZ066-EGFRvIII (Addgene Plasmid# 20737 http://www.addgene.org/20737/) into the expression vector pCDH-CMV-MCS-EF1-Puro. pBabe-HER2YVMA-puro (a kind gift from Carlos Arteaga, Vanderbilt University) encodes HER2 with an in-frame YVMA insertion at residue 776 (Wang, Narasanna et al. 2006). All plasmids were transfected into 293 cells as described (Pao, Miller et al. 2004).

Immunohistochemistry

4um sections were deparaffinized with xylene and rehydrated through graded alcohols into water. Antigen retrieval was carried out in a Milestone RHS microwave rapid histoprocessor for 10 minutes at 110^{o}C in pH9 buffer, Dako S2367 (for phospho-EGFR and phospho-Akt) and pH 6 citrate buffer, Dako S1699 (for phospho-Erk and phospho-S6). Tissues were placed on a LabVision Autostainer, endogenous peroxidase was blocked with 3% H_2O_2 for 10 minutes, followed by washing twice in TBS/0.05% Tween. Serum free protein block (Dako; X0909) was applied for 15 minutes. Slides

were then incubated with the primary antibodes at room temperature, phospho-EGFR Tyr1173 (Cell Signaling Technology, code 4407) at a 1:200 dilution, phospho-ERK (p44/42 Thr202/Tyr204) (Cell Signaling Technology, code 4376) at 1:100, phospho-S6 (Ser 235/236) CST #4857 at 1:150, phospho-PRAS40 (pThr246) (Cell Signaling Technology, code #2997) at 1:200, and phospho-Akt308 CST #2965 at 1:100 dilution. After washing twice, sections were incubated for 30 minutes with Rabbit Envision polymer detection system (Dako K4003), washed twice and then developed in liquid 3,3_-diaminobenzidine (DAB) for 10 minutes. Sections were then counter-stained with Mayer's haematoxylin, dehydrated, cleared, and mounted with coverslips.

Patients

All patients treated on trial NCT01802632 with written informed consent from patients and approval appropriate Institutional Review Boards (For the two patients disclosed in Chapter IV the Ethics committees are as follows; Korean patient: Seoul National University Hospital (EC), UK patient: North West – GM Central, North West Centre of REC, Manchester). Consent to publish study CT scan images is included as part of the patient informed consent, signed by both patients. In the first into man study a cohort size of 6 for the starting dose is standard practice, to provide sufficient safety and tolerability data about a dose level without exposing too many patients to a dose which may not be clinically beneficial. The first two patients in the starting dose cohort with an objective response were selected for inclusion in the publication. The clinical study is ongoing and further study data will be submitted for publication at a later date. Patient tumor tissues were analyzed for EGFR mutations using either the Qiagen EGFR RGQ PCR Kit [Cat #870111] or direct dideoxynucleotide sequencing.

CHAPTER III

Acquired resistance of EGFR-mutant lung adenocarcinomas to afatinib plus cetuximab is associated with activation of mTORC1

Adapted From: Pirazzoli V*, Nebhan C*, Song X, Wurtz A, Walther Z et al. (2014). "Acquired resistance of EGFR-mutant lung adenocarcinomas to afatinib plus cetuximab is associated with activation of mTORC1." *Cell Reports*. *co-first author

Introduction

Targeted therapies effectively treat subsets of solid cancers. However, the inevitable development of acquired resistance (AR) has hampered their success. A paradigm for this concept is the case of *Epidermal Growth Factor Receptor* (*EGFR*)-mutant lung cancer. *EGFR* mutations (Exon 19 deletions or the L858R point mutation) are associated with sensitivity to the first-generation tyrosine kinase inhibitors (TKIs) gefitinib and erlotinib (Pao and Chmielecki 2010), but drug resistance emerges on average 1 year after TKI treatment. In ~50% of resistant tumors, the mutant *EGFR* allele has acquired a secondary mutation in exon 20 (T790M) (Pao and Chmielecki 2010). Additional mechanisms of resistance include amplification of other receptor tyrosine kinases (RTKs) like *MET* and *HER2* (*ERBB2*), mutations in genes encoding downstream signaling components or phenotypic transformations such as epithelial-to-

mesenchymal transition (EMT) and neuroendocrine differentiation (Ohashi, Maruvka et al. 2013).

In a previous study using transgenic mice with *EGFR*$^{L858R+T790M}$-induced LUADs, we showed that resistance due to EGFR T790M could be overcome using a combination of afatinib+cetuximab (A+C) (Regales, Gong et al. 2009). Afatinib is a second-generation TKI that covalently binds EGFR at cysteine 797, while cetuximab is an anti-EGFR antibody. This preclinical study prompted a Phase IB/II clinical trial testing this drug combination in patients with progressive disease after TKI treatment. The trial showed an overall 32% response rate with a median duration of response of eight months (Janjigian, Smit et al. 2012). Unfortunately, patients responding to the drug combination still develop progressive disease.

We used xenografts and transgenic mice to model acquired resistance to the combination of A+C. Molecular analysis of resistant tumors revealed activation of the mTOR signaling pathway. Consistent with these findings, two separate patients with A+C-resistant tumors exhibited alterations in genes (*NF2* and *TSC1*), that when silenced in *EGFR*-mutant cells led to activation of the mTOR pathway. *In vitro* and *in vivo*, A+C resistance can be overcome by addition of an mTOR pathway inhibitor. These studies are the first to demonstrate mechanisms of AR to dual inhibition of EGFR in *EGFR*-mutant lung cancer and provide new insight into the biology of this subset of lung cancers, with immediate therapeutic implications for patients.

Results

Acquired resistance to A+C combination therapy in xenografts

We previously modeled acquired resistance to erlotinib in tetracycline-inducible mouse models of EGFR-dependent lung cancer by intermittently treating mice with the TKI (Politi, Fan et al. 2010). We observed clinically relevant mechanisms of acquired resistance, such as the EGFR T790M mutation and *Met* amplification, validating this experimental approach. We adopted the same strategy to establish models of resistance to A+C, first in xenograft models using the PC-9/BRc1 human LUAD cell line that harbors an $EGFR^{\Delta E746\text{-}A750+T790M}$ mutation (Chmielecki, Foo et al. 2011). Immunocompromised mice with PC-9/BRc1-induced tumors were randomized to receive either vehicle (n=5) or A+C (n=10). After 1 month of treatment, drug administration was interrupted for 1 month, and this on/off drug treatment regimen was repeated 3 times **(Figure 8A**). All tumors in control mice grew continuously. In the A+C treated cohort, tumors initially regressed. During the third cycle of treatment, 2 tumors (#16 and #24) became resistant **(Figure 8A). Thes**e were re-implanted into mice and treated with A+C or vehicle alone for 4 weeks **(Figure 8B**). Eventually, we collected 4 A+C resistant transplants from tumor #16 (labeled 16T-7, 16T-8, 16T-9 and 16T-10) and two from tumor #24 (24T-6, 24T-10) (Error! Reference source not found.). Cell lines were established from tumors 16T-10 and 24T-10. Resistance to A+C in these cell lines compared to parental PC-9 and PC-9/BRc1 cells was confirmed in a 3D colony assay (**Figure 7A**).

Evidence for mTOR pathway activation in A+C resistant xenografts

To identify mechanisms of resistance to A+C, we performed molecular analyses of the tumors collected. We first asked whether resistance to A+C could be explained by the acquisition of new mutations in *EGFR* or *ERBB2*, both of which are targets of A+C.

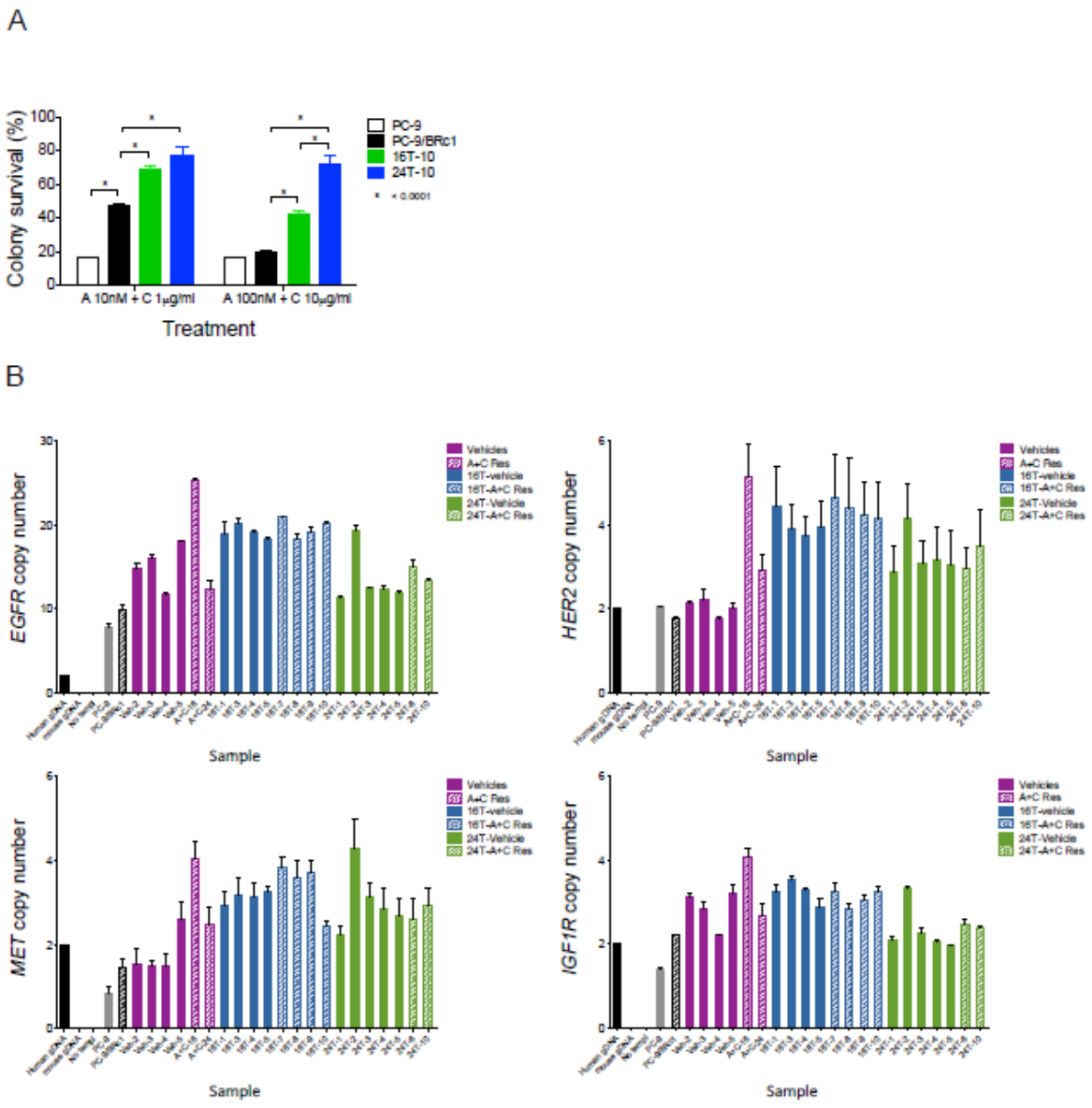

Figure 7. Resistance to afatinib+cetuximab in xenografts and xenograft-derived cell lines, related to Figure 1.

A. Soft agar assay of PC-9, PC-9/BRc1 and the afatinib+cetuximab resistant 16T-10 and 24T-10 cells in response to different doses of A+C. Data are presented as the Mean ± SE.

B. Copy number assay for *EGFR*, *HER2 (ERBB2)*, *MET* and *IGF1R* in xenograft tumors and cell lines as indicated. Afatinib+cetuximab treated tumors (A+C Tx) are shown with patterned bars. The different colors correspond to the origin of the cells used to derive the xenografts: Purple bars represent tumors derived from PC-9/BRc1 cells, blue bars represent tumors derived from afatinib+cetuximab resistant tumor 16, green bars represent tumors derived from afatinib+cetuximab resistant tumor 24. Values have been normalized to normal human gDNA. Two assays were run for each target. The mean and standard error (bar) is shown for each sample.

Sequencing of control and A+C resistant tumors did not detect any mutations in *EGFR* and *ERBB2* (data not shown). Analysis of the tumors revealed increased *EGFR* copy number in both vehicle-treated and A+C-resistant tumors compared to the parental PC-9/BRc1 cell line with tumor #16, but not #24, exhibiting high level *EGFR* amplification (**Figure 7B**). Minor fluctuations in *ERBB2, MET* and *IGF1R* copy number were also observed, the significance of which is likely limited given the magnitude of these changes. Together, the copy number data suggested that RTK amplification alone could not explain the resistance phenotype observed in our samples. These results prompted us to further investigate RTK levels and pathway activation in A+C-resistant samples. The xenograft-derived cell lines exhibited higher levels of phospho (p)-EGFR, pERK and pAKT compared to parental PC-9/BRc1 cells. However, the levels of activation of these proteins decreased in the presence of A+C, suggesting that the drugs retained the ability to block these pathways in A+C-resistant cells (**Figure 8C**). Interestingly, drug treatment did not affect the levels of pS6 or p4EBP1, markers of mTOR pathway activation, in the A+C-resistant lines in contrast to parental PC-9/BRc1 cells. This evidence suggests that pathway re-wiring in resistant tumor cells leads to sustained activation of the mTORC1 pathway. Similarly, *in vivo*, the mTOR pathway was consistently engaged in all A+C-resistant xenografts, as measured by pS6 and p4EBP1 (**Figure 8D and Figure 8E**). The levels of pAKT and pERK in the xenografts did not reveal a consistent pattern that would support either playing a major role in resistance to A+C in this model (**Figure 8D**). Together these results suggest that whilst pAKT and pERK can be inhibited in A+C-resistant tumors, the tumors retain sustained activation of mTOR signaling that may play a role in resistance to A+C combination therapy. Whole

exome sequencing (WES) of the A+C-resistant #16 and #24 tumors did not detect mutations in 23 mTOR-pathway related genes, strongly suggesting that non-mutational processes account for sustained activation of this pathway in these tumors.

Highly penetrant resistance to A+C in genetically engineered mouse models of EGFR-mutant lung cancer

In parallel, we developed models of resistance to A+C using transgenic mice with *EGFR*$^{L858R+T790M}$-induced LUADs. Tumors in these mice are resistant to erlotinib but sensitive to A+C (Regales, Gong et al. 2009). Thirty-eight *CCSP-rtTA*; *TetO-EGFR*$^{L858R+T790M}$ tumor-bearing mice were cycled on and off A+C using the protocol used for the xenograft experiments (**Figure 9A**). Tumor burden before and during treatment was tracked using magnetic resonance imaging (MRI) at the beginning and end of each drug cycle. This on/off drug treatment schedule was repeated until lung tumors no longer responded to treatment and increased in size on MR images (**Figure 9A**). All 38 mice that underwent the intermittent dosing treatment protocol developed resistance to the A+C combination. The majority of mice developed resistance after three cycles of A+C (21 out of 38); 15 mice developed resistance after 2 cycles and 2 mice after 4 cycles of drug treatment (**Table 4**). The median tumor shrinkage during the first cycle of A+C was 80%, but this was attenuated during the second and third cycles of treatment (**Figure 9B)**. Six mice that were treated without interruption with A+C also developed resistance to the drug combination (**Table 4 and Table 5**). Consistent with the emergence of resistance, tumors from the mice with acquired resistance displayed higher levels of proliferation and lower levels of apoptosis, compared to tumors from mice that had undergone short-term A+C treatment (**Table 5**).

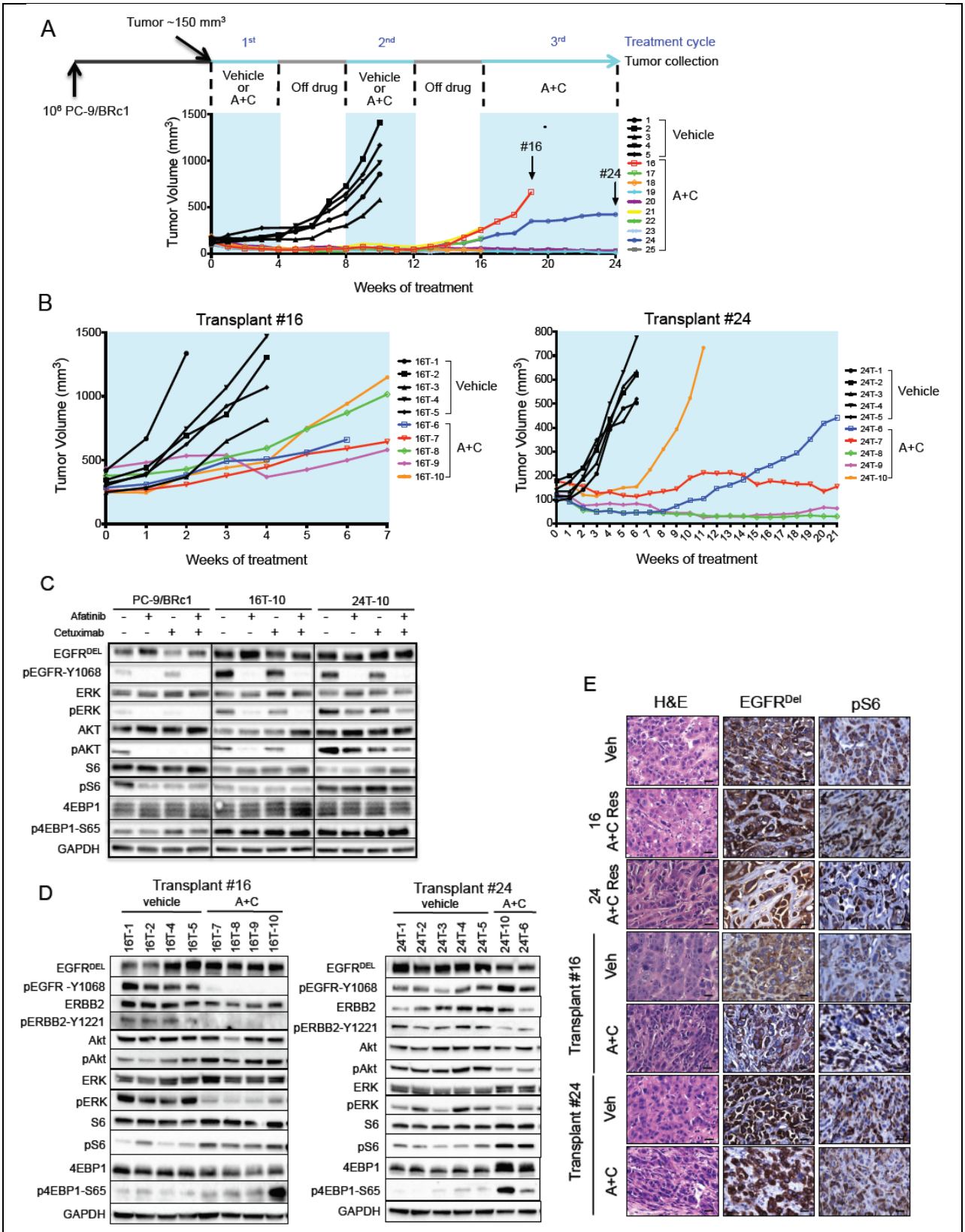

Figure 8. Activation of the mTOR pathway in afatinib+cetuximab-resistant

xenografts

A. Representation of the intermittent dosing protocol used to generate acquired resistance to afatinib and cetuximab in xenografts. 106 PC-9/BRc1 cells were injected s.c. into the flanks of immunocompromised mice. When tumors reached a volume of ~150 mm^3, mice were treated with vehicle (n=5, in black) or A+C (n=10, in color). After one month of treatment, drug administration was stopped for one month. The intermittent drug cycle was repeated three times. Tumor volume measurements are shown. Tumors indicated by the arrows (#16 and #24) acquired resistance to A+C.

B. Tumor growth of the transplants derived from A+C resistant tumors #16 (left panel) and #24 (right panel). The resistant tumors were further transplanted into 10 nude mice and treated continuously with vehicle (in black, n=5) or with A+C (in color, n=5). Transplants are labeled with the number of the original tumor they were derived from (#16 or 24), the letter "T" and a number.

C. Immunoblotting analysis of extracts from PC-9/BRc1, 16T-10 and 24T-10 cells treated with afatinib (100 nM), cetuximab (10 μg/ml) or the A+C combination. Lysates were probed with the indicated antibodies; p, phospho.

D. Immunoblotting analyses of tumor lysates from vehicle- and A+C-treated transplants derived from A+C-resistant tumors 16 and 24. Lysates were probed with the indicated antibodies; p, phospho.

E. Hematoxylin and Eosin staining (H&E) and IHC performed on paraffin sections of tumors derived from vehicle- and A+C-treated mice as indicated. Sections were stained with antibodies to EGFR exon 19 deletion mutant (EGFRDEL) and phospho-S6 (pS6) as indicated. 40X magnification is shown. Bars, 20 μm.

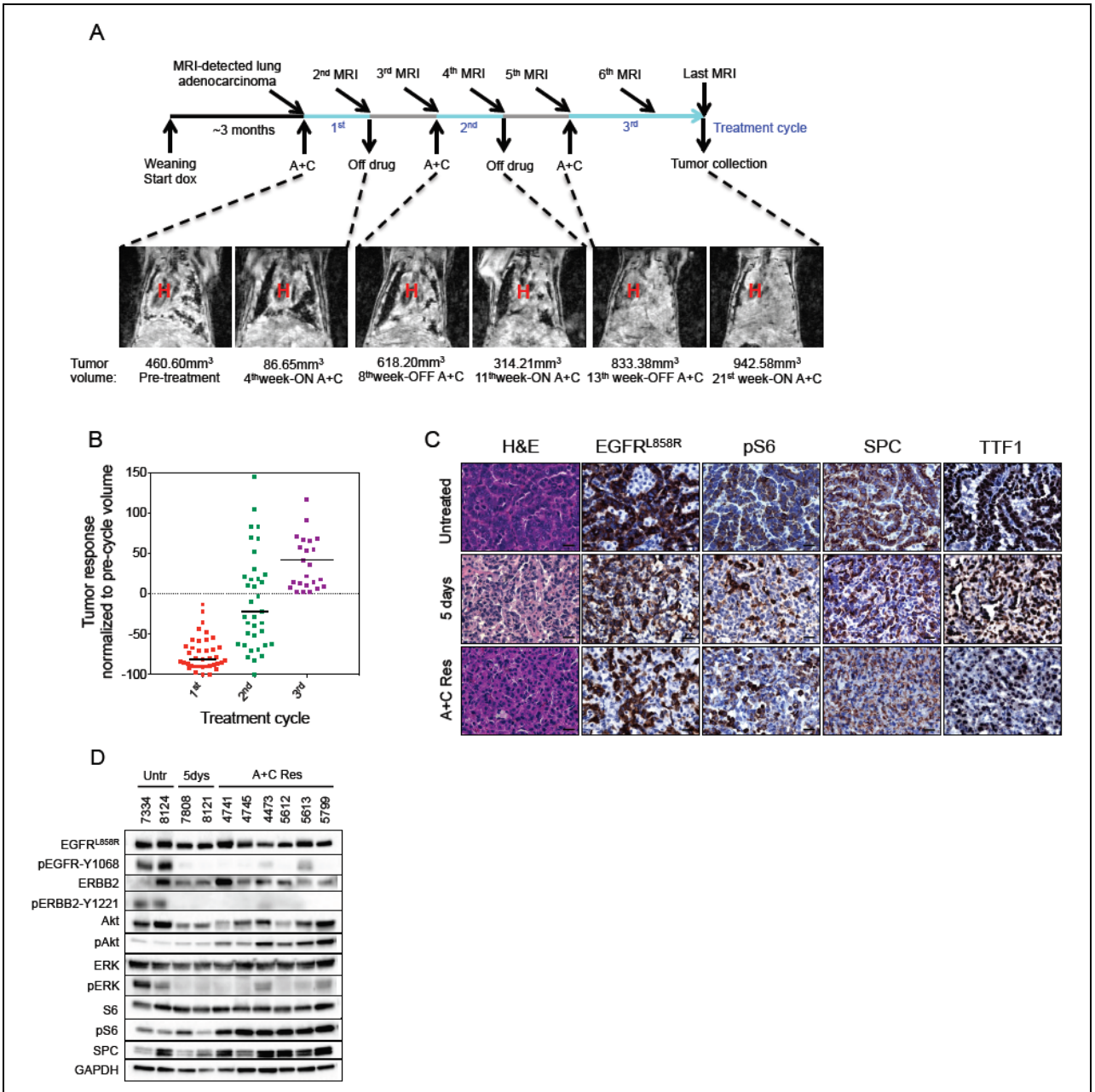

Figure 9. Activation of the mTOR pathway in afatinib+cetuximab-resistant mouse LUADs

A. Intermittent dosing of A+C was performed on a 1 month on drug and 1 month off drug cycle. Doxycycline administration was initiated at weaning and subsequently kept constant throughout the life of the animal. Tumor response was evaluated by MRI at the beginning and at the end of every drug treatment cycle. Coronal MR images of a *CCSP-rtTA*; *TetOEGFR L858R+T790M* mouse subjected to intermittent A+C treatment are shown. Tumor volume measurements are found below each image. H, heart.

B. Tumor response in *CCSP-rtTA*; *TetO-EGFRL858R+T790M* mice subjected to the A+C intermittent treatment protocol. Tumor volume is plotted as the percentage of the tumor volume detected on the pre-cycle MRI. Median tumor volume change is -80% in

the first cycle, -22% in the second cycle and +29% at the third cycle of A+C.
C. Hematoxylin and Eosin staining (H&E) and IHC performed on paraffin sections of LUADs derived from *CCSP-rtTA*; *TetO-EGFRL858R+T790M* untreated mice and mice treated with A+C for 5 days or at resistance to the drug combination (A+C Res). Sections were stained with antibodies to EGFRL858R, pS6, surfactant protein C (SPC) and thyroid transcription factor (TTF1) as indicated. 40X magnification is shown. Bars, 20 μm.
D. Immunoblotting analyses of tumor lysates from LUADs derived from untreated (Untr), A+C-treated (5dys) or resistant (A+C res) *CCSP-rtTA*; *TetO-EGFRL858R+T790M* mice. Lysates were probed with the indicated antibodies; p, phospho. Results representative of one experiment; each lane identified by four-digit number represents a unique mouse.

# Mouse	Months on dox	Lung tumor volume		
		1st cycle of treatment	2nd cycle of treatment	Final cycle of treatment
4473	2.9	n.d.	n.d.	18% increase
3041*	2.3	78% decrease	36% decrease	6% increase
2121*	5.0	71% decrease	3% decrease	67% increase
2846*	4.7	n.d.	84% increase	84% increase
3767	2.4	n.d.	9% decrease	15% increase
4741	3.4	n.d.	10% decrease	3% increase
4745	3.5	93% decrease	62% decrease	13% increase
5373	3.1	nd	29% decrease	66% increase
5612*	2.1	81% decrease	49% decrease	58% increase
4413	4.9	73% decrease	46% decrease	173% increase
5613*	2.1	22% decrease	22% decrease	71% increase
5668	2.5	67% decrease	10% increase	10% increase
5799	3.4	58% decrease	84% increase	84% increase
6033*	3.2	44% decrease	53% increase	53% increase
5883*	2.5	48% decrease	70% increase	70% increase
4515	3.5	n.d.	T1 373% increase T2 19% increase	T1 373% increase T2 19% increase
4659*	4.1	90% decrease	100% decrease	3% increase
6382*	3.9	80% decrease	55% increase	55% increase
6429	3.8	85% decrease	68% increase	68% increase
5670*	2.8	57% decrease	63% decrease	55% increase
5614*	4.9	86% decrease	63% decrease	36% increase
4903*	7.2	69% decrease	62% decrease	14% increase
5796*	4.3	35% decrease	31% increase	31% increase
6231*	4.7	89% decrease	70% decrease	54% increase
6258*	4.5	66% decrease	146% increase	146% increase
6494*	3.1	13% decrease	40% decrease	2% increase
6495*	3.4	57% decrease	36% decrease	11% increase
6654*	3.3	65% decrease	14% increase	14% increase
7336	2.1	83% decrease	28% decrease	92% increase
7488	1.6	87% decrease	69% decrease	42% increase
8435	1.7	90% decrease	24% increase	24% increase
7490	2.2	n.d.	18% increase	18% increase
7494	2.7	100% decrease	82% decrease	22% increase
8128	2.5	85% decrease	21% increase	21% increase
8129	2.5	91% decrease	105% increase	105% increase
7805	2.2	90% decrease	77% decrease	9% increase
7809	1.8	54% decrease	51% decrease	117% increase
7807	2.5	98% decrease	79% decrease	8% increase

*In these mice increased tumor volume was observed when A+C treatment was prolonged beyond 4 weeks in the final round.

Table 4. List of CCSP-rtTA; TetO-EGFR$^{L858R+T790M}$ mice subjected to intermittent treatment with afatinib + cetuximab, related to Figure 9.

# Mouse	Months on dox	Time to resistance (months)	Lung tumor change from baseline	
			After 1 month on A+C	At resistance to A+C
6801	2.3	2	89% decrease	368% increase
6803	2.3	2	70% decrease	55% increase
7495	2	3	92% decrease	367% increase
8616	2.3	2	88% decrease	376% increase
8619	2.3	2	84% decrease	56% increase
7333	2.3	3	80% decrease	154% increase

Table 5. List of CCSP-rtTA; TetO-EGFRL858R+T790M mice subjected to continuous treatment with afatinib + cetuximab, related to Figure 9.

We explored whether A+C resistant tumors showed any phenotypic differences compared to untreated tumors. *CCSP-rtTA*; *TetO-EGFR*$^{L858R+T790M}$ mice developed solid and papillary LUADs, positive for the type II pneumocyte marker surfactant protein-C (SP-C) and for thyroid transcription factor-1 (TTF1) (**Figure 9C**). While most untreated adenocarcinomas were papillary, A+C treated and resistant tumors almost invariably were solid and more poorly differentiated (**Figure 9C**).

Evidence for mTOR pathway activation in the A+C-resistant mouse LUADs

To elucidate further the pathways that may account for resistance to A+C, we sequenced the *EGFR* transgene and *Erbb2* from 23 resistant tumors. Similar to our observations in xenografts, we did not find mutations in these genes or in *Pik3ca, Pik3cb* and *Kras* (n=15, data not shown). A+C-resistant mouse LUADs did not show copy number alterations in the *EGFR* transgene or in endogenous *Egfr*, *Erbb2*, *Met* and *Igf1r* (**Figure 10C**).

We then examined which signaling events might promote acquired resistance to A+C. As expected, we found that upon short-term (5 days) A+C treatment, phosphorylation of EGFR and Erbb2 were decreased. As a consequence reduced levels of phosphorylated Erk were observed, however Akt phosphorylation did not change (**Figure 9D**). Phosphorylation of EGFR was greatly reduced or completely abrogated in all of the resistant tumors, and phosphorylation of Akt was consistently higher than in untreated tumors, suggesting the presence of compensatory mechanisms of activation of the PI3K pathway in these tumors. Similarly, phosphorylation of Erbb2 was not restored to

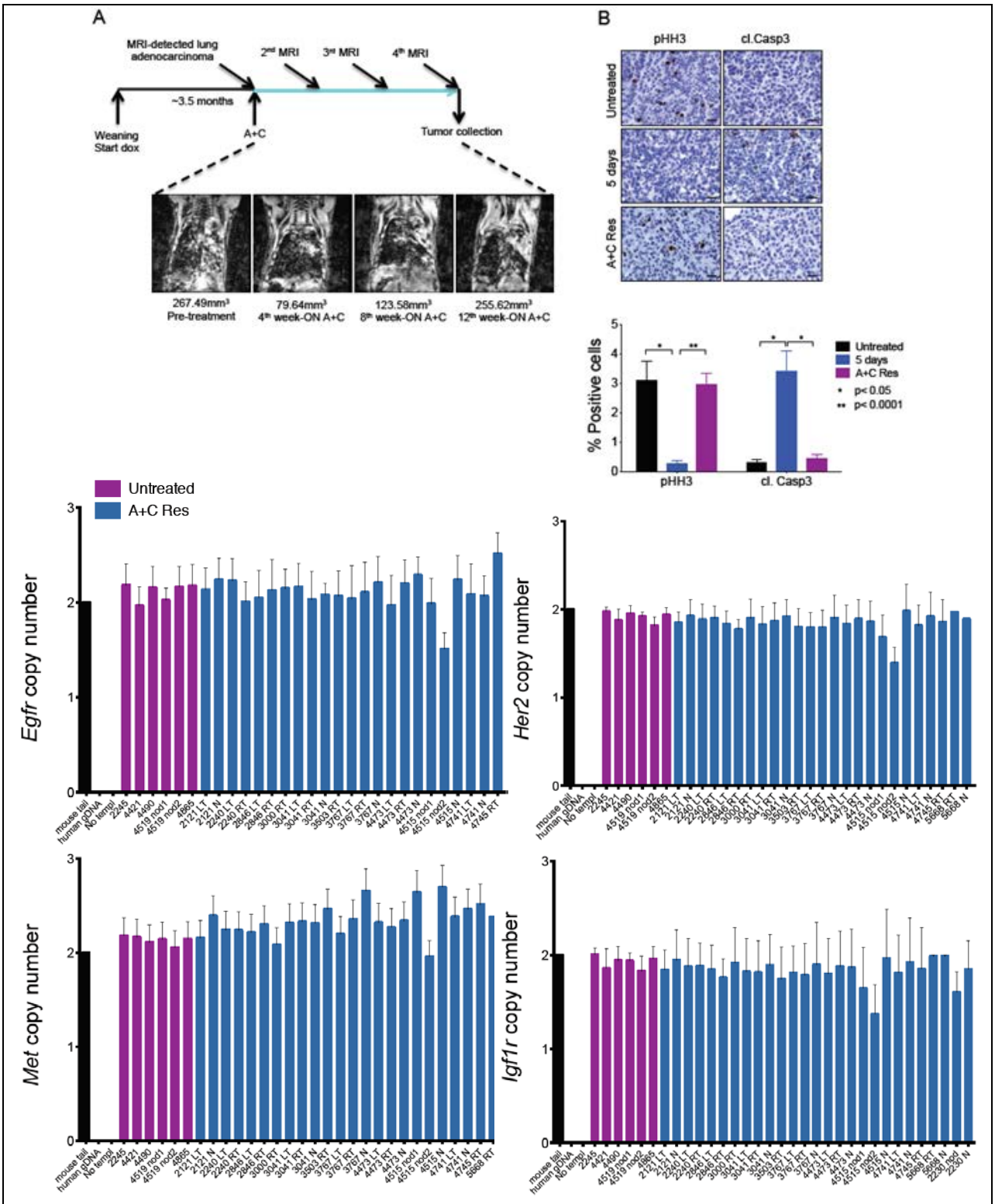

Figure 10. Resistance to A+C in *CCSP-rtTA*; *TetO-EGFRL858R+T790M* mice, related to Figure 9

A. Continuous dosing of afatinib + cetuximab leads to acquired resistance in *CCSP-rtTA*; *TetO-EGFRL858R+T790M* mice. Doxycycline administration was initiated at

weaning and subsequently kept constant throughout the life of the animal. Tumor response was evaluated by MRI every 4 weeks. Coronal MR images of a *CCSP-rtTA*; *TetO-EGFRL858R+T790M* mouse subjected to continuous A+C treatment are shown. Tumor volume measurements are below each image.
B. Decreased mitosis and increased apoptosis upon A+C treatment. Phospho-histone H3 staining (pHH3, left) and cleaved caspase 3 (cl.Casp3, right) of adenocarcinoma sections from *CCSP-rtTA*; *TetO-EGFRL858R+T790M* mice untreated (top), treated with A+C for 5 days (middle) and resistant to A+C (A+C-Res, bottom). Bars, 20 μm. Quantification of pHH3 and cl.Casp3 is shown in the bar graph. Data are represented as the Mean ±SE.
C. Copy number assay for *Egfr*, *Her2 (Erbb2)*, *Met* and *Igf1r* in lung adenocarcinomas from *CCSP-rtTA*; *TetO-EGFRL858R+T790M* mice. Untreated tumors are shown in purple. A+C resistant (A+C Res) tumors are shown in blue. N, normal; LT, left tumor; RT, right tumor; nod, nodule. The mean and standard error (bar) is shown for each sample.

Patient 1

Gene	Nucleotide	Protein	Pre A+C Frequency, Total reads	Post A+C Frequency, Total reads
EGFR	c.2753>G	p.L858R	Positive*	38%, 1162
EGFR	c.2369C>G	p.T790M	Positive*	24%, 1279
NF2	c.592>T	p.R198*	0%, 2301	15%, 631
NF2	c.811-2A>T	splice	0%, 2569	13%, 1168

* as per 2009 retrospective clinical report (Genzyme) of 2006 biopsy sample

Patient 2

Gene	Nucleotide	Protein	Pre A+C Frequency, Total reads	Post A+C Frequency, Total reads
EGFR	c.2753>G	p.L858R	3%, 827	19%, 715
TSC1	c.345_345delT	p.L116fs*	1%, 613	15%, 399

Table 6. List of mutations detected by targeted sequencing in Patient 1 and Patient 2

untreated levels in the A+C-resistant tumors. Similar to the xenografts discussed previously, A+C-resistant tumors consistently showed increased pS6, suggesting that increased activation of mTORC1 may play a role in acquired resistance to A+C (**Figure 9C and Figure 9D**).

Mutations in mTOR signaling pathway genes are associated with resistance to A+C in human tumors

Consistent with the preclinical modeling, we found genetic evidence for potential activation of the mTOR signaling pathway in tumor samples from 2 (of 4 analyzed) separate patients with acquired resistance to A+C (**Figure 11**). Strikingly, the mutated tumor genes were not shared between the two patients, but they both converged on the mTOR pathway. In the first patient, targeted resequencing of 182 genes using the FoundationOne platform **(Table 7)** as well as WES revealed that the resected A+C-resistant tumor (**Figure 11A and Table 7**) still harbored both the L858R and T790M mutations (frequencies of 0.38 of 1162 reads and 0.24 of 1279 reads, respectively in the FoundationOne Assay) (Jeselsohn, Yelensky et al. 2014). Unexpectedly, two additional mutations were found in *NF2* (c.592C>T_p.R198* at frequency 0.15 of 631 reads and c.811-2A>T: splice at 0.13 frequency of 1168 reads). These two mutations were not detected in the 2006 tumor specimen, as assessed by deep amplicon-based resequencing.

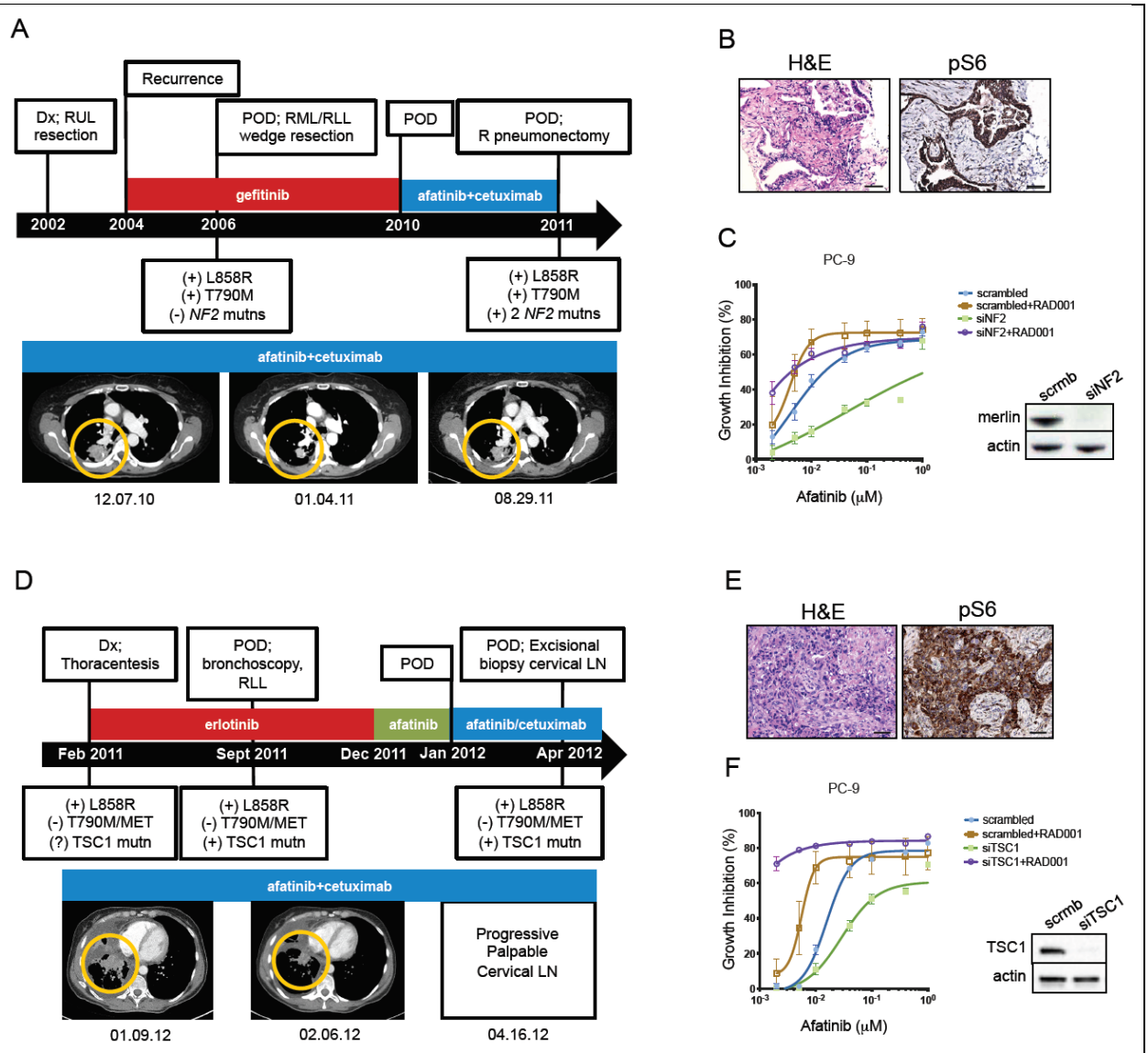

Figure 11. Genetic alterations associated with activation of mTORC1 in human lung tumors resistant to A+C

A. Top, disease milestones for Patient 1. Time from diagnosis to A+C resistance is indicated by the black arrow. Clinical findings, procedures and drug-treatments are indicated above the arrow. Molecular findings are shown below the black arrow. Dx, diagnosis; POD, progression of disease; RUL, right upper lobe; RML, right middle lobe; RLL, right lower lobe; R, right; Mutns, mutations. Bottom, computed tomography scans of the lungs are shown prior (12.07.10), during (01.04.11) and at resistance (08.29.11) to A+C. Tumors areas are circled.

B. Hematoxylin and eosin (H&E, left panel) and IHC for pS6 (right panel) of the A+C resistant tumor harboring the *NF2* mutations. 20X magnification is shown. Bars, 50 μm.

C. Growth inhibition of PC-9 cells after knockdown of *NF2* in response to afatinib (left). Viable cells were measured after 72 hours of treatment and plotted relative to untreated

controls. Data are presented as the mean ± SE. Immunoblotting of PC-9 cells showing efficient knock-down of Merlin expression is shown on the right. Lysates were probed with the indicated antibodies.
D. Top, disease milestones for Patient 2. Time from diagnosis to A+C resistance is indicated by the black arrow. Clinical findings, procedures and drug treatments are indicated above the arrow. Molecular findings are shown below the black arrow. Dx, diagnosis; POD, progression of disease; RLL, right lower lobe; Mutn, mutation; LN, lymph node. Bottom, computed tomography scans of the lungs are shown prior (01.09.12) and during treatment with A+C (02.06.12). Tumor areas are circled.
E. Hematoxylin and eosin (H&E) staining of the excised cervical lymph node from Patient 2 (left) and IHC showing phosphorylation of S6 (pS6, right). Bars, 50 μm.
F. Growth inhibition of PC-9 cells after knockdown of *TSC1* in response to afatinib (left). Viable cells were measured after 72 hours of treatment and plotted relative to untreated controls. Data are presented as the mean ± SE. Immunoblotting of PC-9 cells showing efficient knock-down of TSC1 expression is shown on the right. Lysates were probed with the indicated antibodies.

The *NF2* gene encodes merlin, a protein with putative tumor-suppressive function. Both mutations are predicted to cause loss of protein function. The R198* mutation is a truncating mutation that causes loss of two-thirds of Merlin and has previously been described in cancers including ependymoma (Lamszus, Lachenmayer et al. 2001). The c.811-2A>T alteration is a splice-site mutation that at a minimum affects the FERM domain, important for Merlin's localization and activation. In support of a functional role of this mutation, a 69bp deletion encompassing this exon 9 splice site and causing *NF2* exon 9 skipping has been associated with familial autosomal dominant intramedullary ependymoma (Zemmoura, Vourc'h et al. 2014).

In different cellular contexts, *NF2* has been shown in independent studies to negatively regulate EGFR signaling and mTORC1 (Curto, Cole et al. 2007; James, Han et al. 2009; Lopez-Lago, Okada et al. 2009). To determine whether the mTORC1 pathway was activated in this sample, we used immunohistochemistry (IHC) to stain the biopsy collected at the time of resistance to A+C with a pS6 antibody and observed a strong signal (**Figure 11B**). In support of a role for *NF2* on TKI-sensitivity, knockdown of *NF2* led to a decrease in the sensitivity of PC-9 cells to afatinib (**Figure 11C**). Importantly, the addition of an mTOR inhibitor, everolimus (RAD001), re-sensitized PC-9 cells with *NF2* knockdown to afatinib *in vitro* (**Figure 11C**). Notably, everolimus alone was not able to inhibit cell proliferation in cells treated with either control (scrambled) or *NF2* siRNAs (**Figure 12C**). The same effect was observed in HCC827 cells upon cetuximab treatment (**Figure 12B**). Moreover, A+C treatment in LUAD HCC827 cells did not decrease the levels of pS6 upon *NF2* knock down (**Figure 12B**)**.** Taken together, this patient and *in vitro* data suggest that the *NF2* mutations were acquired

during treatment on A+C and that *NF2* loss leads to activation of the mTORC1 signaling pathway to mediate drug resistance.

In the second patient, initial molecular analysis of the A+C-resistant tumor (**Figure 11D**) did not detect the T790M mutation, *MET* amplification or *ERBB2* amplification. Further analysis using a more recent FoundationOne panel (Frampton, Fichtenholtz et al. 2013) revealed the presence of the L858R mutation (c.2573T>G; frequency of 0.19 of 715 reads) plus a mutation in the *Tuberous Sclerosis 1 (TSC1)* gene (c.345_345delT_p.L116fs*; frequency 0.15 of 399 reads; this sample contained approximately 70% tumor cells) (**,** Error! Reference source not found.). The observed L116fs* frame-shift mutation leads to the creation of a stop codon immediately downstream of codon 116, truncating the protein. The somatic status and zygosity of the *TSC1* L116fs*2 alteration (see Supplemental Experimental Procedures) were consistent with a somatic alteration clonally present on a single *TSC1* copy in the tumor, indicating that LOH occurred. The *TSC1* mutation status of the pleural fluid collected at diagnosis was not assessed due to insufficient tumor material. FoundationOne analysis of the erlotinib-resistant lung specimen (before A+C) identified the presence of the *L858R* mutation (c.2573T>G; frequency of 0.03 of 827 reads) and of the *TSC1* mutation (c.345_345delT_p.L116fs*; frequency 0.01 of 613 reads), indicating that it did pre-exist treatment with A+C (Error! Reference source not found.**,** Error! Reference source not found.). The low allele frequency of both of the mutations is due to low tumor purity of this sample (10% purity). These data suggest that selection of the deleterious *TSC1* mutant may have occurred during A+C treatment.

Patient 1. Post-A+C targeted re-sequencing by FoundationMedicine

Alteration	Gene	Chromosome	Nucleotide	Protein	Post-A+C frequency, total reads
Somatic Variant	*EGFR*	7	c.2753T>G	L858R	38%, 1162
	EGFR	7	c.2369C>G	T790M	24%, 1279
	NF2	22	c.592C>T	R198*	15%, 631
	NF2	22	c.811-2A>T	splice	13%, 1168
Copy number gains					none
Homozygous gene deletions	*CDKN2A*	9	deletion	deletion	n/a
	CDKN2B	9	deletion	deletion	n/a
Chromosomal region deletions	*SMARCA4*	19: 11.1-11.2 deletion	deletion	deletion	n/a

n/a, not applicable

Patient 1. Pre-A+C targeted deep re-sequencing by MiSeq

Mutation	Pre-A+C frequency, total reads	Post-A+C frequency, total reads
NF2 c.592C>T p.R198*	0.13%, 2298	12.1%, 2821
NF2 c.811-2A>T p.splice	0.27%, 2563	9.98%, 1560

Note: The pre-A+C sample for patient 1 was insufficient for sequencing by FoundationMedicine. Therefore, targeted deep sequencing using the MiSeq platform was used to analyze pre-treatment *NF2* status.

Patient 2. Pre- and post-A+C targeted re-sequencing by FoundationMedicine

Alteration	Gene	Chromosome	Nucleotide	Protein	Pre-A+C frequency, total reads	Post-A+C frequency, total reads
Somatic Variants	*EGFR*	7	c.2753>G	L858R	3%, 827	19%, 715
	TP53	17	c.431_431delA	Q144fs*26	n.d.	13%, 599
	TSC1	9	c.345_345delT	L116fs*2	1%, 613	15%, 399
Copy number gains					none	none
Homozygous gene deletions					none	none
Chromosomal region deletions					none	none

n.d., not determined

Table 7. Data from targeted sequencing of A+C-resistant patient samples, related to Figure 11

The *TSC1* gene encodes for Hamartin, which together with Tuberin (*TSC2)* forms a complex that suppresses mTORC1 signaling (Laplante and Sabatini 2012). To determine whether this pathway was active in the sample collected after A+C treatment, we performed IHC for pS6 and observed strong staining (**Figure 11E**). The functional role of disruption of TSC1 on drug response was tested using siRNAs. Knockdown of *TSC1* in PC-9 cells led to a decrease in sensitivity of the cells to afatinib, and sensitivity to afatinib was restored by the addition of everolimus upon *TSC1* loss **(Figure 11F)**. Moreover, cells treated with either scrambled or *TSC1* siRNAs were not sensitive to everolimus treatment **(Figure 12C)**. These results indicate that the absence of *TSC1* mediates resistance to EGFR-directed therapies by activating the mTORC1 signaling pathway.

Xenografts and LUADs resistant to A+C are sensitive to concurrent EGFR and mTOR inhibition

Activation of the mTOR pathway in mouse models and patient samples led us to explore whether A+C resistant tumors responded to inhibition of this pathway. To test this, we treated 4 *CCSP-rtTA*; *TetO-EGFR*$^{L858R+T790M}$ mice with A+C resistant tumors with rapamycin as a single agent. Rapamycin treatment alone was ineffective in all 4 cases (**Figure 13A** and **Figure 13C**). This result is in line with previous findings showing that inhibition of mTOR alone is not sufficient to abolish Akt signaling and that the combination of an mTOR inhibitor with an RTK inhibitor is more likely to have anti-tumor activity (Li, Ambrogio et al. 2008; Rodrik-Outmezguine, Chandarlapaty et al. 2011). To

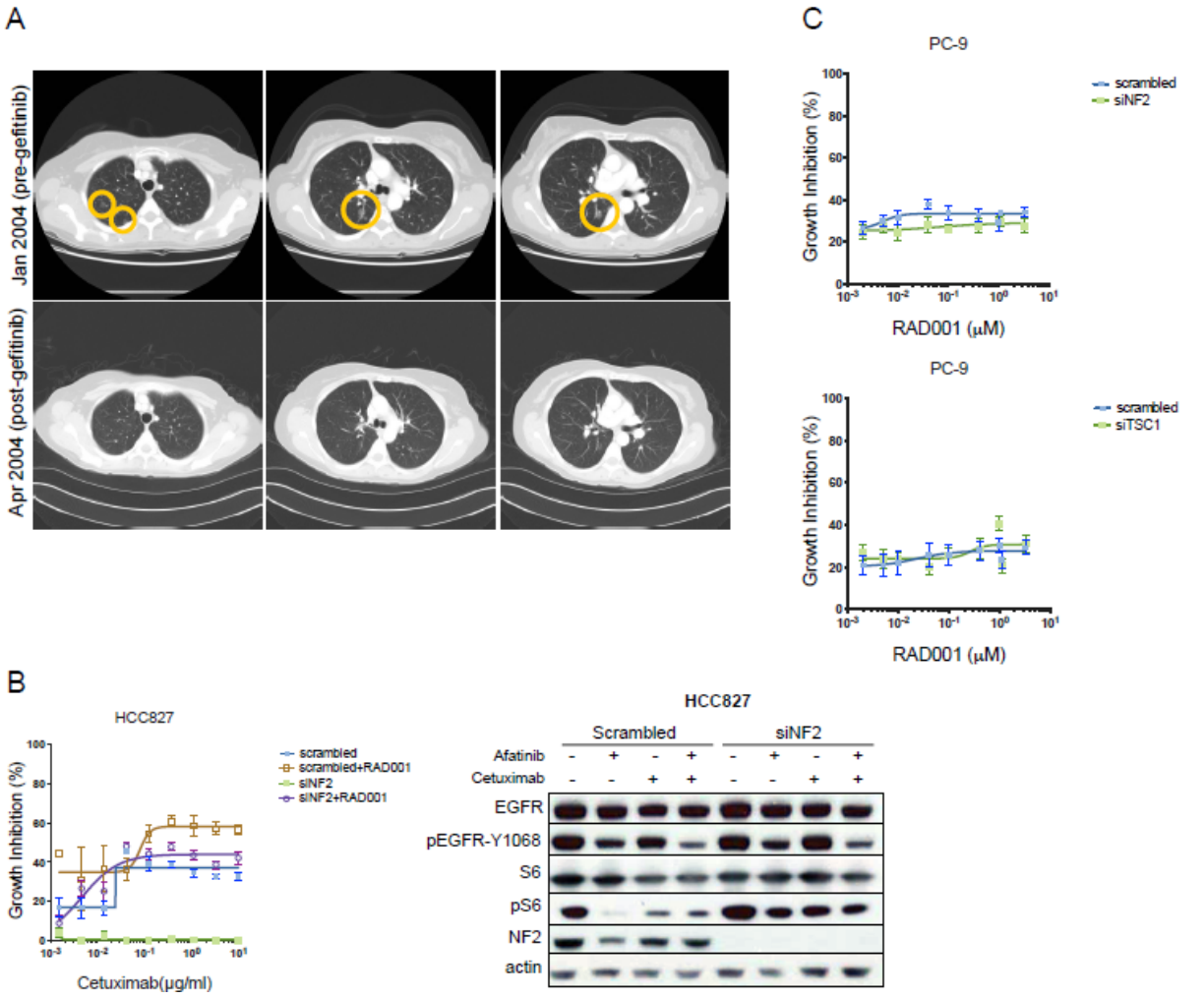

Figure 12. Activation of mTORC1 upon loss of Merlin in Patient 1, related to Figure 11.

A. Partial response of Patient 1 to gefitinib. (Top) Pre-gefitinib computed tomography images, January 2004. Tumors areas are circled. (Bottom) Post-gefitinib computed tomography images, April 2004.

B. Growth inhibition of HCC827 cells after knockdown of *NF2* in response to cetuximab (left). Viable cells were measured after 72 hours of treatment and plotted relative to untreated controls. Data are presented as the mean ± SE. On the right, immunoblot analysis of HCC827 cells showing activation of S6 upon knock-down of *NF2* and treatment with afatinib (100 nM), cetuximab (10 μg/ml) or the A+C combination. Lysates were probed with the indicated antibodies; p, phospho.

C. Growth inhibition of PC-9 cells after knockdown of *NF2* (left) or *TSC1* (right) in response to rapamycin. Viable cells were measured after 72 hours of treatment and plotted relative to untreated controls. Data are presented as the mean ± SE.

test whether combined inhibition of EGFR and mTOR could overcome resistance to A+C, we added rapamycin to the treatment regimen of *CCSP-rtTA*; *TetO-EGFR*$^{L858R+T790M}$ mice at the time of emergence of resistance to A+C (A+C+R). All 8 mice with LUADs resistant to A+C responded dramatically to the addition of rapamycin (**Figure 13B** and **Figure 13C**). In the mice with tumor burden lower than 600 mm^3 (6/8), tumor shrinkage was greaterthan 72% after one month of treatment with A+C+R (**Figure 13B** and **Table S4**). We also stained paraffin-embedded sections of A+C-resistant LUADs treated with rapamycin alone or in combination with A+C with antibodies against phospho-histone H3 and cleaved caspase 3 (**Figure S4**). Tumors treated with rapamycin alone were not growth inhibited whilst tumors treated with A+C+R exhibited both proliferation arrest and cell death. We further found that addition of rapamycin to A+C decreased pS6 in the LUADs (**Figure 13D**). All 4 of the A+C-resistant tumors treated with rapamycin alone showed activation of EGFR and Erbb2, as expected by the absence of EGFR-directed therapies (**Figure 13D**).

To evaluate the effect of concurrent EGFR and mTOR inhibition in xenografts, we injected 10^6 cells derived from the A+C-resistant xenografts 16T-10 and 24T-10 into immunodeficient mice. Upon the growth of A+C-resistant tumors, mice were divided into 3 groups (Figure 13E). One group was maintained on A+C for 4 weeks (n=7). The second group was treated with rapamycin alone (R, n=2) and the third group was treated with rapamycin in addition to A+C (A+C+R, n=5). Tumors in the A+C combination and rapamycin arms grew throughout the 4 weeks. In contrast, all of the tumors in mice that received A+C+R shrank (Figure 13F). Together these data indicate that inhibition of mTORC1 can re-sensitize cells to A+C treatment.

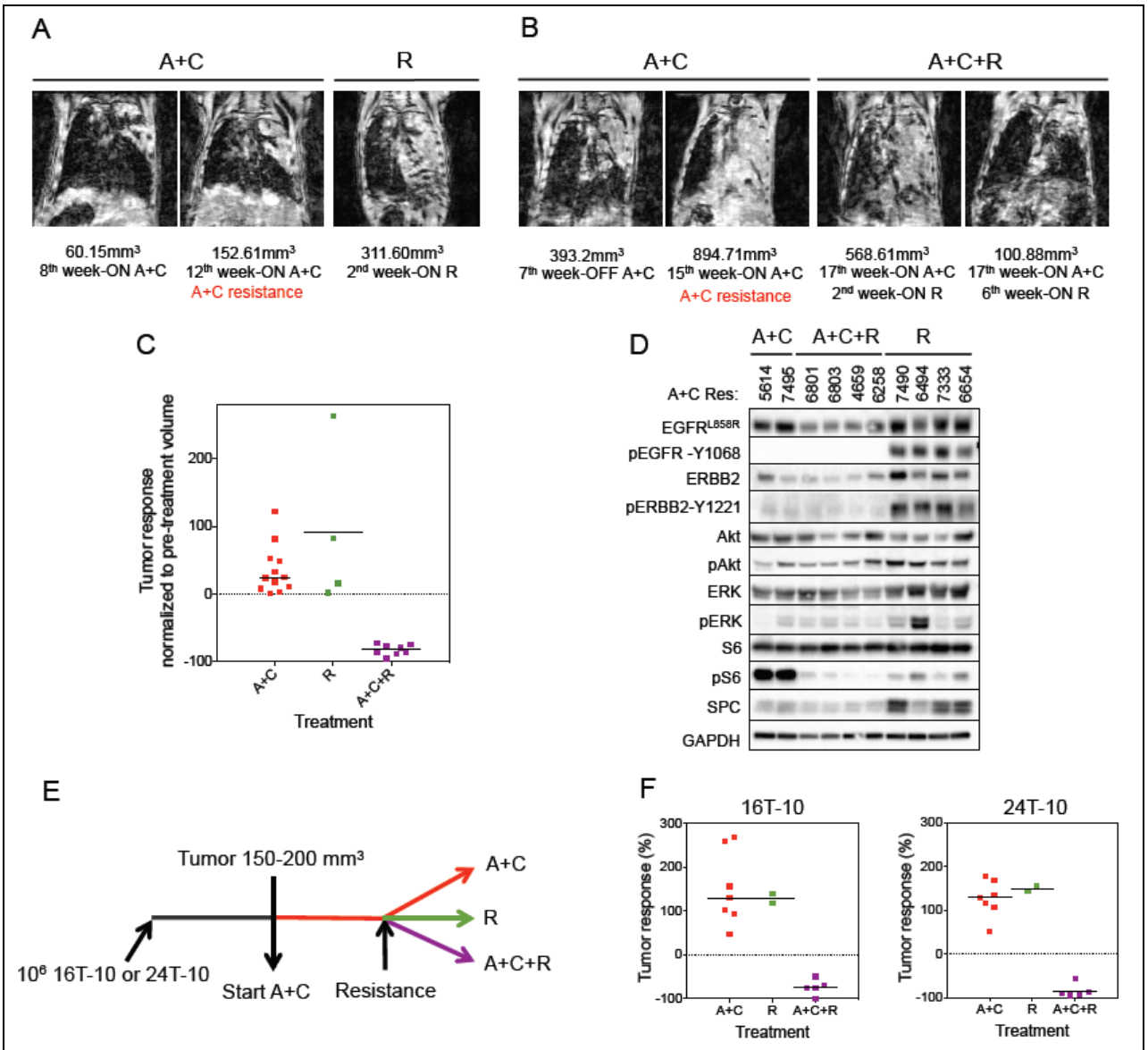

Figure 13. Tumors resistant to afatinib+cetuximab are sensitive to concurrent EGFR and mTOR Inhibition

A. Coronal MR images of *CCSP-rtTA*; *TetO-EGFRL858R+T790M* mouse lungs prior to and upon treatment with rapamycin (R) following the development of resistance to A+C as indicated in red. Tumor volume measurements are shown.

B. Coronal MR images of *CCSP-rtTA*; *TetO-EGFRL858R+T790M* mouse lungs prior to and upon treatment with rapamycin in combination with afatinib and cetuximab (A+C+R) following the development of resistance to A+C as indicated in red. Tumor volume measurements are shown.

C. Response of A+C-resistant LUADs from *CCSP-rtTA*; *TetO-EGFRL858R+T790M* mice to 4 weeks of treatment with Rapamycin alone (R) or in combination with afatinib and cetuximab (A+C+R). The increase in tumor volume in the presence of A+C before the randomization to R or A+C+R is shown on the left. Tumor volumes are plotted as the percentage of the tumor volume detected in the pre-cycle MRI. Median tumor

volume change to R is +52%; to A+C+R is -79%.
D. Immunoblotting analysis of LUADs resistant to A+C, following 4 weeks of treatment with rapamycin alone or in combination with afatinib and cetuximab. Lysates were probed with the indicated antibodies; p, phospho.
E. Strategy used to test the response of A+C-resistant xenograft tumors to concurrent EGFR and mTOR inhibition. 106 16T-10 or 24T-10 cells were injected s.c. into immunocompromised mice. When tumors reached a volume between 150-200 mm3, mice were treated with A+C (n=14). When resistance emerged, 2 mice were switched to rapamycin treatment (R, 2mg/Kg/day) and 5 mice received A+C+R. The rest of the mice were maintained on A+C. Mice were treated for 4 weeks from the randomization point.
F. Tumor response to A+C, rapamycin alone (R) or in combination (A+C+R) in xenografts. Data are plotted as percentage of tumor volume change from the randomization point. The median response to A+C+R was -75% in xenografts derived from 16T-10 cells (left) and -91% in xenografts derived from 24T-10 cells (right).

Discussion

We show that resistance to dual inhibition of *EGFR*$^{L858R+T790M}$ with A+C is due to activation of mTORC1 signaling in mouse models. Addition of drugs targeting mTOR re-sensitizes tumors to A+C treatment. Consistent with these findings, we have identified mutations in genes that affect the mTOR signaling cascade in A+C-resistant biopsy samples from two separate patients with *EGFR*-mutant lung cancer.

Previous studies have shown that the presence of active mTORC1 in untreated *EGFR* mutant tumors is a direct consequence of mutant EGFR signaling. Effective. therapies that target mutant EGFR lead to a decrease in mTORC1 signaling and consequent tumor regression. Indeed, in cell lines harboring EGFR TKI-sensitizing mutations (e.g. *EGFR*^{L858R}), EGFR blockade using TKIs leads to a decrease in pS6 equivalent to that observed with rapamycin, accompanied by a decrease in cell viability(Li, Shimamura et al. 2007). Further supporting the critical role of mTORC1 signaling in the maintenance of *EGFR*-mutant lung tumors, the combination of either afatinib or HKI-272 with rapamycin together was required to elicit regression of *EGFR*$^{L858R+T790M}$-induced tumors (Li, Shimamura et al. 2007; Li, Ambrogio et al. 2008). Our study shows that in addition to playing a role in the maintenance of *EGFR*-mutant lung tumors, the mTORC1 pathway also plays a role in resistance to EGFR-directed therapies, specifically following A+C treatment. First, pS6 is observed in cell lines, xenografts and GEM models of A+C-resistant *EGFR*-mutant lung cancer. Second, these tumors regress following the addition of rapamycin to A+C. These data highlight the importance of mTORC1 for the survival of lung cancer cells with *EGFR* mutations and

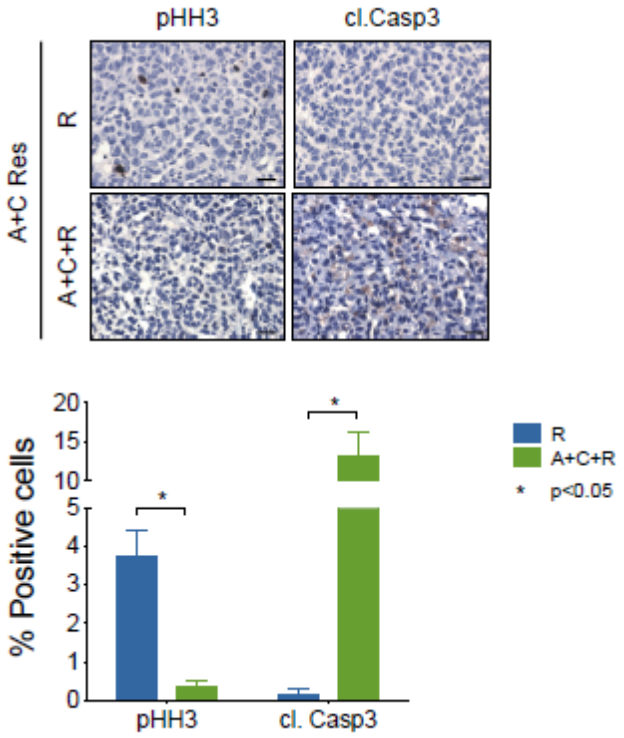

Figure 14 Rapamycin alone does not block proliferation in A+C-resistant lung adenocarcinomas, related to Figure 13.
Phospho-histone H3 (pHH3, left) and cleaved caspase 3 (cl.Casp3, right) staining of A+C-resistant adenocarcinoma sections from *CCSP-rtTA*; *TetO-EGFRL858R+T790M* mice treated with rapamycin alone (R, top) or in combination with A+C (A+C+R, bottom). Bars, 20 μm. Quantification of pHH3 and cl.Casp3 are shown in the bar graph below. Data are represented as the Mean ±SE.

suggest that as resistance emerges, tumors increasingly rely on mTORC1 activation to survive.

The presence of a *TSC1* frameshift mutation coupled with LOH at the same locus in a sample from a patient biopsied upon progression with A+C provides further evidence for dysregulation of the mTOR pathway as a mechanism of resistance to A+C. Indeed, strong pS6 staining was observed in tumor cells in this sample and disruption of *TSC1* in human *EGFR*-mutant lung cancer cell lines increased their viability in the presence ofEGFR TKIs. Unexpectedly, acquired *NF2* inactivating mutations were observed in A+C-resistant specimens from a separate patient on the same trial. Recent work has found that a downstream biochemical consequence of *NF2* loss is activation mTORC1 (Lopez-Lago, Okada et al. 2009). We show that the effects of both *TSC1* and *NF2* loss can be reversed in cells by treatment with a rapalog, suggesting that the presence of genomic changes in these genes indicates sensitivity to mTOR inhibition. Further studies to determine the prevalence of *NF2* and *TSC1* mutations in *EGFR*-mutant lung cancer are ongoing.

mTORC1 represents the output of several signaling pathways and external stimuli. In addition to genetic mechanisms like those described above that lead to its activation, it can be engaged through non-genetic mechanisms. Increased growth factor receptor signaling, through, for example, IGF1R, activates mTORC1 through the PI3K pathway. In this setting, one would expect to observe higher levels of phosphorylation of mTORC1 and AKT. Consistent with the possibility of similar mechanisms occurring in some of our models, we observed increased phosphorylation of AKT in the #16 xenograft-derived tumors and in the A+C-resistant GEMM tumors (**Figure 8D and**

Figure 9D). An increase in the levels of phosphorylation of IGF1R was indeed observed in the #16 derived tumors (data not shown) and may explain the increased mTORC1 signaling found in these tumors. These results also highlight how activation of mTORC1 can occur both via signals upstream and downstream of AKT. Moreover, our data from cell lines, xenografts and patient samples suggest that mTORC1 activation acts cell autonomously in the tumor cells to confer resistance. Whether this pathway is also activated in other cells in the tumor microenvironment cannot be excluded and is under further investigation.

Our findings suggest that patients with acquired resistance to A+C may benefit from drug combinations that include EGFR-directed therapies and mTOR inhibitors. In this regard, a phase IB trial of afatinib with the rapalog sirolimus in patients with *EGFR*-mutant lung cancer is currently ongoing. Phase III trials of A+C in patients with TKI-naïve and refractory *EGFR*-mutant lung cancer are planned. Inhibition of mTOR in this context may delay resistance. Due to concerns about the toxicity of this multi-drug combination, it will be important to use preclinical models to determine whether continuous or intermittent dosing of the mTOR inhibitor are equally effective at countering drug resistance. Moreover, rapalogs only partially block downstream functions of mTOR in contrast to mTORC1/2 kinase inhibitors. Investigation of these latter novel agents will be informative to determine their efficacy in the context of *EGFR*-mutant lung cancer. Finally, the recent development of mutant specific EGFR inhibitors that induce reduced toxicity due to less inhibition of wild-type EGFR may open the door to use of drug combinations including those of EGFR inhibitors with mTOR inhibitors (Walter, Sjin et al. 2013).

In summary, resistance to targeted therapies remains the major hurdle to the long-term success of EGFR-directed therapies. Our data in multiple preclinical models and human tumor samples show increased mTORC1 signaling after long-term treatment with A+C, identifying this node as a critical vulnerability of drug-resistant cells.

CHAPTER IV

AZD9291, an irreversible EGFR TKI, overcomes T790M-mediated resistance to EGFR inhibitors in lung cancer

Adapted From: Cross DA, Ashton SE, Ghiorghiu S, Eberlein C, Nebhan CA et al (2014). "AZD9291, an irreversible EGFR TKI, overcomes T790M-mediated resistance to EGFR inhibitors in lung cancer." *Cancer Discovery.*

Introduction

Gefitinib (Barker, Gibson et al. 2001) and erlotinib (Moyer, Barbacci et al. 1997) are reversible small molecule ATP analogues originally designed to inhibit the tyrosine kinase (TK) activity of wild-type epidermal growth factor receptor (EGFR). During their clinical development, these first-generation TK inhibitors (TKIs) were serendipitously found to be most effective in advanced non-small-cell lung cancer (NSCLC) patients whose tumors harbor recurrent somatic activating mutations occurring in the exons encoding the kinase domain of EGFR, i.e. small multi-nucleotide in-frame deletions in exon 19 (ex19del) and a point mutation in exon 21 leading to substitution of leucine for arginine at position 858 (L858R) (Lynch, Bell et al. 2004; Paez, Janne et al. 2004; Pao, Miller et al. 2004). Tumors with these activating mutations account for approximately 10-15% and 40% of NSCLC in Western and Asian populations respectively (Pao and Chmielecki 2010). Unfortunately, while patients with EGFR-mutant tumors typically

show good initial responses to first generation TKIs, most patients who respond to therapy ultimately develop disease progression after about 9-14 months of treatment (Mok, Wu et al. 2009; Maemondo, Inoue et al. 2010; Mitsudomi, Morita et al. 2010; Zhou, Wu et al. 2011; Rosell, Carcereny et al. 2012). Furthermore, these first generation TKIs are associated with side effects that include skin rash and diarrhea that are due to the inhibition of wild-type EGFR in skin and gastrointestinal organs (Burtness, Anadkat et al. 2009).

Preclinical modeling and analysis of tumor tissue obtained from patients after the development of disease progression has led to the identification of a number of mechanisms that mediate EGFR TKI resistance. Such genetic and other signaling aberrations that drive resistance mechanisms include HER2 amplification (Takezawa, Pirazzoli et al. 2012), MET amplification (Bean, Brennan et al. 2007; Engelman, Zejnullahu et al. 2007), PIK3CA mutation (Sequist, Waltman et al. 2011), BRAF mutation (Ohashi, Sequist et al. 2012), NF1 loss (de Bruin, Cowell et al. 2014) and potentially FGFR signaling (Ware, Marshall et al. 2010). In addition, resistant tumors have also been reported to show histologic changes such as small cell lung cancer (SCLC) transformation or epithelial mesenchymal transition (EMT) (Sequist, Waltman et al. 2011). However, it is now well established that acquisition of a second mutation in EGFR, resulting in substitution of threonine at the “gatekeeper” amino acid 790 to methionine (T790M) is the most common resistance mechanism and is detected in tumor cells from more than 50% of patients after disease progression (Kobayashi, Boggon et al. 2005; Pao, Miller et al. 2005). The T790M mutation is believed to render the receptor refractory to inhibition by these reversible EGFR TKIs through exerting

effects on both steric hindrance (Sos, Rode et al. 2010) and increased ATP affinity (Yun, Mengwasser et al. 2008).

Current targeted therapeutic strategies for patients with acquired resistance are limited. Second-generation irreversible EGFR TKIs such as afatinib (Li, Ambrogio et al. 2008) and dacomitinib (Engelman, Zejnullahu et al. 2007) are effective in untreated EGFR mutant lung cancer (Ramalingam, Blackhall et al. 2012; Sequist, Yang et al. 2013). However, as monotherapy, they have failed to overcome T790M-mediated resistance in patients (Miller, Hirsh et al. 2012; Katakami, Atagi et al. 2013), because concentrations at which these irreversible TKIs overcome T790M activity pre-clinically are not achievable in humans due to dose-limiting toxicity related to non-selective inhibition of wild-type EGFR (Eskens, Mom et al. 2008). Furthermore, these inhibitors can drive resistance through acquisition of T790M *in vitro* (Chmielecki, Foo et al. 2011) and in patients (Kim, Ko et al. 2012), providing supportive evidence that they have low potency against T790M. One regimen that showed potential activity is afatinib plus the anti-EGFR antibody, cetuximab, which induced a 32% unconfirmed response rate in a phase IB trial for patients with EGFR-mutant lung cancer and acquired resistance to erlotinib (Janjigian et al, *Can Disc* in press). However, this combination has substantial skin toxicity with 18% of patients reporting CTCAE grade 3 or higher rash.

Therefore, there remains a significant unmet need for an EGFR TKI agent that can more effectively target T790M tumors while sparing the activity of wild-type EGFR. This has led to the development of “third generation” EGFR TKIs that are designed to target T790M and EGFR TKI-sensitizing mutations more selectively than wild-type

EGFR. WZ4002 was the first such agent to be published (Zhou, Ercan et al. 2009), although it has not progressed to clinical trials. A second agent closely related to the WZ4002 series, CO- 1686, has been recently reported (Walter, Sjin et al. 2013), and is currently in early Phase II clinical trials. HM61713 is another “third generation” agent that is currently in early Phase I trials. Here, we describe identification, characterization, and early clinical development of AZD9291, a novel, irreversible, EGFR TKI with selectivity against mutant versus wild-type forms of EGFR. AZD9291 is a mono-anilino-pyrimidine compound that is structurally and pharmacologically distinct from all other TKIs including CO-1686 and WZ4002.

Results

AZD9291 is a mutant-selective, irreversible inhibitor of EGFR kinase activity

AstraZeneca developed a novel series of irreversible, small-molecule inhibitors to target the sensitizing and T790M resistant mutant forms of the EGFR tyrosine kinase with selectivity over the wild-type form of the receptor. These compounds bind to the EGFR kinase irreversibly by targeting the cysteine-797 residue in the ATP binding site via covalent bond formation (Ward, Anderton et al. 2013)**,** as depicted in the modeling structure for AZD9291 **(Figure 15A)**. Further work on this chemotype allowed additional structure activity relationships (SAR) to be discerned that enabled target potency to be increased without driving increased lipophilicity, thus maintaining favorable drug-like properties. Continued medicinal chemistry efforts achieved further improvements

A

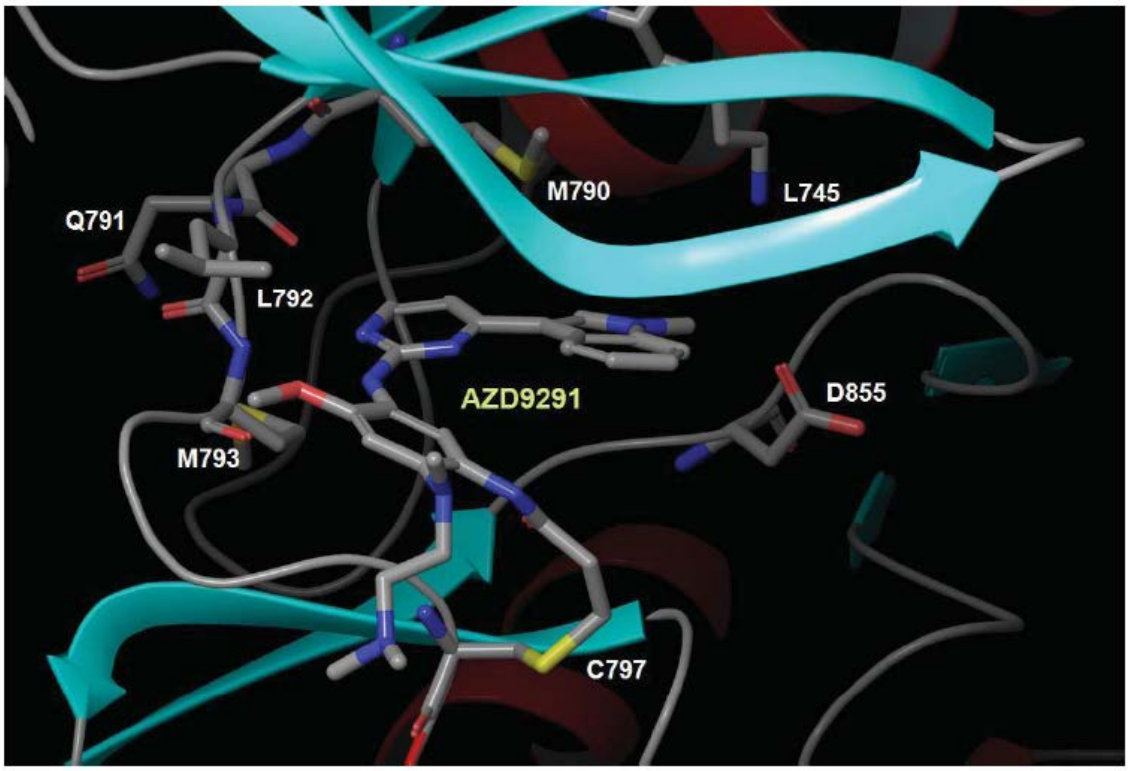

B

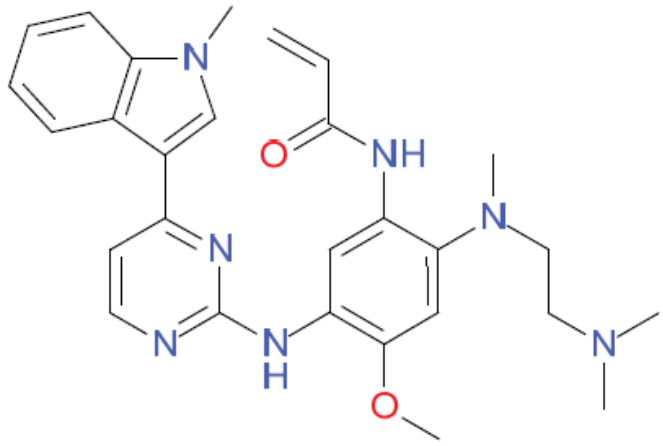

Figure 15. AZD9291 binding mode and structure
A. Structural model showing the covalent mode of binding of AZD9291 to EGFR T790M via Cys-797. Shows pyrimidine core forming two hydrogen bonds to the hinge region (Met-793), orientation of the indole group adjacent to the gatekeeper residue, the amine moiety positioned in the solvent channel and the covalent bond formed to Cys-797 via the acrylamide group of AZD9291.
B. Chemical structure of AZD9291.

including increased kinase selectivity, ultimately arriving at the mono-anilino-pyrimidine AZD9291 **(Figure 15B)**. Mass spectrometry of chymotrypsin digests confirmed that AZD9291 can covalently modify recombinant EGFR (L858R/T790M) at the target cysteine 797 amino acid.

AZD9291 has a distinct chemical structure from the other third-generation TKIs, WZ4002 (Zhou, Ercan et al. 2009) and CO-1686 (Walter, Sjin et al. 2013). Whilst the former two compounds share a number of common structural features (e.g. positioning of the electrophilic functionality that undergoes reaction with a conserved cysteine residue present in EGFR (Cys 797), heteroatom-linked pyrimidine 4-substituents, and presence of a pyrimidine 5- substituent), AZD9291 is architecturally unique. Amongst other differences, the electrophilic functionality resides on the pyrimidine C-2 substituent ring, the pyrimidine 4-substituent is C-linked and heterocyclic, and the pyrimidine 5-position is devoid of substitution.

In EGFR recombinant enzyme assays (Millipore), AZD9291 showed an apparent IC_{50} of 12 nM against L858R and 1 nM against L858R/T790M; these are called apparent since the amount of active enzyme changes over time and thus IC_{50} is time-dependent for irreversible agents. The drug exhibited nearly 200 times greater potency against L858R/T790M than wild-type EGFR, consistent with the design goal of a mutant EGFR selective agent in comparison to early generation TKIs. Subsequent murine *in vivo* studies revealed that AZD9291 was metabolized to produce at least two circulating metabolite species, AZ5104 and AZ7550. In biochemical assays, AZ7550 had a comparable potency and selectivity profile to the parent. In contrast, although AZ5104 exhibited the same overall profile, it was more potent against mutant and wild-type

EGFR forms, thus demonstrating a smaller selectivity margin compared to parent (data not shown).

To explore a broader kinome selectivity profile, we tested AZD9291 and metabolites at 1 μM across approximately 280 other kinases available on a commercial biochemical kinome panel (Millipore). AZD9291 showed minimal off-target kinase activity, with only a limited number of additional kinases showing greater than 60% inhibition at 1 μM and moderate IC_{50} potencies such as ErbB2/4, ACK1, ALK, BLK, BRK, MLK1 and MNK2. The active metabolites displayed a similar secondary target profile as parent. Given that AZD9291 makes a covalent bond with Cys797 in EGFR as described, we were specifically interested to explore potency in other kinases that have a cysteine residue in the analogous kinase domain position. Of the nine other kinases present within the human kinome with the analogous Cys797 to EGFR, AZD9291 showed significant activity only in a biochemical assay against ErbB2, ErbB4 and BLK**,** supporting the overall high degree of selectivity that AZD9291 confers**.**

Like the T790M double-mutant EGFR receptor, the insulin-like growth factor receptor (IGF-1R) and insulin receptor (IR) also have a methionine gatekeeper in their kinase domains. We considered it important to develop selectivity against these kinases to minimize potential dose limiting toxicities related to hyperglycemia. Using a commercially available cellular IGF-1R phosphorylation assay as a surrogate, AZD9291 and the metabolite AZ5104 did not exhibit significant activity towards this receptor family. Moreover, a single oral dose of 200 mg/kg of AZD9291 in rats did not cause a significant change in blood glucose or insulin levels over a 24 hour period, consistent with lack of IGF-1R activity (data not shown).

Finally, we evaluated cellular potency against HER2 (ErbB2), using three different cellular approaches: surrogate kinase assays involving expression of wild-type HER2 in HEK293 cells, PC-9 cells (ex19del) engineered to overexpress HER2 (Takezawa, Pirazzoli et al. 2012) and biochemical reconstitution studies in HEK293 cells involving intracellular domain constructs encoding L858R/T790M, wild-type EGFR, or wild-type HER2 (Red Brewer, Yun et al. 2013). Consistently, treatment of cells with AZD9291 inhibited phosphorylation of HER2 at moderate potency levels. However, consistent with its greater wild-type EGFR potency, the AZ5104 metabolite showed more potency than AZD9291 against phospho-HER2.

AZD9291 potently and selectively targets mutant EGFR cell lines in vitro

We compared AZD9291 with other early generation EGFR TKIs in EGFR phosphorylation and cell death (Sytox) assays using a number of tumor cell lines harboring either wild-type or different forms of mutant EGFR. Compared with other EGFR inhibitors of both first (gefitinib and erlotinib) and second generation (afatinib and dacomitinib), AZD9291 demonstrated a unique third generation TKI profile. AZD9291 showed similar potency to early generation TKIs in inhibiting EGFR phosphorylation in EGFR cells harboring sensitizing EGFR mutants including PC-9 (ex19del), H3255 (L858R) and H1650 (ex19del) **(Figure 16A),** with mean IC_{50} values ranging from 13 to 54nM for AZD9291. AZD9291 also potently inhibited phosphorylation of EGFR in T790M mutant cell lines (H1975 (L858R/T790M), PC-9VanR (ex19del/T790M) **(Figure 16A)**, with mean IC_{50} potency less than 15 nM. First generation reversible TKIs were

A

	H1975 (L858R/ T790M)	PC-9 VanR (ex19del/ T790M)	PC-9 (ex19del)	H3255 (L858R)	H1650 (ex19del)	LoVo (WT)	A431 (WT)	NCI-H2073 (WT)
AZD9291	15 (10, 20)	6 (3, 13)	17 (13, 22)	60, 49	14, 12	480 (320, 720)	2376, 1193	1865 (872, 3988)
Dacomitinib	40 (24, 65)	6 (2, 17)	0.7 (0.5, 1)	1.2, 1.3	0.04, 0.06	12 (8, 17)	51, 22	26 (7, 99)
Afatinib	22 (15, 31)	3 (2, 6)	0.6 (0.5, 0.8)	1, 0.8	0.6, 3	15 (10, 24)	27, 40	25 (5, 129)
Gefitinib	3102 (1603, 6001)	741 (484, 1136)	7 (5, 11)	11, 12	16, 19	59 (42, 82)	60, 88	61 (34, 110)
Erlotinib	6073 (3634, 10150)	1262 (588, 2711)	6 (4, 7)	8, 11	5, 8	91 (53, 156)	244, 260	108 (52, 223)

B

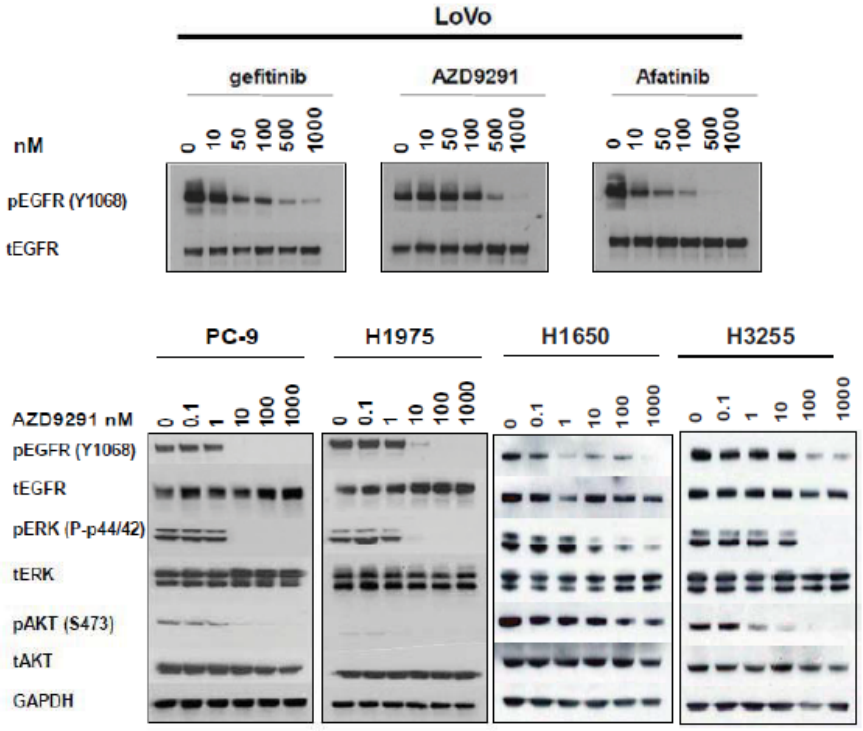

Figure 16. Effect of AZD9291 on EGFR phosphorylation *in vitro*
A. In comparison to early generation TKIs, AZD9291 inhibits EGFR phosphorylation across cell lines
harboring sensitising (PC-9, H3255, H1650) or T790M resistance (H1975, PC-9VanR) mutations, whilst having less activity against wild-type EGFR phosphorylation (LOVO, A431, H2073). Apparent geomean IC50 (nM) values quantified in cell extracts after 2 h compound treatment using a phospho-EGFR ELISA from at least two separate experiments (expressed with 95% confidence intervals where n>3, or individual IC50 values where n=2).

B. AZD9291 inhibits EGFR phosphorylation and downstream signaling pathways across representative mutant EGFR lines (PC-9, H1975, H1650, H3255), whilst having less activity against EGFR phosphorylation in the LOVO wild-type EGFR cell line compared to early generation TKIs, after 6 h treatment. The data is representative of at least two separate experiments.

ineffective at inhibiting phosphorylation of T790M EGFR **(Figure 16A)**. The second generation irreversible TKIs, afatinib and dacomitinib, showed activity against T790MEGFR *in vitro*, although this activity is may not be achievable at exposures that can be reached in the clinic. AZD9291 was less potent at inhibiting phosphorylation of EGFR in wild-type cell lines (A431, LOVO, NCI-H2073), with mean IC50 range of 480 to 1865 nM **(Figure 16A)**. This is in clear contrast to the early generation TKIs which all potently inhibited EGFR phosphorylation in wild-type lines with similar potency to sensitizing-mutant EGFR **(Figure 16A)**. Similar results were found when phosphorylation of EGFR and downstream signaling was determined by immunoblot analysis of lysates from PC-9, H1975, LOVO, H1650 and H3255 lines **(Figure 16B)**. Consistently, results showed that AZD9291 more potently inhibited phospho-EGFR and downstream signaling substrates (pAKT, pERK) in cells with mutant EGFR compared with wild-type **(Figure 16B),** although H1650 cells retained higher phospho-AKT levels due to loss of PTEN (Sos, Rode et al. 2010).

As previously described, AZD9291 has active circulating metabolites, so we also profiled their activity against EGFR. Consistent with presented biochemical data, AZ7550 exhibited very similar potency and profile to AZD9291 against mutant and wildtype cell lines tested, whilst AZ5104 harbored somewhat greater potency against ex19del (2 nM in PC-9), T790M (2 nM in H1975) and wild-type EGFR (33 nM in LOVO) cell lines. Therefore, AZ5104 exhibited a reduced selectivity margin against wild-type EGFR when compared to AZD9291. However, taken together, this mechanistic data confirmed the third generation TKI properties of AZD9291 compared to earlier

generation agents: equivalent activity against sensitizing mutant EGFR, superior activity towards T790M and increased selectivity margin against wild-type EGFR.

We then explored how the pharmacological activity against mutant and wild-type EGFR signaling translated into cell proliferation effects using a Sytox live/dead cell phenotype endpoint. In line with the phosphorylation data, AZD9291 showed high levels of phenotype potency in both sensitizing-mutant (mean IC_{50} of 8 nM in PC-9) and T790M (mean IC_{50} of 11 and 40 nM in H1975 and PC-9VanR respectively) EGFR cell lines, whilst having much less activity towards wild-type EGFR (mean IC_{50} of 650 and 461 nM in Calu3 and H2073 respectively) **(Figure 17A)**. Again, this contrasted to second generation TKIs, afatinib and dacomitinib, which showed much less activity against T790M lines and were associated with much greater potency towards wild-type EGFR **(Figure 17A).** To confirm these results, we determined the efficacy of AZD9291 in an independent laboratory against a panel of isogenic pairs of drug-sensitive /resistant EGFR-mutant lung cancer cell lines (Chmielecki, Foo et al. 2011). Parental EGFR-mutant lines (PC-9, H3255, HCC827, HCC4006, 11-18) were sensitive to AZD9291 as well as erlotinib, afatinib, and AZD8931 (a reversible equipotent inhibitor of EGFR, HER2 and HER3 signaling (Mu, Klinowska et al. 2014)) **(Figure 17B)**. However, only AZD9291 displayed low nanomolar activity against the lines harboring EGFR T790M (H1975, HCC827/ER1, PC-9/BRc1 and H3255/XLR) **(Figure 17B)**. Interestingly, AZD9291 was not effective against lines harboring non-T790M resistance such as 11-18/ER (NRAS), HCC827/ER2 (MET amplification), and HCC4006/ER (EMT) (Ohashi, Sequist et al. 2012) **Figure 17B)**. In a separate large cell panel proliferation profiling study, AZD9291 was also poorly active *in vitro* (IC_{50} ~1 μM) against both NSCLC NCI-

A

	H1975 (T790M/L858R)	PC-9 VanR (ex19del/T790M)	PC-9 (ex19del)	Calu 3 (WT)	NCI-H2073 (WT)
AZD9291	11 (6,19)	40 (30, 54)	8 (7, 9)	650 (457, 924)	461 (230, 924)
Dacomitinib	335 (265, 424)	531 (465, 607)	0.4 (0.3, 1)	65 (37, 116)	54 (ND)
Afatinib	483 (403, 579)	679 (532, 868)	0.8 (0.7, 0.9)	71 (35, 144)	30 (9, 99)
Gefitinib	6962 (6304, 7688)	4232 (1998, 8965)	23 (20, 25)	1933 (1299, 2876)	200 (41, 974)
Erlotinib	6165 (5392, 7050)	5778 (4766, 7029)	28 (22, 36)	4101 (2732, 6156)	692 (193, 2478)

B

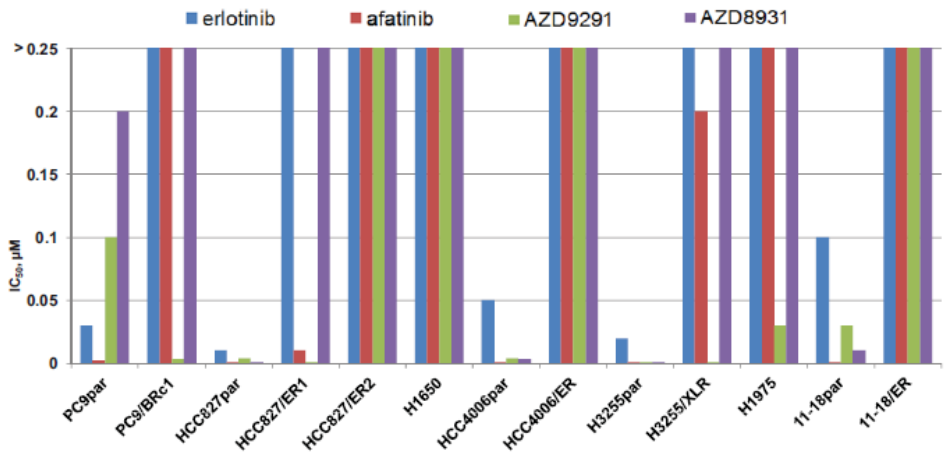

C

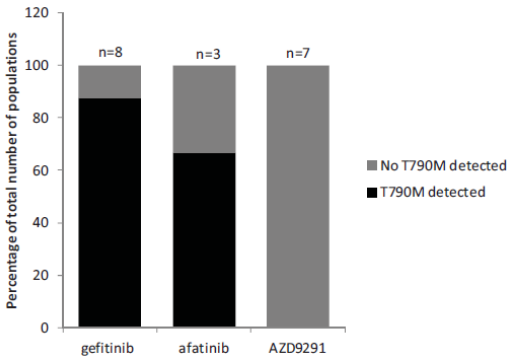

Figure 17. Additional characteristics of AZD9291 *in vitro*

A. AZD9291 demonstrates greater inhibition of viability against mutant EGFR cell lines compared to wild-type, as assessed using a Sytox Green live/dead assay measured after 3 days treatment. The data represents the geomean IC_{50} nM value from at least two separate experiments (expressed with 95% confidence intervals where n>3).

B. Sensitivity of isogenic pairs of EGFR mutant drug-sensitive and –resistant lung cancer cell lines (PC-9, ex19del; PC-9/BRc1, ex19del/T790M; HCC827, ex19del;

HCC827/ER1, ex19del/T790M; HCC827/ER2, ex19del/METamplification; H1650, ex19del/PTEN loss; HCC4006, ex19del; HCC4006/ER, EMT (epithelial mesenchymal transition); H3255, L858R; H3255/XLR, L858R/T790M; H1975, L858R/T790M; 11-18, L858R; 11-18/ER, L858R/NRAS) to AZD9291, erlotinib, and afatinib. IC_{50}s (μM) were based on data obtained from growth inhibition assays measured with CellTiter Blue (Promega) and calculated using Excel (Microsoft). Data represent n=3 replicates for each cell line/drug condition.

C. T790M mutation was detected in multiple independent populations of PC-9 cells with acquired resistance to gefitinib or afatinib, but not in populations resistant to AZD9291.

H820 and EBC-1 cell lines that harbor MET amplification and mutant EGFR (data not shown). Consistent with phospho-EGFR data, the metabolite AZ5104 again demonstrated much greater potency across cell lines in a phenotypic assay, whereas AZ7550 was broadly similar, with the same overall profile maintained.

Due to their low activity against T790M EGFR, it has been suggested that treatment with early generation TKIs can induce the growth selection of tumor cells harboring EGFRm+/T790M leading to TKI resistant populations both pre-clinically and clinically (Chmielecki, Foo et al. 2011). We therefore hypothesized that such resistance would not occur upon treatment with AZD9291, given its superior potency against T790M. Indeed, whilst chronic treatment with gefitinib or afatinib commonly caused acquired resistance in PC-9 cells *in vitro* through gain of T790M, acquired resistance to AZD9291 through T790M was not observed **(Figure 17C)**. Studies are ongoing to characterize the T790M independent mechanisms of acquired resistance to AZD9291 (Eberlein et al.,manuscript in preparation).

Activity of AZD9291 against rare EGFR and HER2 mutants in vitro

In addition to activity against the common activating/sensitizing EGFR mutants, we assessed the potency of AZD9291 against other rarer EGFR mutants associated with sensitivity or resistance to first-generation EGFR TKIs. 293 cells were transfected with cDNAs encoding EGFR G719S, L861Q, an exon 20 insertion (H773-V774HVdup), exon 19 insertion (I744-K745insKIPVAI) or an EGFR variant III (EGFRvIII; found in brain glioblastomas (Wong, Ruppert et al. 1992)), and treated with increasing concentrations of either erlotinib, afatinib, AZD9291, the metabolite AZ5104, or AZD8931 for 6 hours. Immunoblotting was performed on corresponding lysates using

antibodies against phospho-EGFR (Y1173) and total EGFR. All EGFR TKIs were effective against EGFR L861Q, G719S, and the exon 19 insertion, although AZD9291 was somewhat less potent compared with the AZ5104 metabolite against these mutant EGFR forms. None of the TKIs was effective against the exon 20 insertion mutation. For the EGFRvIII mutant, AZD9291 demonstrated lower potency compared to afatinib and AZD8931. AZ5104, however displayed a higher level of activity. These data are consistent with the kinase activity of the vIII mutant being similar to that of their wild-type EGFR.

We similarly explored activity against HER2 mutations found in NSCLC. Compared to afatinib and AZ5104, AZD9291 exhibited moderate potency against H1781 cells, which harbor a VC insertion at G776 in exon 20 of *HER2* (Shigematsu, Takahashi et al. 2005), with an IC_{50} of 80 nM. However, AZD9291 was more effective at inhibiting growth of these cells than erlotinib. The effect of various TKIs on HER2-associated signaling in H1781 cells was consistent with these results. Similar activity was observed in 293 cell transfectants harboring the most common HER2 mutant in NSCLC (exon20 YVMA 776-779ins) (Wang, Narasanna et al. 2006) (data not shown). Thus, in patients, AZD9291 and its metabolite AZ5104, may also be able to target HER2 in tumors, depending on the clinical exposures that are achieved.

AZD9291 causes profound and sustained regression in mutant EGFR in vivo xenograft models

AZD9291 demonstrated good bioavailability, was widely distributed in tissues, and had moderate clearance resulting in a half-life of around 3 hours after oral dosing in the mouse. The circulating active metabolites in plasma each had a similar half-life, and

the total exposure levels (AUC) were approximately 68 and 33% compared to the parent compound for AZ7550 and AZ5104, respectively.

To explore *in vivo* activity of AZD9291, we administered the drug as monotherapy against various mutant EGFR xenografts representing clinical NSCLC settings. Once daily dosing of AZD9291 induced significant dose-dependent regression in both PC-9 (ex19del) and H1975 (L858R/T790M) tumor xenograft models, with tumor shrinkage observed at doses as low as 2.5mg/kg/day in both models after 14 days **(Figure 18A, B)**. Similar tumor shrinkage was seen after administration of 5 mg/kg/day AZD9291 in H3255 (L858R) and PC-9VanR (ex19 del/ T790M) xenografts after 14 days. These studies showed that AZD9291 can induce profound shrinkage at low doses against both EGFR drug-sensitizing and T790M-resistant EGFR mutant disease models.

We next explored the durability of tumor shrinkage. Chronic long term daily oral dosing of AZD9291 resulted in complete and durable macroscopic responses of both PC-9 **(Figure 18C)** and H1975 xenografts **(Figure 18D)**. For PC-9 cells, no visible tumors were evident following 40 daily doses with 5 mg/kg of AZD9291 in 8 of 8 tumors, and this complete response was sustained out to 200 days when the study was terminated (data not shown). As a comparison, gefitinib at 6.25 mg/kg/day, a clinically representative dose, induced less tumor regression, and tumors began to re-grow after approximately 90 days. In H1975 xenografts, 5 mg/kg/day AZD9291 resulted in

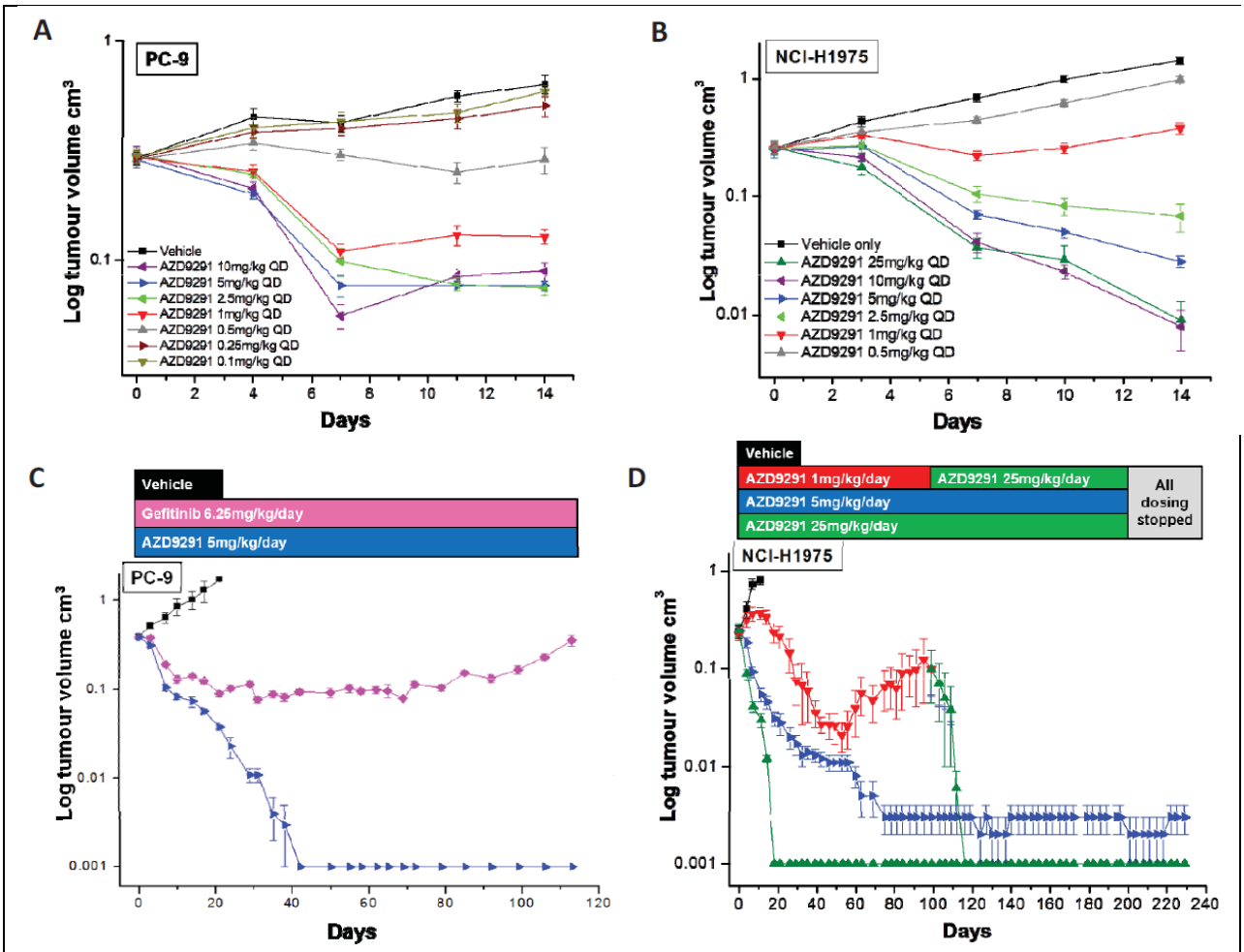

Figure 18. *In vivo* anti-tumor efficacy of AZD9291 in subcutaneous xenograft models of EGFR-TKI sensitising and T790M resistant lung cancer

A., PC-9 (ex19del) xenograft following 14 days of daily treatment (n=6 or 8 animals depending on treatment group).

B. H1975 (L858R/T790M) xenograft following 14 days of daily treatment (n=6 or 8 animals depending on treatment group).

C. PC-9 following chronic daily oral dosing of 5mg/kg AZD9291 (n=8) or 6.25 mg/kg gefitinib (n=11)

D. H1975 following chronic daily oral dosing of 1, 5 or 25 mg/kg AZD9291 (n=10 or 12 animals depending on dose group). Data are plotted as mean standard error.

complete responses in 10 of 12 tumors. Re-growth was observed after approximately 50 days treatment with 1 mg/kg/day, but an increased dose of 25 mg/kg/day AZD9291 re-induced tumor regression possibly suggesting re-growth was still driven by T790M EGFR. No visible

tumors were evident after 20 days dosing of 25 mg/kg/day AZD9291 in the H1975 xenograft model. Moreover, the complete responses were maintained for the duration of the study period with no evidence of tumor progression during 200 days of treatment. No growth was observed for an additional 30 days after treatment was stopped. AZD9291 daily dosing was well tolerated in the animals with minimal body weight loss, (less than 5% of starting body weight) even after dosing for 200 days Similar long term dosing studies were performed in the H3255 model, with 5 mg/kg/day AZD9291 causing non-measurable tumors in all 8 dosed mice by day 53. By contrast, only one mouse treated with 6.25 mg/kg gefitinib achieved non-measurable tumor status (data not shown).

To explore comparative efficacy against wild-type EGFR, AZD9291 was tested in A431 xenografts. These cells are used as a model for wild-type EGFR activity, but they are highly dependent on amplified wild-type EGFR and therefore are unlikely to reflect normal tissue EGFR pharmacology/physiology (Merlino, Xu et al. 1984). AZD9291 did induce some moderate tumor growth inhibition at 5 mg/kg/day, suggesting AZD9291 or associated metabolites are not entirely inactive against wildtype EGFR in this model. By contrast, this same 5 mg/kg/day dose level was sufficient to induce profound and sustained tumor shrinkage in both H1975 and PC-9 mutant EGFR tumor xenograft

models **(Figure 18A-B)**, consistent with AZD9291 having a significant selectivity margin over wild-type EGFR.

AZD9291 causes profound and sustained regression in mutant EGFR in vivo transgenic tumor models

We further examined tumor responses in previously generated mouse tumor models that develop lung adenocarcinomas driven by $EGFR^{L858R}$ (Politi, Zakowski et al. 2006) or $EGFR^{L858R\ +T790M}$ (Regales, Balak et al. 2007). These models employ a tetracycline–inducible (tet-inducible) system, involving bitransgenic animals. One transgene carries a tet transactivator in lung epithelia (i.e., Clara cell secretory protein – reverse tetracycline transactivator [CCSPrtTA], herein referred to as “C” mice). The 2 relevant strains are referred to as C/L858R and C/L+T, respectively. As expected, tumors harboring $EGFR^{L858R}$ were sensitive to erlotinib, while tumors expressing $EGFR^{L858R\ +\ T790M}$ were resistant (Regales, Balak et al. 2007). Here, we treated tumor-bearing mice with AZD9291 (5 mg/kg/day), afatinib (7.5 mg/kg/day), or vehicle control for one to two weeks. Within days of treatment, 5 of 5 C/L858R mice displayed nearly 80% reduction in tumor volume by magnetic resonance imaging MRI (see Methods and (Regales, Gong et al. 2009)) after therapy with both afatinib or AZD9291, while 5 of 5 mice treated with vehicle showed tumor growth **(Figure 19A (top) and Figure 19B)**. Upon histological examination, only vehicle-treated mice showed viable tumor **(Figure 19B)**. By contrast, in C/L+T animals, only AZD9291 treatment induced significant tumor shrinkage **(Figure 19A (middle & bottom) and Figure 19C)**, while both vehicle- and afatinib-treated mice showed viable tumor **(Figure 19C)**. The difference in tumor responses was more pronounced after 2 weeks of treatment **(Figure 19A (bottom))**.

Furthermore, preliminary data in a single mouse with tumor driven by an ex19del mutant alone (Politi, Zakowski et al. 2006) also responded rapidly to AZD9291 The metabolite, AZ5104 (5 mg/kg/day), was also effective in shrinking tumors in both C/L858R and C/L+T mice (data not shown).

Pharmacodynamic confirmation of target inhibition by AZD9291

To confirm on-target and pathway activity of AZD9291, we examined tumor tissues from the H1975 xenograft and L858R/T790M transgenic model after drug treatment. Mice bearing H1975 xenografts were given a single dose of AZD9291 (5 mg/kg) and tumors were harvested 1, 6, 16, 24, and 30 hours later. Sections from formalin-fixed paraffin-embedded tumors were then stained for the phosphorylated forms of-EGFR (Tyr1173), ERK (Thr202/Tyr204), S6 (Ser235/236), and PRAS40 (Thr246). In the H1975 model, AZD9291 treatment strongly inhibited both phospho-EGFR and downstream signaling pathways after 6 hours **(Figure 20A)**. Although in mice, the pharmacokinetic half-life of AZD9291 is only ~3 hours, phospho-EGFR staining remained significantly diminished even after the 30 hour time point, consistent with its expected irreversible mode of action. Interestingly, although downstream signaling molecules similarly showed maximal inhibition after 6 hours, in contrast to phospho-EGFR, they displayed more transient inhibition **(Figure 20A)**.

In the transgenic model, we similarly observed target inhibition after 5mg/kg dosing of AZD9291 via immunohistochemical staining of sections for phospho-EGFR and downstream markers **(Figure 20B)** or immunoblotting of lysates **(Figure 20C)** from treated tumors.

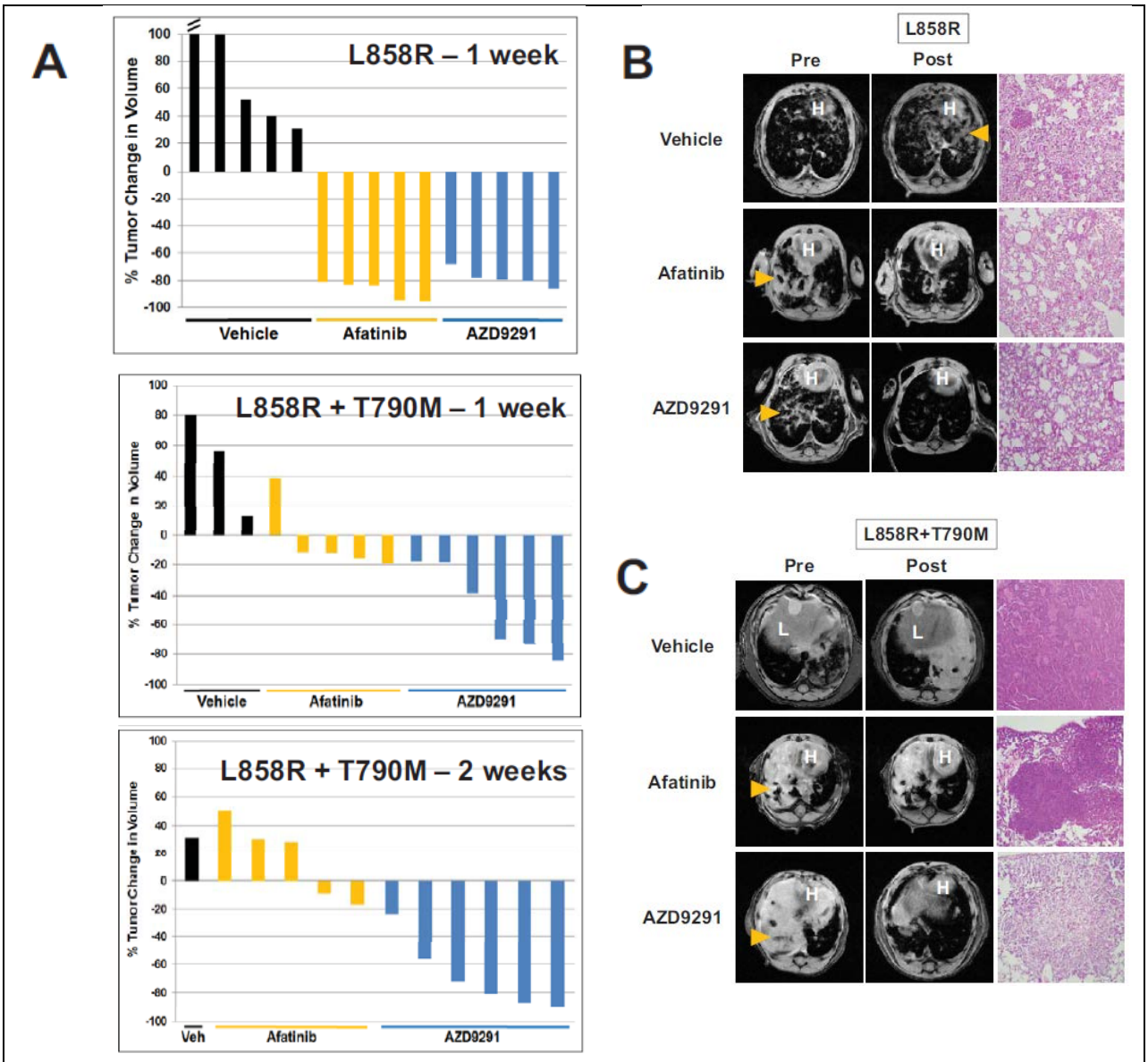

Figure 19. AZD9291 induces significant and sustained tumor regression in transgenic models of EGFR-TKI sensitizing (C/L858R) and T790M resistant (C/L+T) lung cancer

A. Percent change in radiographic tumor volume from baseline by treatment for individual lung tumor-bearing C/L858R (top) and C/L+T (middle, bottom) animals with vehicle, afatinib (7.5 mg/kg/day), or AZD9291 (5 mg/kg/day).

B and C. Representative MRI images and H&E staining (original magnification, ×40) of lungs from tumor-bearing animals (**B.** C/L858R and **C.** C/L+T) pre and post treatment with vehicle, afatinib, or AZD9291 for 1 week. H – heart; L – liver; arrow denotes tumor.

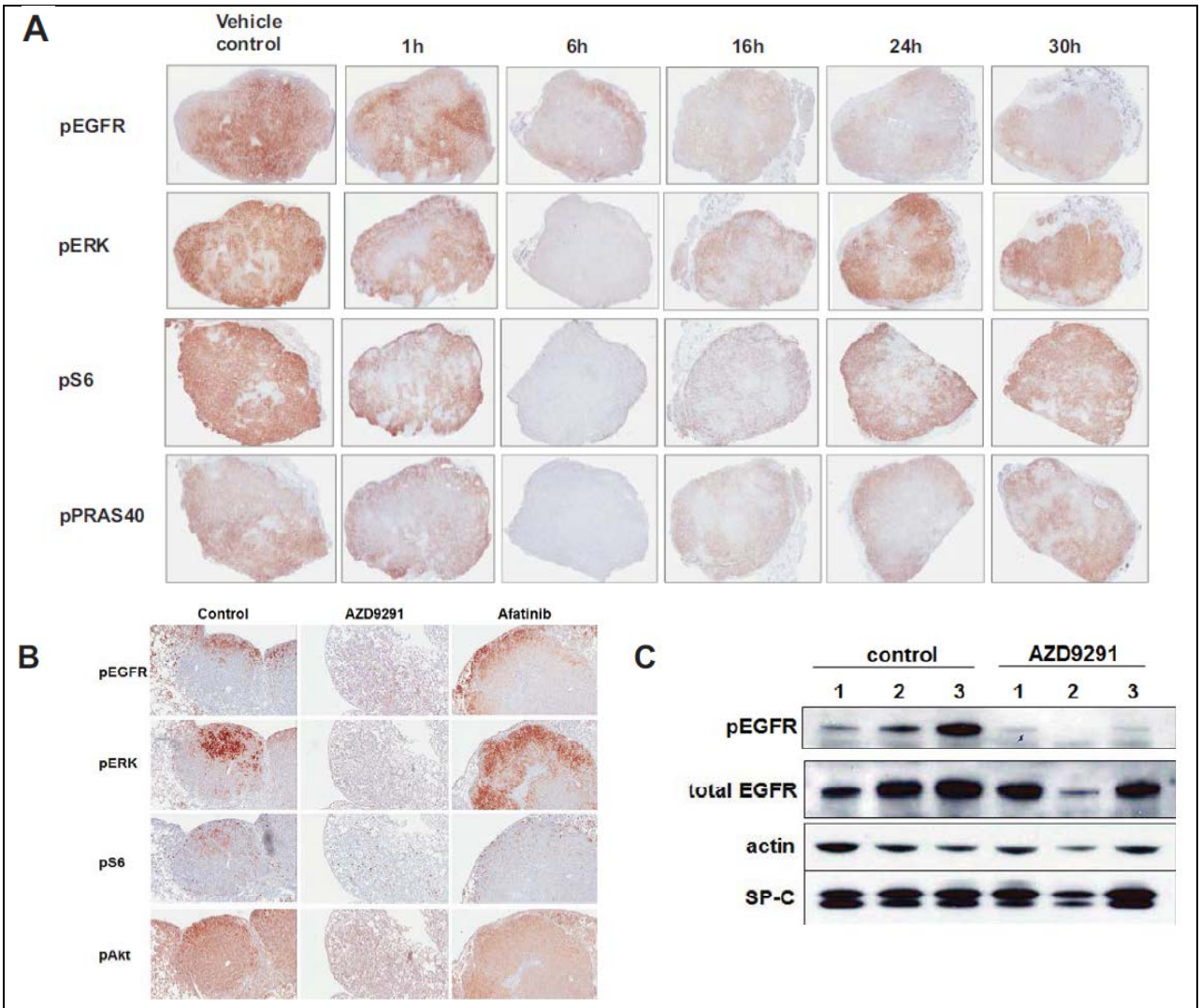

Figure 20. AZD9291 inhibits EGFR phosphorylation and downstream signallng in murine models of EGFR T790M resistant lung cancer

A. Subcutaneous H1975 (L858R/T790M) xenografts, treated with a single 5 mg/kg dose of AZD9291 for the indicated times, were examined for phospho-EGFR, -ERK, -S6, and -PRAS40 status by immunohistochemistry. Representative images were taken from scans at 20x magnification and then size adjusted to fill the screen.

B. Lungs from representative transgenic mice treated with control, AZD9291, or afatinib were harvested 6 hours after dose administration. Formalin-fixed paraffin-embedded sections were stained with the indicated antibodies. Representative images were taken from Aperio scans at 100x magnification.

C. Lungs were harvested from either untreated tumor-bearing transgenic mice (as confirmed by MRI) (control) or from tumor-bearing mice 8 hours after a single treatment with AZD9291 5 mg/kg. Corresponding lysates from individual animals were immunoblotted with the indicated antibodies. Anti-SP-C (surfactant protein C) antibody was used as a surrogate marker for tumor burden, as tumors express the protein.

Proof of principle clinical activity of AZD9291 in patients with acquired resistance to EGFR TKIs

The mesylate salt of AZD9291 is currently in a first-in-human phase I dose escalation clinical trial (AURA; NCT01802632; AstraZeneca) in patients with advanced EGFR-mutant NSCLC who had disease progression following treatment with any EGFR TKI (including gefitinib or erlotinib). As proof-of-principle, here we present preliminary results of the first two patients in the study with confirmed radiographic responses (as per RECIST 1.1 (Eisenhauer, Therasse et al. 2009) treated at the lowest dose cohort (20 mg once daily) **(Figure 21)**. Both patients' tumors harbored drug sensitive EGFR mutations in addition to documented T790M mutations (according to local testing results). Consistent with AZD9291 being less active against wild-type EGFR, in these two cases there were no rash events and only one reported CTCAE Grade 1 diarrhea. Preliminary clinical pharmacokinetic analysis indicates that AZD9291, AZ5104 and AZ7550 have a half-life of at least 50 hours, longer than would be predicted from the preclinical data, which results in a desirable flat PK profile after multiple once daily dosing **(Figure 21A)**. Further Phase 1 clinical data for this study will be submitted for publication at a later date.

The first patient was a 57-year old East Asian female patient from South Korea diagnosed with Stage IV EGFR mutant (ex 19 del) NSCLC in May 2011. The patient had disease progression following 2 cycles of gemcitabine plus carboplatin combination chemotherapy. The patient next had a partial response on gefitinib before developing disease progression after 10 months. She then had stable disease with 4 cycles of pemetrexed followed by 4 cycles of paclitaxel plus carboplatin with a best response of

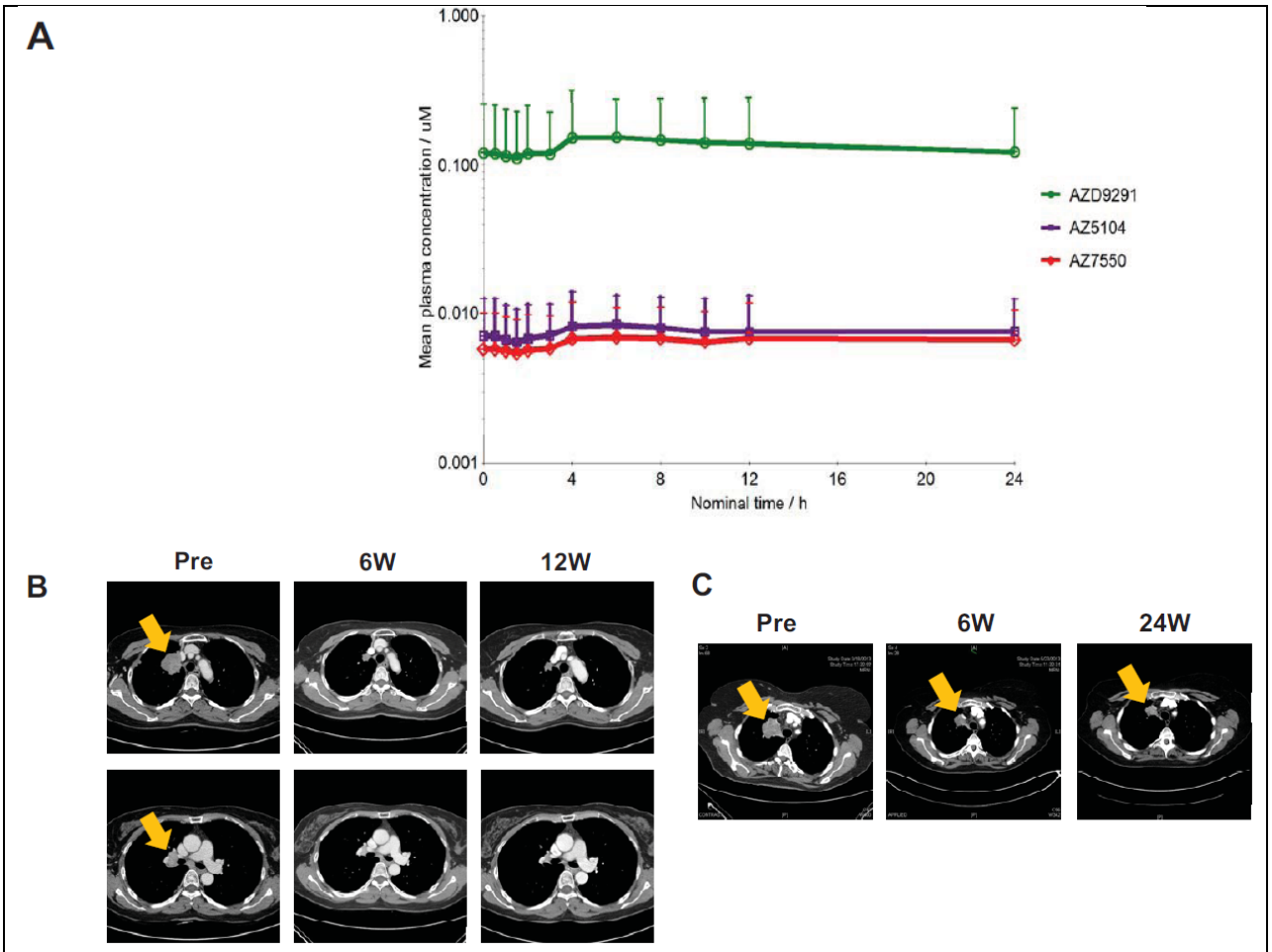

Figure 21. Proof of concept clinical studies validating AZD9291 as a mutant-selective EGFR kinase T790M inhibitor

A. Preliminary pharmacokinetic profile showing mean (+SD) total plasma levels of AZD9291, AZ5104 and AZ7550 versus time from cohort of 6 advanced NSCLC patients. After a single dose of AZD9291 mesylate salt, followed by a 7 day washout and then 8 days of once daily 20 mg oral dosing in AURA Phase 1 study (NCT01802632).

B and C. Serial computed tomography scans of the chest from patients before and after treatment with AZD9291 in a phase I trial. **B**, Images from a 57-year old Korean female patient diagnosed with Stage IV non-small cell lung cancer in May 2011. See main text for details. **C**, Images from a 57-year old British female never smoker diagnosed with Stage IV lung adenocarcinoma in December 2010. The patient was previously treated with first-line gefitinib for 14 months, achieving a partial response before eventually developing progressive disease. See main text for details.

partial response before progressing immediately before study. Analysis of tumor tissue, from a biopsy taken immediately before AZD9291 study entry, using direct dideoxynucleotide-based sequencing, revealed presence of a T790M mutation (data not shown). Tumor shrinkage on AZD9291 was 39.7% at scan 1, 48.3% by scan 2 **(Figure 21B)**, remained at 48.3% at both scan 3 and scan 4, and was 51.7% at scan 5 (data not shown).

The second patient was a 57-year old white female never smoker from England diagnosed with Stage IV lung adenocarcinoma in December 2010. Analysis of tumor tissue obtained at diagnosis in a local molecular pathology lab using the Qiagen EGFR RGQ PCR test revealed evidence of exon 19 deletion and T790M mutations (data not shown). The patient was treated with first-line gefitinib, achieving a partial response before eventual progressive disease 14 months later, suggesting that the T790M mutation was present at only a low allele frequency. Re-biopsy prior to starting AZD9291 was not performed. At the cycle 1 day 15 assessments on AZD9291, the patient reported full resolution of pre-existing persistent nocturnal cough. Tumor shrinkage was 38% at scan 1, 39.3% at scan 2, 56.7% by scan 3 **(Figure 21C)**, 62% by scan 4, and 59.3% by scan 5 (data not shown). By Cycle 7 Day 1, the patient reported significant improvement in pre-existing hair and eyelash abnormalities which had developed during the immediately prior gefitinib therapy. Since this patient received AZD9291 after developing acquired resistance whilst on continuous gefitinib (after initial > 6 months duration of partial response) with no intervening treatment, strict Jackman clinical criteria for acquired resistance were fulfilled (Jackman, Pao et al. 2010). No significant aberration of blood glucose levels were noted in either patient during the

study. Both patients had duration of response of approximately 9 months and were progression-free on 20 mg/day AZD9291 for approximately 11 months, until disease progression by RECIST 1.1. Both patients continue to receive AZD9291 treatment on study as per protocol, as they continue to derive clinical benefit according to their treating physicians.

Discussion

Mutations in EGFR occur in 10-35% of NSCLCs and confer sensitivity to the EGFR TKIs erlotinib, gefitinib, and afatinib (Pao and Chmielecki 2010). In randomized studies, the median overall survival of patients with EGFR mutant lung cancer receiving first-line EGFR TKIs is ~19-36 months, while median progression free survival is about a year. In more than half of patients, tumor cells at the time of progression harbor a second-site T790M mutation, which confers resistance to these EGFR TKIs (Yun, Mengwasser et al. 2008). No specific treatments for patients with acquired resistance to current EGFR TKIs have yet been approved.

We describe here the identification, characterization and early clinical development of AZD9291, a novel oral, irreversible, third generation TKI with a distinct profile from gefitinib, erlotinib, afatinib, and dacomitinib. Notably, AZD9291 has a distinct chemical structure from the other third-generation TKIs, WZ4002 (Zhou, Ercan et al. 2009) and CO-1686 (Walter, Sjin et al. 2013). Biochemical profiling together with *in vitro* cellular phosphorylation and phenotype studies have collectively shown that AZD9291 is highly potent against EGFR-mutant and T790M resistant EGFR mutants with a wide margin of selectivity against wild type EGFR activity and exhibits a high degree of selectivity against other kinases outside the EGFR family. Moreover, the profound anti-

tumor activity of AZD9291 across xenograft and transgenic mutant T790M EGFR disease models *in vivo* suggests the potential to target T790M tumors following progression on early generation TKIs.

Prior to identification of “third generation” EGFR TKIs, the most promising targeted regimen in patients with acquired resistance had been the combination of afatinib plus cetuximab, which induced a 32% response rate and median progression-free survival of 4.7 months in a heavily pre-treated cohort (Janjigian et al) with a significant degree of skin and gastrointestinal (diarrhea) toxicity. In the phase I trial of AZD9291 in EGFR-mutant NSCLC patients that had progressed on earlier generation TKIs, evidence of efficacy has been seen at all doses studied so far, with AZD9291 induced partial radiographic responses in patients whose tumors were known to harbor T790M, from the first dose cohort onwards (Burtness, Anadkat et al. 2009). Rash and diarrhea were mostly mild and reported in only a minority of patients, consistent with low activity against wild-type EGFR. Out of the two confirmed partial responses described in this paper, in addition to both patients’ tumors harboring the T790M mutations (according to local tests), one patient’s disease fits strict Jackman criteria for acquired resistance (Jackman, Pao et al. 2010), receiving the drug directly after prolonged response and progression on gefitinib. Thus, based on the above, AZD9291 has already demonstrated proof-of-principle clinical activity in patients with acquired resistance for whom there are no approved targeted therapies. Similarly, results from a phase I trial with CO-1686 have also shown evidence of efficacy in TKI-resistant tumors harboring T790M, providing further proof of principle for potential use of “third generation” TKIs in this setting. A surprising finding in the afatinib plus cetuximab study

was that tumors with undetectable levels of T790M also displayed tumor shrinkage, suggesting that a T790M-independent but EGFR-dependent pathway of resistance exists. The current phase I study of AZD9291 will test whether the drug is effective in both T790M-positive and –negative cohorts, through planned dose expansion cohorts. Full Phase I data will be presented at completion of study.

The existence of cell populations harboring T790M within a proportion of TKI-naive EGFR-mutant tumors has been reported, although the prevalence depends on the diagnostic assay being used. Studies using more conventional diagnostic assays have reported detection in about 2% of TKI-naive tumors (Sequist, Martins et al. 2008). Recently, groups using more sensitive technologies have reported higher detection rates ranging from 40% to 60% (Costa, Molina et al. 2014), although it remains unclear whether all these observations are real or analytical artifacts (Ye, Zhu et al. 2013). However, overall the data supports the hypothesis that T790M clones pre-exist in a proportion of EGFR-mutant tumors prior to TKI treatment. In addition to T790M, AZD9291 also potently inhibits sensitizing mutant EGFR across *in vitro* and *in vivo* disease models at similar potencies to T790M-mutant EGFR. Therefore, taken together, this supports the hypothesis that AZD9291 could also offer an attractive treatment option in EGFR-mutant TKI-naive patients, through targeting both sensitizing and T790M tumor cell populations that co-exist in a proportion of tumors, which may then lead to delayed disease progression and ultimately increased survival benefit. However, it remains to be determined what the optimal sequencing of EGFR TKIs will be and whether maximum benefit to most patients will be achieved through using AZD9291 after TKI progression or earlier in the treatment pathway.

Patients harboring EGFR-mutant tumors often progress during TKI treatment due to growth of secondary brain metastases (Porta, Sanchez-Torres et al. 2011). Although there are reports of TKIs providing benefit in treatment of EGFR-mutant brain metastases, current TKIs are believed to have generally poor properties for penetrating across the blood brain barrier (BBB), and thus their activity will be variable and influenced by such factors as dose, level of BBB disruption and efflux transporter expression across individuals. Therefore, there is also a need for EGFR TKIs with improved brain penetrance. Quantitative whole body autoradiography (QWBA) studies in rat brain with [$_{14}$C]AZD9291 have indicated AZD9291 had a brain-to-blood ratio of up to 2 over the first 24 hours, suggesting the potential of AZD9291 to penetrate the brain (data not shown). This is in contrast to [$_{14}$C]gefitinib which had a maximum brain-to-blood ratio of only 0.2 (McKillop, Hutchison et al. 2004). Although further pre-clinical studies are required to explore the translatable potential of AZD9291 to target brain metastases, together with future clinical studies, the preliminary data look promising in this area.

Despite the potential of AZD9291 to prevent resistance via T790M, tumors are likely to engage alternative escape mechanisms. If TKIs such as AZD9291 become a prominent feature in the treatment of EGFR-mutant disease across multiple lines of therapy, it will be critical for future pre-clinical and clinical research to identify the most prevalent future resistance mechanisms. Consistent with its pharmacological profile, we have not observed acquired resistance to AZD9291 *in vitro* due to emergence of T790M. It is also interesting to note that we have not yet seen resistance to AZD9291 due to direct mutation of cysteine 797 (data not shown), which would render the

receptor refractory to irreversible agents, in an analogous manner T790M prevents inhibition by early generation drugs. Therefore, non-EGFR related resistance mechanisms may become more dominant for agents such as AZD9291. Indeed, pre-clinical reports have suggested that “third generation” agents can induce switching to multiple signaling mechanisms that bypass EGFR dependency such as ERK and AKT pathways (Ercan, Xu et al. 2012; Cortot, Repellin et al. 2013; Walter, Sjin et al. 2013). Since AZD9291 is structurally distinct, it will be critical to understand which resistance mechanisms are induced through treatment with AZD9291 and whether different “third generation” TKIs engage common escape mechanisms. Furthermore, identification of molecular mechanisms of resistance will support the investigation of strategies to combine additional novel targeted therapies with AZD9291 as a foundation EGFR TKI partner, to achieve potentially greater clinical benefit.

AZD9291 and its active circulating metabolite AZ5104 display similar and minimal off-target activity against other non-HER family kinases, but *in vitro* data suggests the potential to target both HER2 and HER4 kinase activity. This property may be important as HER2 amplification may mediate acquired resistance to EGFR TKI in some cases (Takezawa, Pirazzoli et al. 2012). AZD9291 and AZ5104 also appear to be effective against other rare drug-sensitive EGFR mutants and potentially lung cancer-associated HER2 mutants, but like other EGFR TKIs are not potent against an EGFR exon 20 insertion. Further pre-clinical and clinical studies are required to understand the potential utility of AZD9291 in these additional molecular phenotypes.

Earlier generation EGFR TKIs have revolutionized the treatment of EGFR-mutant

NSCLC and have demonstrated the power of precision medicine in genetically-defined tumors. However, toxicities related to wild-type EGFR and the emergence of resistance mechanisms have limited the effectiveness of these drugs. Third-generation EGFR TKI agents such as AZD9291 have the potential to overcome these limitations and improve markedly the treatment options to patients who have progressed on TKI treatment due to T790M. Evaluation of AZD9291 in the 1st line setting in patients with EGFR-mutant tumors should also be considered based on AZD9291's third generation EGFR TKI profile. Moreover, if AZD9291 is confirmed to have a mild side effect profile together with its clinical efficacy and mechanistic hypothesis, this raises the option for investigation as a foundation EGFR TKI for combinations with other therapies to provide further treatment options for patients.

CHAPTER V

Merlin regulates EGFR expression in some, but not all, EGFR-mutant lung cancer cell lines

Introduction

Lung cancer is the leading cause of cancer-related deaths in the US and worldwide (Molina, Yang et al. 2008). Historically, lung cancers have been treated with cytotoxic chemotherapies, with mixed results. Over the past decade, tremendous advances in genomic technologies have enabled the identification of specific mutations that drive lung tumors. Such mutations are causally implicated in oncogenesis and positively selected for throughout tumor generation (Weinstein 2002; Stratton, Campbell et al. 2009). Importantly, some of these mutations can be targeted by drugs, matching the specific driver mutation of patient's tumor to a specific drug. This personalized approach to cancer medicine often results in far better outcomes for patients, including both reduced tumor burden and decreased toxicity profile.

In 2004, mutations in the epidermal growth factor receptor (EGFR) were identified as an essential biomarker for sensitivity to first-generation anti-EGFR tyrosine kinase inhibitors (TKIs), erlotinib and gefitinib (Lynch, Bell et al. 2004) (Pao, Miller et al. 2004) (Paez, Janne et al. 2004). Patients whose tumors harbor activating mutations in EGFR now routinely receive erlotinib or gefitinib as first-line therapy; most patients will

respond and experience decreased tumor burden. However, within a median of 9-16 months, all patients will invariably experience disease progression, defined as primary acquired resistance. Much work has focused on mechanisms of and treatment methods to overcome primary acquired resistance. One such therapy combines a second-generation EGFR TKI, afatinib, plus monoclonal anti-EGFR antibody, cetuximab (Regales, Gong et al. 2009). A phase Ib trial within patients with primary acquired resistance observed a 29% response rate to afatinib + cetuximab. Unfortunately, all responders will eventually fail second-line anti-EGFR targeted therapy and experience secondary acquired resistance.

We previously identified two of the first patients to experience secondary acquired resistance (Pirazzoli, Nebhan et al. 2014).In one patient, we identified two mutations in *NF2* that were present at the point of disease progression, but not prior to starting afatinib+cetuximab. Mutations in merlin, the protein product of the *NF2* gene, had not previously been reported in the context of acquired resistance. The first mutation, c.592C>T_p.R198* at frequency 0.15 of 631 reads, is a truncating mutation, while the second, c.811-2A>T: splice at 0.13 frequency of 1168 reads, is a splice site mutation expected to cause a deletion of eight amino acids. Both mutations are predicted to cause loss-of-function due to their location in the protein's FERM domain, essential for merlin's function and localization **(Figures 3, 4)**. Mutations in *NF2* piqued our interest as a potential mechanism of acquired resistance to afatinib+cetuximab because loss of merlin has been shown to activate EGFR signaling, at least in non-cancerous cells with wild-type EGFR (Curto, Cole et al. 2007). After we established that knockdown of merlin induces resistance to anti-EGFR agents in EGFR-mutant lung

cancer cell lines, which may be abrogated by concurrent treatment with mTOR inhibitor (see Chapter III), we sought to understand the mechanism by which merlin regulates EGFR in EGFR-mutant cells.

Results

Merlin is expressed in EGFR-mutant lung cancer cell lines

Because the function of merlin is dependent on cell density, all experiments described herein were conducted at 100% total cell confluence at the time of cell lysis. To begin evaluating the mechanism of merlin in EGFR-mutant lung cancer cells, we first evaluated a panel of EGFR-mutant cell lines for the presence of full-length merlin. As a control, we acquired the only commercially-available *NF2-/-* lung adenocarcinoma cell line, SW1573. This cell line does not harbor any *EGFR* mutation but does contain a *KRAS* G12C mutation. EGFR-mutant lung cancer cell lines evaluated included those harboring both exon 19 deletions and L858R mutations in EGFR. All cell lines harbored full-length merlin by immunoblot analysis; though protein levels were not totally consistent among cell lines, no patterns were identified (**Figure 22, upper panels**).

Because the *NF2* mutations discovered in a patient were found in the context of acquired resistance to anti-EGFR agents, we next evaluated isogenic pairs of TKI-sensitive and -resistant EGFR-mutant cell lines for merlin loss. Resistant cell lines were developed in our lab by prolonged drug exposure of parental cells as previously described (Chmielecki, Foo et al. 2011). No evidence of merlin loss upon resistance to

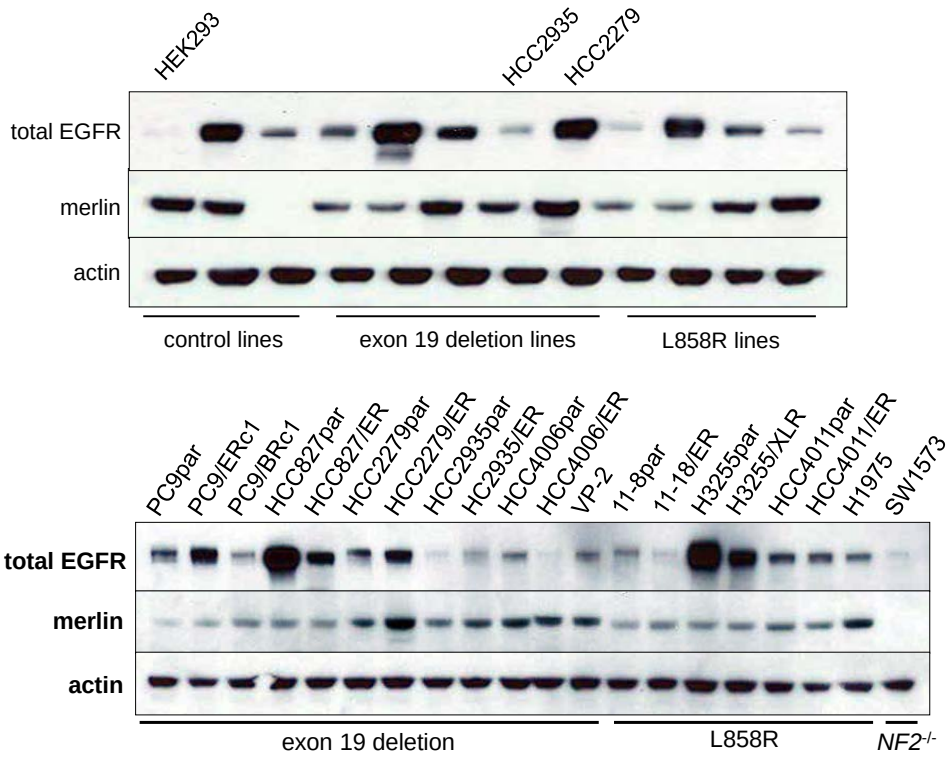

Figure 22. Merlin is expressed in EGFR-mutant lung cancer cell lines
Immunoblot ananalysis of endogenous merlin expression in EGFR-mutant TKI sensitive cell lines (top) and isogenic pairs (bottom) of TKI-sensitive (par, parental) and –resistant (/ER, erlotinib-resistant; /BR, afatinib-resistant; XLR, XL647-resistant). SW1573 is an wtEGFR, mtKRAS, $NF2^{-/-}$ lung adenocarcinoma cell line used as a control. Results are representative of at least three experiments per cell line.

drug was seen by immunoblot analysis within various isogenic pairs (**Figure 22, lower panels**).

Merlin expression is not affected by treatment with anti-EGFR targeted therapies

Next, we evaluated whether treatment with anti-EGFR agents affected levels of merlin in EGFR-mutant cell lines. PC9par and HCC827par cells were exposed to erlotinib (data not shown), afatinib or cetuximab over a 4-day time period (Figure 23). In all cases, drug was effective at reducing or eliminating phosphorylated EGFR. When treated with cetuximab, prolonged exposure resulted in the expected downregulation of total EGFR. However, in all cases, merlin levels remained stable, suggesting that merlin expression is not affected by short-term treatment with anti-EGFR tyrosine kinase inhibitors or an anti-EGFR antibody.

Merlin expression regulates EGFR expression in some EGFR-mutant cell lines

To explore further the mechanism of merlin regulation of EGFR in the context of EGFR-mutant cells, we transiently transfected an si*NF2* construct into PC9par and HCC827par cell lines. In both cell lines, we observed efficient merlin knockdown. However, we saw an unexpected decrease in total EGFR upon merlin knockdown in PC9par cells. This decrease in total EGFR was not observed in HCC827par cells, suggesting that the observation was not due to off-target effects against *EGFR* by the si*NF2* construct. To further investigate, we conducted a time course analysis in which either a scrambled, si*EGFR*, or si*NF2* construct was transfected into cells. We saw that knockdown of EGFR resulted in no change in merlin expression in both cell lines, suggesting that merlin expression is not dependent on EGFR expression. However, we

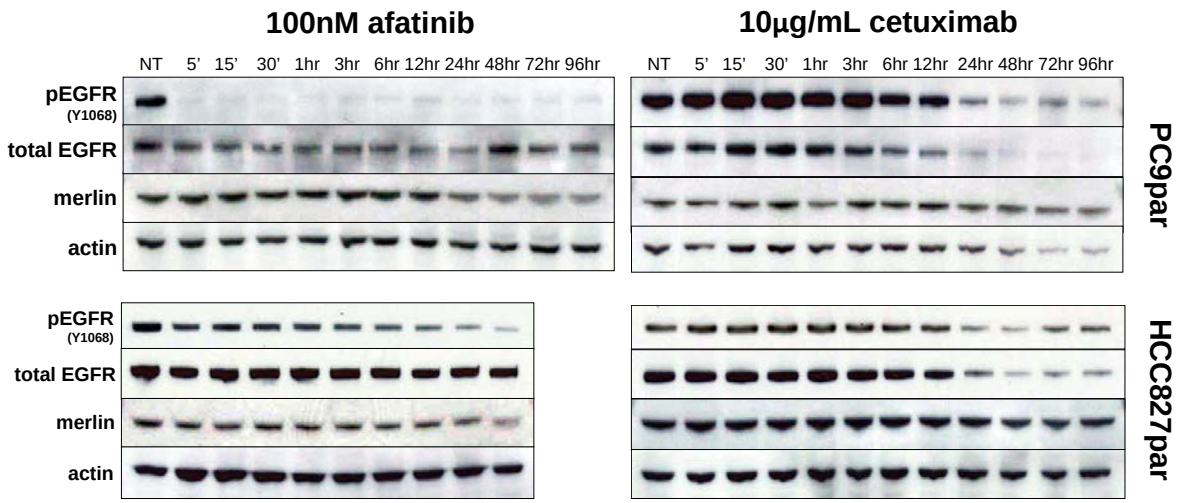

Figure 23. Merlin expression is not decreased by treatment with anti-EGFR targeted therapies

Time course treatment of PC9par cells (top panels) and HCC827par cells (bottom panels) with 100nM afatinib (left panels) or 10μg/mL cetuximab (right panels). Results are representative of at least three experiments.

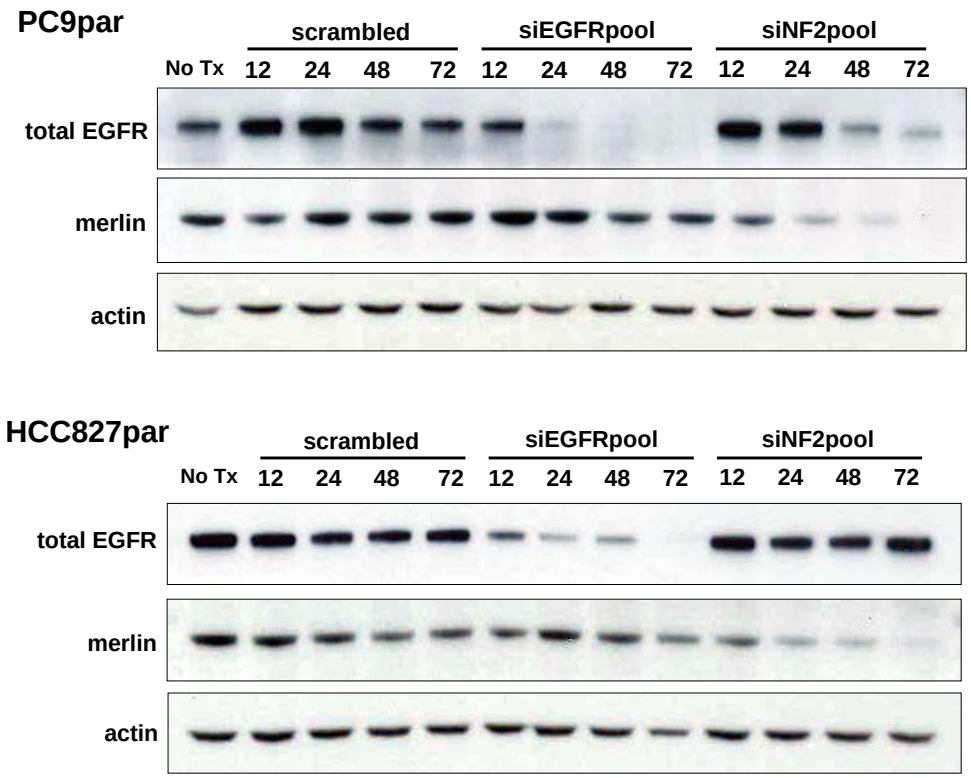

Figure 24. Merlin expression regulates EGFR expression in some EGFR-mutant cell lines

Time course transfection of PC9par cells (top panel) or HCC827par cells (bottom panels) with scrambled siRNA construct, siEGFR, or siNF2 for 12-72hr timecourse of treatment. For all treatments, reverse transfection protocol was used to ensure cell confluence at the time of lysis. Results are representative of at least three experiments for each cell line/transfection condition.

again observed that loss of merlin in PC9par cells resulted in a simultaneous loss of total EGFR (**Figure 24, upper panels**). This phenomenon was absent in HCC827par cells (**Figure 24, lower panels**). Two unique non-pooled si*NF2* constructs were also evaluated individually to ensure further that results were not due to off-target effect of the RNAi constructs (data not shown).

Next, we used an expanded panel of EGFR-mutant cell lines to evaluate the effect of *NF2* knockdown on EGFR. Surprisingly, we discovered that EGFR-mutant cell lines can be stratified into two groups based on total EGFR expression upon *NF2* knockdown (**Figure 25**). To quantify change in EGFR expression, we conducted densitometry analysis to compare total EGFR expression after 72 hours of si*NF2* transfection to total EGFR expression after 72 hours of scrambled construct transfection. The experiment was repeated at least three times in all cell lines. For purposes of further study, we designated those cell lines with total EGFR expression (siNF2/siSCR) < 80% to have a 'decreased EGFR' phenotype, while those cell lines with total EGFR expression (siNF2/siSCR) > 80% to have an 'unchanged EGFR' phenotype. Parental EGFR-mutant cell lines in the decreased EGFR phenotype group include PC9, H1975, H1650, VP-2, HCC4011, and HCC2279; parental EGFR-mutant cell lines in the unchanged EGFR phenotype group include H3255, HCC2935, HCC4006, and HCC827.

Interestingly, with the exception of HCC4011, both members of an isogenic pair of cell lines stratified to the same group, indicating that in most cases, the effect of merlin on EGFR is not altered by the sensitivity or resistance of that cell line to tyrosine kinase inhibitor. In addition, there was no discernable pattern of specific EGFR mutation

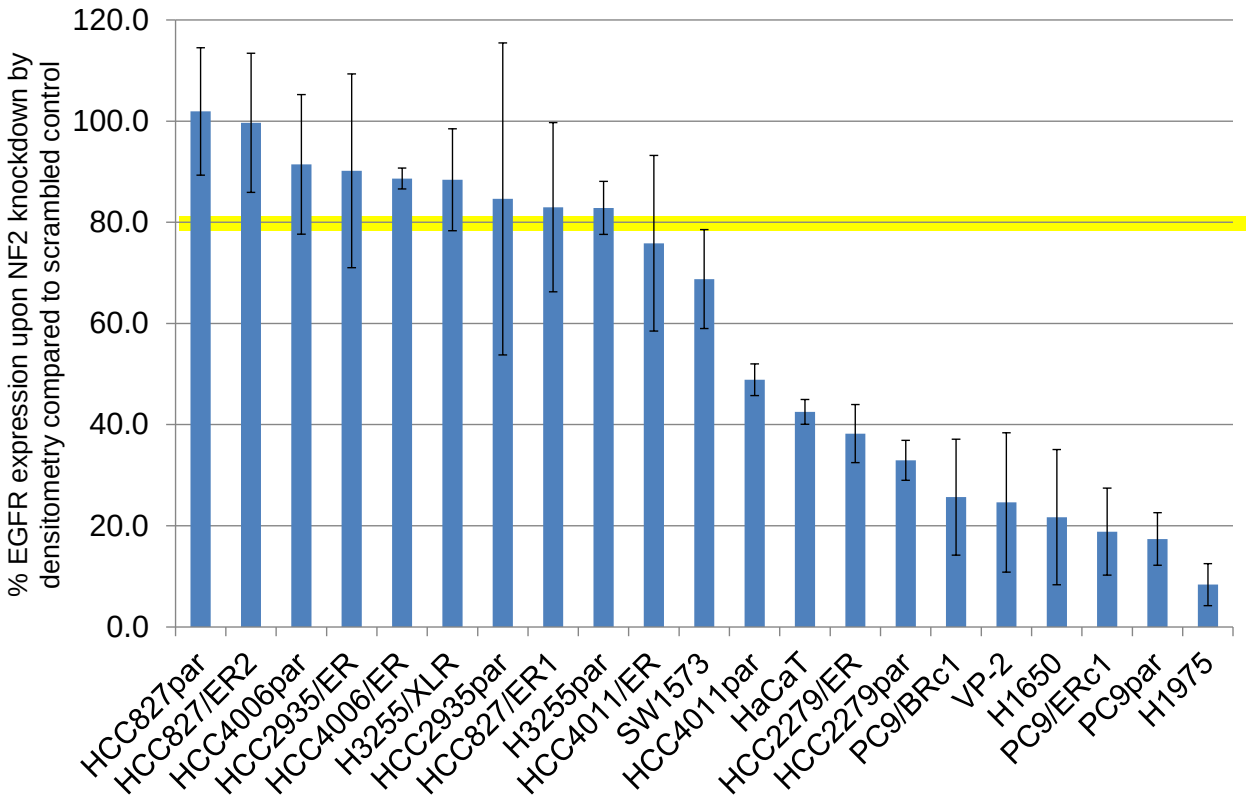

Figure 25. Quantified change in total EGFR expression upon *NF2* knockdown in an expanded panel of EGFR-mutant cell lines

Densitometry analysis comparing total EGFR expression after 72 hours of si*NF2* transfection to total EGFR expression after 72 hours of scrambled construct transfection; % change in EGFR expression quantified as (siNF2/siSCR). Cell lines above the yellow line (left side) indicate the 'unchanged EGFR phenotype' group; cell lines below the yellow line indicate the 'decreased EGFR phenotype' group. The experiment was repeated at least three times in all cell lines.

among the two phenotype groups; cell lines harboring L858R, exon19del, and T790M belong to both the decreased EGFR and unchanged EGFR groups.

To further explore the regulation of total EGFR expression by merlin in some, but not all, EGFR-mutant cell lines, we conducted cell proliferation assays. We hypothesized that upon *NF2* knockdown, cell lines in the decreased EGFR phenotype group would show a decreased proliferation rate compared to cell lines in the unchanged EGFR phenotype group. Analysis of growth rate supported this hypothesis. PC9par cells transfected with si*NF2* showed a significant decrease in growth rate as compared to untransfected or scrambled-transfected cells (**Figure 26, left panel**). The decrease in proliferation rate upon knockdown of *NF2* was not as dramatic as observed upon knockdown of *EGFR*. Among HCC827par cells, there was no significant difference in growth rate among untransfected, scrambled-transfected, and siNF2-transfected cells (**Figure 26, right panel**). The differences in proliferation rate further supports the existence of two distinct phenotypes among EGFR-mutant lung cancer cells upon merlin knockdown.

Decreased EGFR expression upon merlin knockdown does not correlate with cadherin-catenin or NHERF1 expression

In attempt to identify any underlying mechanism responsible for the disparate EGFR regulation of merlin in EGFR-mutant lung cancer cell lines, we recalled that PC9 cells are known to lack α-catenin (Shimoyama, Nagafuchi et al. 1992). This was particularly interesting because merlin is known to directly bind α-catenin. Additionally, α-catenin is a required member of the cadherin-catenin complex, an essential regulator

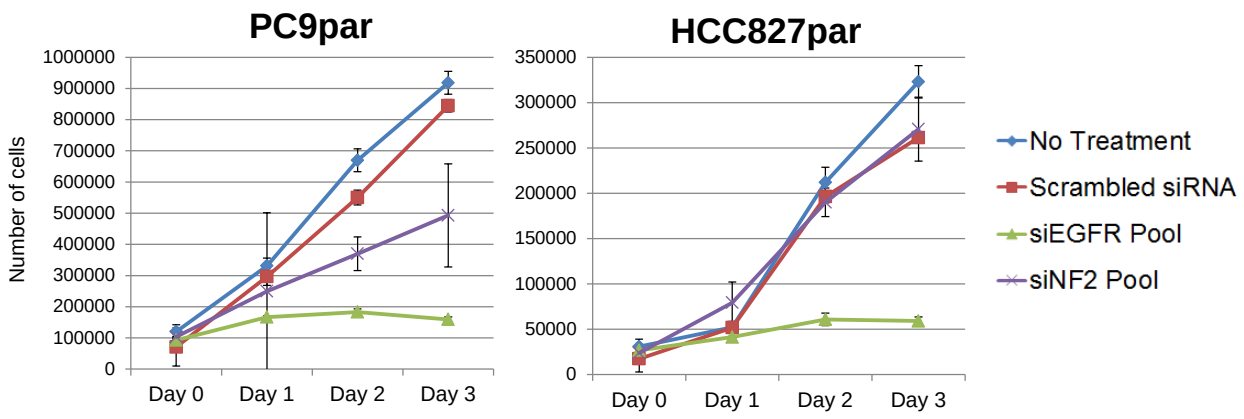

Figure 26. Proliferation rate of EGFR-mutant cells upon knockdown of *NF2*
PC9par cells (left) and HCC827par cells (right) were transfected with scrambled siRNA construct, siEGFR, or siNF2 and plated in triplicate by reverse transfection. Each sample was counted in triplicate on successive days. Concurrent immunoblot analysis was conducted to verify appropriate protein knockdown (data not shown).

of cell-to-cell and cell-to-matrix interaction. The cadherin-catenin complex is composed of p120, α-catenin, β-catenin (which may be compensated for by plakoglobin/γ-catenin), and E-cadherin (Reynolds, Daniel et al. 1994), (Shibamoto, Hayakawa et al. 1995). All members of the cadherin-catenin complex are required for complex function. BecausePC9 cells are known to lack α-catenin, we hypothesized that the decreased EGFR phenotype group and the unchanged phenotype group may be stratified by the presence of a complete cadherin-catenin complex.

To evaluate the cadherin-catenin complex, we conducted immunoblot analysis for all complex members in a panel of EGFR-mutant cell lines **(Figure 27)**. As expected, all isogenic PC9 cell lines lacked α-catenin, but full-length α-catenin was present in the remaining EGFR-mutant lines. All cell lines expressed full-length β-catenin. While plakoglobin expression was more varied, the presence of β-catenin negates the requirement of plakoglobin to form functioning cadherin-catenin complexes. All EGFR-mutant cell lines expressed full length p120. With two exceptions, full-length E-cadherin was expressed in all cell lines. The two lines in which E-cadherin was absent, HCC2279/ER and HCC4006/ER, undergo epithelial-mesenchymal transition (EMT) as part of their erlotinib-resistance phenotype; as such, resultant decrease or loss of E-cadherin is expected. In total, only PC9 cells lack an essential component of the cadherin-catenin complex, so alterations in the expression of this complex cannot fully explain the dichotomy of the decreased EGFR and unchanged EGFR phenotype groups.

Next, we checked for expression of NHERF1 in our panel of EGFR-mutant cell lines. Current literature suggests that NHERF1 is a necessary adaptor protein that links

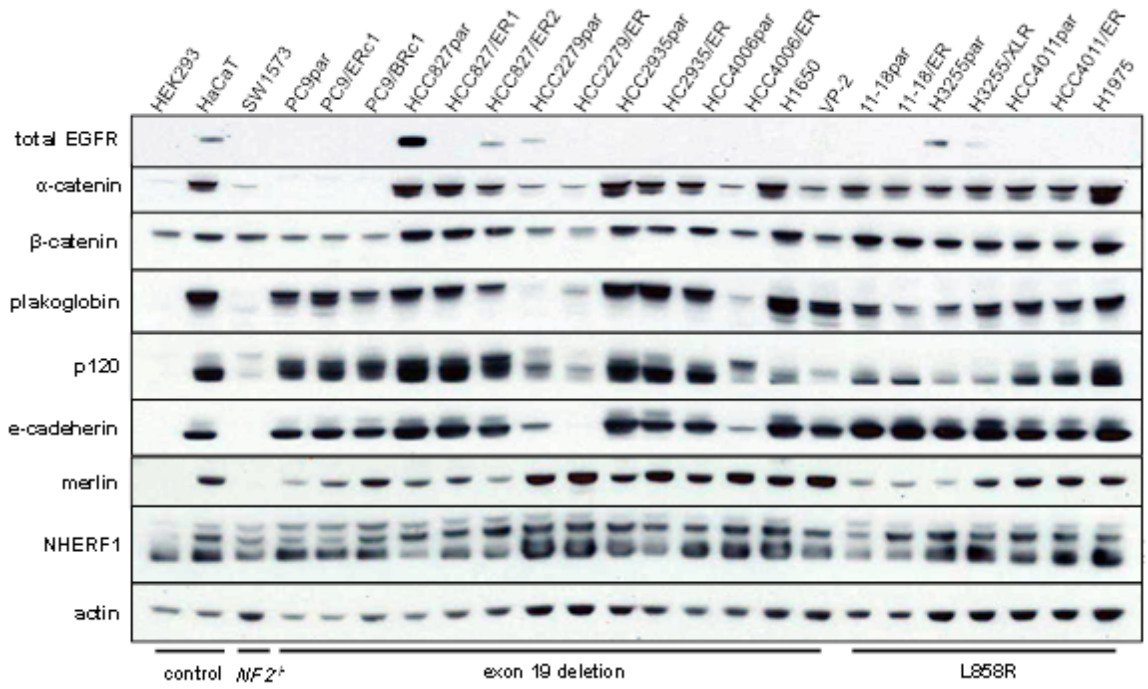

Figure 27. Decreased EGFR expression upon merlin knockdown does not correlate with cadherin-catenin or NHERF1 complex expression
Immunoblot analysis of control and EGFR-mutant cell lines for cadherin-catenin complex proteins. Of note, HCC2935/ER and HCC4006/ER are known to develop acquired primary acquired resistance through epithelial-mesenchymal transition (EMT), as indicated by the loss of E-cadherin in these resistant lines compared to their respective TKI-sensitive parent line.

merlin to EGFR (Curto, Cole et al. 2007). As such, we hypothesized that the presence or absence of NHERF1 may stratify the EGFR phenotype groups we observed. If NHERF1 links merlin to EGFR, loss of NHERF1 may disrupt the ability of merlin to regulate EGFR and define the unchanged EGFR expression group. To explore this, we conducted immunoblotting for NHERF1 but saw expression of full-length NHERF1 in all EGFR-mutant cell lines **(Figure 27)**. Taken together, neither expression of cadherin-catenin proteins nor expression of NHERF1 can explain the merlin-regulated EGFR phenotype we observe in some EGFR-mutant cell lines.

Treatment with TKI does not disrupt merlin-NHERF1-EGFR binding in EGFR-mutant cells

After observing full-length NHERF1 in all EGFR-mutant lung cancer cell lines evaluated, we investigated whether canonical merlin-NHERF1-EGFR binding occurs in the context of mutant EGFR by co-immunoprecipitation of endogenous protein. Using a representative cell line from both EGFR phenotype groups, cells were cultured to confluence before subjected to pulldown of EGFR, merlin, or NHERF1 and immunoblot analysis to determine the status of the remain two complex members. In both H1975, a member of the decreased EGFR phenotype, and HCC827par, a member of the unchanged EGFR phenotype group, the three proteins precipitate together **(Figure 28, left panels)**. Next, we evaluated the effect of treatment with anti-EGFR TKI on the stability of the merlin-NHERF1-EGFR interaction. Cells were treated for six hours with 100nM AZD9291, a third-generation, mutant-specific TKI. Drug treatment did not alter the interaction of merlin, NHERF1 and EGFR, suggesting that wild-type merlin is

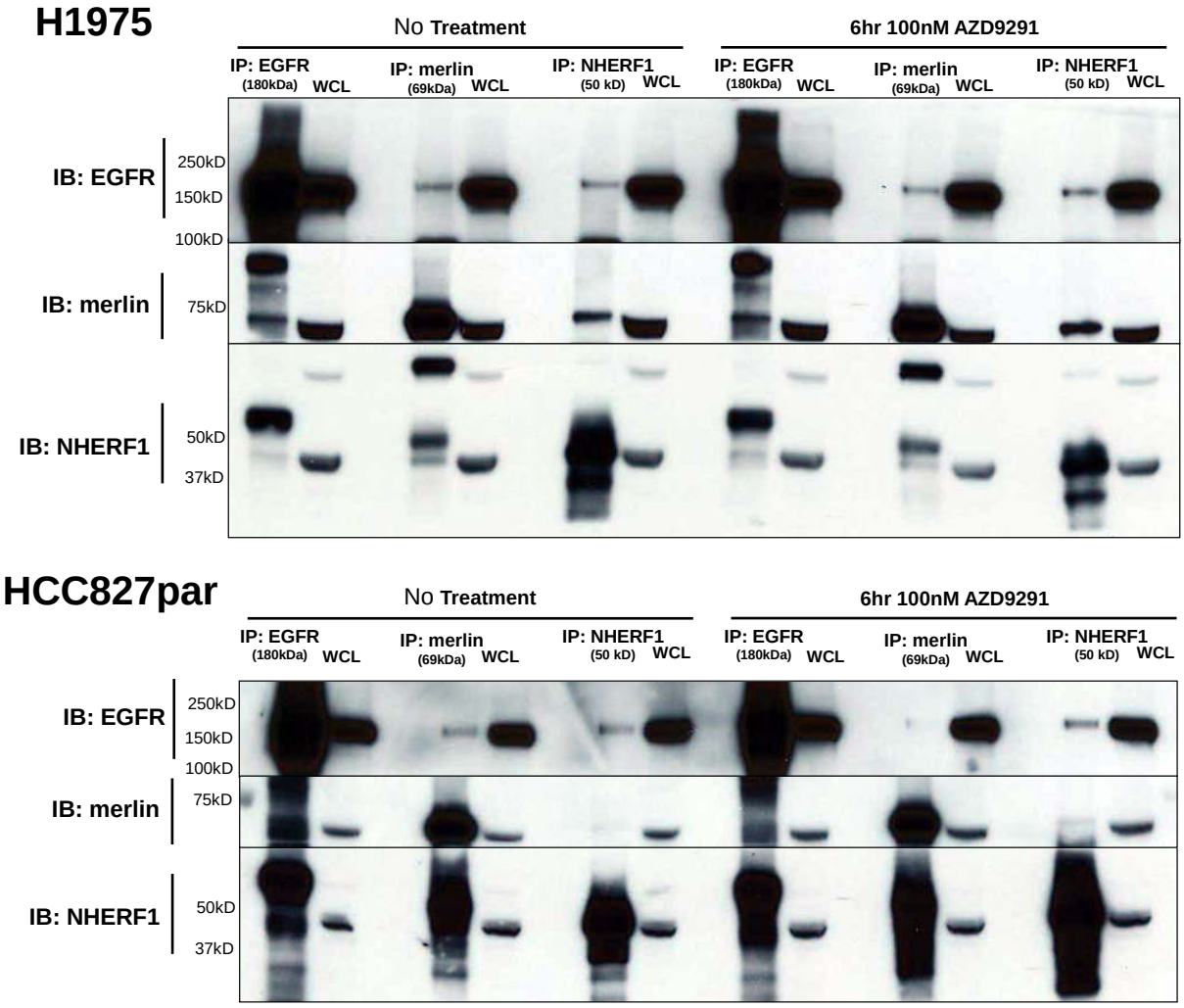

Figure 28. Treatment with TKI does not disrupt merlin-NHERF1-EGFR binding in EGFR-mutant cells

Co-immunoprecipitation of EGFR, merlin, and NHERF1 in untreated (left panels) or TKI-treated (right panels) cell lines (H1975, top panels; HCC827par, bottom panels). WCL, whole cell lysate. For treatment, cells were drugged with 100nM AZD9291 for 6hr immediately prior to crosslinking and lysis. Blots were cut in thirds as indicated to visualize all three proteins in the same lane. EGFR runs at 190kDa; merlin runs at 69kDa, and NHERF1 runs at 48kDa. To eliminate contamination by heavy-chain IgG/IgA signal, a light-chain specific secondary antibody was used to probe for NHERF1 by immunoblot.

capable of interacting with and potentially regulating EGFR in a manner that is independent of the kinase activity of EGFR **(Figure 28, right panels)**.

Discussion

The interaction and regulation of merlin and EGFR is poorly understood in wild-type epithelial cells and has never been examined in the aberrant signaling context of mutant EGFR. We recently identified two mutations in *NF2* predicted to cause loss-of-function of merlin in a lung adenocarcinoma patient with secondary acquired resistance to anti-EGFR targeted therapy. Our previous studies demonstrated that merlin loss was sufficient to induce resistance to anti-EGFR therapy in EGFR-mutant lung cancer cell lines, and that re-sensitization occurs upon con-treatment with mTOR pathway inhibitor everolimus. Because *NF2* mutation has been identified in a patient and shown to have targetable consequences *in vitro* and *in vivo*, the mechanism of merlin in the context of aberrant EGFR-driven cell signaling merits further investigation.

The experiments described here show that full-length merlin is expressed in a panel of EGFR-mutant cell lines and their TKI-resistant isogenic pairs. Merlin expression is unaffected by short-term treatment with either EGFR TKI or anti-EGFR antibody. While tyrosine kinase inhibitor and antibody have different mechanisms of action, neither affects merlin status. This indicates that inhibition of EGFR does not alter merlin biology. Furthermore, using co-immunoprecipitation assays, we show that merlin binds to EGFR via adaptor protein NHERF1, and this interaction is similarly unperturbed by treatment with TKI.

When conducting transient transfections to knockdown merlin expression in EGFR-mutant cells, we were surprised to see the emergence of two distinct EGFR phenotypes upon merlin knockdown. In four of ten parental cell lines, including HCC827, HCC4006, HCC2935, and H3255, knockdown of merlin results in no significant change in total EGFR (defined by the authors as decrease of $\leq$ 20%). We therefore defined this group as the 'unchanged EGFR phenotype' group. In six of ten parental cell lines, including PC9, H1975, VP-2, H1650, HCC2279, and HCC4011, knockdown of merlin results in a decrease in total EGFR of $\geq$ 20% or more, earning the designation of the 'decreased EGFR phenotype' group. Consistent with the definition of two distinct phenotype groups, we observe that upon knockdown of merlin, cell proliferation rate among one cell line in the decreased EGFR phenotype group is significantly slower than scrambled-transfected cells, but there is no difference in cell proliferation rate upon merlin knockdown in a cell line in the unchanged EGFR phenotype group.

We next sought to elucidate an underlying mechanism to explain the stratification of lung cancer cell lines driven by the same activating mutation in EGFR. Because PC9 cells lack α-catenin but HCC827 cells do not, we hypothesized that expression of full-length α-catenin and all other members of the cadherin-catenin complex may separate HCC827 cells and it other unchanged EGFR phenotype group members from the decreased EGFR phenotype group. This hypothesis was unproven, as all cell lines evaluated expressed full-length copies of all cadherin-catenin complex protein (with the expected exceptions of the PC9 family and those resistance cell lines known to have

undergone EMT). The presence of full-length NHERF1 in all cell lines also eliminated the possibility of phenotype stratification due to lack of merlin-EGFR adaptor protein.

Thus, we cannot yet completely explain the mechanism by which merlin regulates EGFR in the context of some EGFR-mutant tumor cells. Our data suggests possibly that the decreased EGFR phenotype we observe in some cells after merlin knockdown is due to indirect effects (e.g. transcriptional) rather than direct effects mediated by protein-protein interactions. Future studies will need to address such considerations. Nevertheless, very recent data published by another group shows that merlin biology is certainly deserving of further investigation. For example, a genome-scale CRISPR-Cas9 knockout screen in human melanoma cells identified hits in the *NF2* gene as involved in resistance to BRAF inhibitor vemurafenib (Shalem, Sanjana et al. 2014). To our knowledge, this is the only report besides our own suggesting *NF2* mutation may contribute to acquired resistance to targeted therapy. As acquired resistance is arguably the greatest obstacle to effective targeted therapy in cancer, it is not insignificant that *NF2* has now been identified as a potential mechanism of acquired resistance in cancers of two unique origins (lung and melanoma).

In addition to the potential role for merlin in acquired resistance to targeted therapy, two recent studies have elucidated potential drug targets for tumors associated with merlin deficiency. As a relatively small cytoplasmic protein that also localizes to the cell cortex and nucleus, merlin is difficult to directly target, but proteins whose expression is elevated upon merlin loss may provide better targets. Work by Shapiro et al suggests that merlin-negative tumors may benefit from treatment with a focal adhesion kinase (FAK) inhibitor. Studies using mesothelioma cell lines as well as other

merlin-positive and merlin-negative cell lines show that merlin-negative status is an excellent biomarker for FAK inhibitor sensitivity (Shapiro, Kolev et al. 2014). Work by Petrilli et al similarly identifies the LIM domain kinases 1 and 2 (LIMK1/2) as potential targets in tumors with merlin deficiency (Petrilli, Copik et al. 2014). Development and eventual clinical trials of drugs targeting merlin-deficient cells may result in much-needed advancements not only for patients with neurofibromatosis type 2, but also for a new subset of patients with acquired resistance to targeted therapeutics.

CHAPTER VI

Future Directions

Introduction

The objective of this research was to identify potential mechanisms of secondary acquired resistance to targeted anti-EGFR therapy in EGFR-mutant lung adenocarcinoma and evaluate novel drugs or drug combinations designed to overcome acquired resistance. First, using patient-generated data, we showed that knockdown of merlin in EGFR-mutant lung cancer cell lines can induce resistance to anti-EGFR therapy. We then hypothesized that combination therapy with mTOR pathway inhibitor everolimus could re-sensitize cells to anti-EGFR therapy. This hypothesis was validated in both cell line and mouse models. Second, we have worked with AstraZeneca to characterize AZD9291, a novel, mutant-specific inhibitor of EGFR. Data generated in EGFR-mutant cell lines supports the use of AZD9291 in patients with T790M-driven primary acquired resistance to anti-EGFR agents, and a phase 2 clinical trial is currently underway (NCT02094261). These findings have expanded our understanding of acquired resistance in EGFR-mutant lung cancer and provided preclinical rationale for the application of new drugs and drug combinations to be evaluated in translational studies. Additionally, insights into the potential role of merlin in secondary acquired resistance have provided impetus for continued study of the mechanism of interaction

and regulation of EGFR and merlin in the context of the aberrant signaling networks that dominate a cancer cell.

AZD9291 clinical trial

Clinical trials of AZD9291 are underway. As part of the ongoing phase 1 trial of the drug in a cohort of lung cancer patients with acquired resistance to first- or second-generation TKI has shown, AZD9291 has been administered to 232 patients. No dose-limiting toxicity has been observed. Impressively, a partial response rate of 64% has been observed in a cohort of patients with central confirmed EGFR T790M-positive tumors. In May 2014, the phase 2 clinical trial of AZD9291 began in a stratified cohort of patients whose EGFR-mutant lung tumors have met the criteria for acquired resistance to first- or second-generation TKI and are T790M-positive.

As AZD9291 and other third-generation EGFR TKIs currently under development enter clinical trials, it is also worth considering the best strategy for use of our anti-EGFR drug arsenal in combatting disease in patients. Studies to evaluate the optimal sequence of anti-EGFR therapy in EGFR-mutant lung cancer will allow clinicians to treat patients in a highly rational manner while also informing the direction of research in this ever-expanding field of targeted therapies. While large-scale pharmaceutical industry-sponsored trials seem unlikely at the moment, researchers can use available tools to generate data within cell line and animal models to understand which course of treatment will lead to greatest progression-free survival. The generation of cancer cell lines with acquired resistance to various first-, second-, and third-generation TKIs and anti-EGFR drug combinations will be valuable tools in this endeavor. In addition, transgenic mouse models may be treated with various lines of anti-EGFR therapy to

determine a drug sequence which maximizes PFS, using animal models to imitate clinical trials of human subjects and potentially produce sufficient data to become the biological rationale for a clinical trial in human patients.

Clinical application of concurrent EGFR and mTOR inhibition in A+C-resistant patients

Data discussed in Chapter III show in both cell line and mouse models that combination therapy of second-line anti-EGFR therapy plus mTOR inhibition may be an effective strategy to overcome secondary acquired resistance in patients. These findings, along with supporting evidence generated by other groups, may provide preclinical rationale to establish a clinical trial of this drug combination. Indeed, results reported by Kawabata and colleagues demonstrate that concurrent second-line anti-EGFR therapy and mTOR inhibition can prevent the development and progression of T790M-positive EGFR-mutant tumors in mouse models (Kawabata, Mercado-Matos et al. 2014).

A clinical trial (NCT00456833) of erlotinib monotherapy versus RAD001 plus erlotinib combination therapy in a population of TKI-naive non-small cell lung cancer patients treated with one or two previous rounds of chemotherapy was reported in 2011. This trial demonstrated only a modest progression-free survival benefit of combination therapy over monotherapy (2.9 and 2.0 months, respectively), and combination therapy recipients experience more than twice the frequency of grade 3/4 toxicity events than monotherapy recipient (Besse, Leighl et al. 2014). Importantly, this trial was conducted in a non-stratified lung cancer patient population. At the trial's initiation in 2006, routine evaluation for *EGFR* and other mutations in lung cancer patients was not widely

performed. Furthermore, the field of acquired resistance in this disease was still in its infancy at the time of the study's design in 2005; the T790M resistance mutation was first reported in 2005. As such, the only clinical trial evaluating EGFR TKI plus mTOR inhibition may have been executed "before its time;" our data suggest that such a trial certainly bears repeating today in a highly-selected cohort of patients whose tumors harbor confirmed EGFR mutations and/or have developed acquired resistance to secondary anti-EGFR therapy.

A trial conduced today should evaluate afatinib+cetuximab+rapamycin or AZD9291+rapamycin versus salvage chemotherapy in a patient cohort whose EGFR-mutant tumors have demonstrated secondary acquired resistance to afatinib+cetuximab dual therapy. Interestingly, a phase 1 trial of afatinib + rapamycin was announced in July 2014 (NCT00993499). The trial, currently enrolling patients in eight locations in Spain, is recruiting only highly stratified patients with EGFR-mutant non-small-cell lung cancer who have experienced disease progression after treatment with erlotinib or gefitinib. Our data support these efforts to evaluate highly stratified patient groups, using evidence-based rationale for treatment regimens in specific instances of acquired resistance to targeted therapy.

In addition to providing evidence for future clinical trials, our data also suggest new areas for preclinical research. As clinical pharmacology progresses, new and potentially better drugs are continually produced. While much of the work presented here focuses on first-, second-, and third-generation EGFR TKIs, novel compounds for the inhibition of mTOR are also being developed and are worth evaluating for both drug synergy and toxicity effects. Drugs targeting mTOR may be broadly classified as

allosteric or catalytic inhibitors (Garcia-Echeverria 2010). Both everolimus, the drug used throughout experiments detailed in Chapter 3, and its close analog discussed above, rapamycin (sirolimus), are allosteric inhibitors of mTORC1 (Rolfo, Giovannetti et al. 2014). Other such drugs in this group include timsirolimus and ridaforolimus (Porta, Paglino et al. 2014). Allosteric mTOR inhibitors function by complexing with the immunophilin FK506-binding protein of 12kDA (FKDP12), which binds to a region of the mTOR carboxy-terminus that is adjacent to the catalytic site (Choi, Chen et al. 1996). This binding interferes exclusively with the kinase activity of the mTORC1 complex, leaving mTORC2 activity intact. More recently, ATP-competitive kinase inhibitors of mTOR have been developed; these catalytic mTOR inhibitors are also known to block the activity of PI3K. Inhibitors in development include NVP-BEZ235, NVP-BGT226, XL765, SF1126, and GSK1059615 (Dienstmann, Rodon et al. 2014). Importantly, mTOR inhibition with catalytic inhibitors targets mTORC1, mTORC2, and PI3K. Thus, not only do catalytic inhibitors have greater anti-tumor effect by targeting the entire mTOR complex, but negative feedback of mTORC1 leading to Akt phosphorylation and tumor progression is abrogated with the concomitant PI3K inhibitory properties of these drugs (O'Reilly, Rojo et al. 2006). Favorable pharmacokinetic/pharmacodynamics properties of catalytic mTOR inhibitors have led to numerous clinical trials of these agents, particularly BEZ235. Future studies will need to determine the best inhibitor in the mTORC pathway to combine with anti-EGFR agents for patients.

Targeting merlin in acquired resistance

We present the identification of two novel mutations in *NF2* that may directly induce secondary acquired resistance in EGFR-mutant lung adenocarcinomas.

Mutations in merlin, the protein product of *NF2*, has also been identified in a variety of other solid and liquid tumors, including but not limited to mesothelioma, squamous cell carcinoma, hepatocellular carcinoma, renal cell carcinoma, and acute myeloid leukemia (Yoo, Park et al. 2012). Patients suffering from neurofibromatosis type 2, the namesake tumor syndrome of the *NF2* gene, also stand to benefit from an increased understanding of merlin pathobiology and its translational application.

Merlin is thought to be a poor candidate for direct drug targeting due to its lack of enzymatic activity. To date, no agents directly targeting merlin have been reported. However, recent interest in the role of merlin in cancer has increased interest in identifying druggable targets that are hyperactivated when *NF2* is mutated. Results generated by Shapiro and colleagues identify merlin mutation as a biomarker of sensitivity to focal adhesion kinase (FAK) inhibition by VS-4718 (Shapiro, Kolev et al. 2014). Encouragingly, a phase 1 clinical trial of this drug in metastatic solid tumors is currently underway (NCT01849744). Should phase 1 results demonstrate good tolerability, a phase 2 trial should specifically evaluate VS-4718 in patients with *NF2*-mutant tumors. Furthermore, results shown by our group and others provide support for the inclusion of EGFR-mutant lung adenocarcinoma patients with acquired resistance to secondary acquired resistance to anti-EGFR therapy. As this work was published following our studies, we did not determine if FAK inhibition could overcome acquired resistance in EGFR mutant lung cancers in the setting of *NF2* loss. If FAK inhibitors do prove useful in this regard, then patients with EGFR-mutant tumors and *NF2* mutations could potentially benefit from addition of FAK inhibitors to anti-EGFR therapy as well.

The goal of the research described herein was to evaluate potential mechanism of acquired resistance to afatinib + cetuximab therapy in EGFR-mutant lung cancer, as well as assess the efficacy of a novel mutant-specific EGFR inhibitor, AZD9291. We have shown that loss of *NF2* may induce resistance to anti-EGFR therapy in EGFR-mutant lung cancer cells, and that this resistance may be overcome with the addition of an mTORC1 inhibitor. We also demonstrate with *in vitro* and *in vivo* studies that AZD9291 may have potential to overcome limitations of previous TKIs in EGFR-mutant lung cancer, and provide some of the preclinical rationale for this compound's use in human trials. Understanding mechanisms of acquired resistance and developing novel therapeutic strategies to overcome acquired resistance are major challenges in the field of targeted cancer therapy; the research described here may aid our understanding to ultimately benefit the survival time of our patients.

REFERENCES

Ahronowitz, I., W. Xin, et al. (2007). "Mutational spectrum of the NF2 gene: a meta-analysis of 12 years of research and diagnostic laboratory findings." Hum Mutat **28**(1): 1-12.

Alam, N., K. S. Gustafson, et al. (2010). "Small-cell carcinoma with an epidermal growth factor receptor mutation in a never-smoker with gefitinib-responsive adenocarcinoma of the lung." Clin Lung Cancer **11**(5): E1-4.

Alfthan, K., L. Heiska, et al. (2004). "Cyclic AMP-dependent protein kinase phosphorylates merlin at serine 518 independently of p21-activated kinase and promotes merlin-ezrin heterodimerization." J Biol Chem **279**(18): 18559-18566.

Arakawa, H., N. Hayashi, et al. (1994). "Alternative splicing of the NF2 gene and its mutation analysis of breast and colorectal cancers." Hum Mol Genet **3**(4): 565-568.

Arcila, M. E., G. R. Oxnard, et al. (2011). "Rebiopsy of lung cancer patients with acquired resistance to EGFR inhibitors and enhanced detection of the T790M mutation using a locked nucleic acid-based assay." Clin Cancer Res **17**(5): 1169-1180.

Arkhipov, A., Y. Shan, et al. (2013). "Architecture and membrane interactions of the EGF receptor." Cell **152**(3): 557-569.

Barker, A. J., K. H. Gibson, et al. (2001). "Studies leading to the identification of ZD1839 (IRESSA): an orally active, selective epidermal growth factor receptor tyrosine kinase inhibitor targeted to the treatment of cancer." Bioorg Med Chem Lett **11**(14): 1911-1914.

Bean, J., C. Brennan, et al. (2007). "MET amplification occurs with or without T790M mutations in EGFR mutant lung tumors with acquired resistance to gefitinib or erlotinib." Proc Natl Acad Sci U S A **104**(52): 20932-20937.

Benhamouche, S., M. Curto, et al. (2010). "Nf2/Merlin controls progenitor homeostasis and tumorigenesis in the liver." Genes Dev **24**(16): 1718-1730.

Besse, B., N. Leighl, et al. (2014). "Phase II study of everolimus-erlotinib in previously treated patients with advanced non-small-cell lung cancer." Ann Oncol **25**(2): 409-415.

Bianchi, A. B., S. I. Mitsunaga, et al. (1995). "High frequency of inactivating mutations in the neurofibromatosis type 2 gene (NF2) in primary malignant mesotheliomas." Proc Natl Acad Sci U S A **92**(24): 10854-10858.

Bono, P., E. Cordero, et al. (2005). "Layilin, a cell surface hyaluronan receptor, interacts with merlin and radixin." Exp Cell Res **308**(1): 177-187.

Bretscher, A., K. Edwards, et al. (2002). "ERM proteins and merlin: integrators at the cell cortex." Nat Rev Mol Cell Biol **3**(8): 586-599.

Burtness, B., M. Anadkat, et al. (2009). "NCCN Task Force Report: Management of dermatologic and other toxicities associated with EGFR inhibition in patients with cancer." J Natl Compr Canc Netw **7 Suppl 1**: S5-21; quiz S22-24.

Cao, T. T., H. W. Deacon, et al. (1999). "A kinase-regulated PDZ-domain interaction controls endocytic sorting of the beta2-adrenergic receptor." Nature **401**(6750): 286-290.

Carpenter, G., L. King, Jr., et al. (1978). "Epidermal growth factor stimulates phosphorylation in membrane preparations in vitro." Nature **276**(5686): 409-410.
Carpenter, G., K. J. Lembach, et al. (1975). "Characterization of the binding of 125-I-labeled epidermal growth factor to human fibroblasts." J Biol Chem **250**(11): 4297-4304.
Carter, T. A., L. M. Wodicka, et al. (2005). "Inhibition of drug-resistant mutants of ABL, KIT, and EGF receptor kinases." Proc Natl Acad Sci U S A **102**(31): 11011-11016.
Chadee, D. N., D. Xu, et al. (2006). "Mixed-lineage kinase 3 regulates B-Raf through maintenance of the B-Raf/Raf-1 complex and inhibition by the NF2 tumor suppressor protein." Proc Natl Acad Sci U S A **103**(12): 4463-4468.
Chmielecki, J., J. Foo, et al. (2011). "Optimization of dosing for EGFR-mutant non-small cell lung cancer with evolutionary cancer modeling." Sci Transl Med **3**(90): 90ra59.
Chmielecki, J., J. Foo, et al. (2011). "Optimization of Dosing for EGFR-Mutant Non-Small Cell Lung Cancer with Evolutionary Cancer Modeling." Science translational medicine **3**(90): 90ra59.
Choi, J., J. Chen, et al. (1996). "Structure of the FKBP12-rapamycin complex interacting with the binding domain of human FRAP." Science **273**(5272): 239-242.
Cools, J., E. H. Stover, et al. (2003). "PKC412 overcomes resistance to imatinib in a murine model of FIP1L1-PDGFRalpha-induced myeloproliferative disease." Cancer Cell **3**(5): 459-469.
Cortot, A. B., C. E. Repellin, et al. (2013). "Resistance to irreversible EGF receptor tyrosine kinase inhibitors through a multistep mechanism involving the IGF1R pathway." Cancer Res **73**(2): 834-843.
Costa, C., M. A. Molina, et al. (2014). "The impact of EGFR T790M mutations and BIM mRNA expression on outcome in patients with EGFR-mutant NSCLC treated with erlotinib or chemotherapy in the randomized phase III EURTAC trial." Clin Cancer Res **20**(7): 2001-2010.
Cross, D. A., S. E. Ashton, et al. (2014). "AZD9291, an irreversible EGFR TKI, overcomes T790M-mediated resistance to EGFR inhibitors in lung cancer." Cancer Discov.
Curto, M., B. K. Cole, et al. (2007). "Contact-dependent inhibition of EGFR signaling by Nf2/Merlin." J Cell Biol **177**(5): 893-903.
Dalgliesh, G. L., K. Furge, et al. (2010). "Systematic sequencing of renal carcinoma reveals inactivation of histone modifying genes." Nature **463**(7279): 360-363.
de Bruin, E. C., C. Cowell, et al. (2014). "Reduced NF1 expression confers resistance to EGFR inhibition in lung cancer." Cancer Discov **4**(5): 606-619.
Dienstmann, R., J. Rodon, et al. (2014). "Picking the point of inhibition: a comparative review of PI3K/AKT/mTOR pathway inhibitors." Mol Cancer Ther **13**(5): 1021-1031.
Donowitz, M., B. Cha, et al. (2005). "NHERF family and NHE3 regulation." J Physiol **567**(Pt 1): 3-11.
Doody, J. F., Y. Wang, et al. (2007). "Inhibitory activity of cetuximab on epidermal growth factor receptor mutations in non small cell lung cancers." Mol Cancer Ther **6**(10): 2642-2651.

Downward, J., P. Parker, et al. (1984). "Autophosphorylation sites on the epidermal growth factor receptor." Nature **311**(5985): 483-485.
Downward, J., Y. Yarden, et al. (1984). "Close similarity of epidermal growth factor receptor and v-erb-B oncogene protein sequences." Nature **307**(5951): 521-527.
Eisenhauer, E. A., P. Therasse, et al. (2009). "New response evaluation criteria in solid tumours: revised RECIST guideline (version 1.1)." Eur J Cancer **45**(2): 228-247.
Engelman, J. A., K. Zejnullahu, et al. (2007). "PF00299804, an irreversible pan-ERBB inhibitor, is effective in lung cancer models with EGFR and ERBB2 mutations that are resistant to gefitinib." Cancer Res **67**(24): 11924-11932.
Engelman, J. A., K. Zejnullahu, et al. (2007). "MET amplification leads to gefitinib resistance in lung cancer by activating ERBB3 signaling." Science **316**(5827): 1039-1043.
Ercan, D., C. Xu, et al. (2012). "Reactivation of ERK signaling causes resistance to EGFR kinase inhibitors." Cancer Discov **2**(10): 934-947.
Eskens, F. A., C. H. Mom, et al. (2008). "A phase I dose escalation study of BIBW 2992, an irreversible dual inhibitor of epidermal growth factor receptor 1 (EGFR) and 2 (HER2) tyrosine kinase in a 2-week on, 2-week off schedule in patients with advanced solid tumours." Br J Cancer **98**(1): 80-85.
Evans, D. G. (2009). "Neurofibromatosis type 2 (NF2): a clinical and molecular review." Orphanet J Rare Dis **4**: 16.
Fernandez-Valle, C., Y. Tang, et al. (2002). "Paxillin binds schwannomin and regulates its density-dependent localization and effect on cell morphology." Nat Genet **31**(4): 354-362.
Frampton, G. M., A. Fichtenholtz, et al. (2013). "Development and validation of a clinical cancer genomic profiling test based on massively parallel DNA sequencing." Nat Biotechnol **31**(11): 1023-1031.
Fukuoka, M., S. Yano, et al. (2003). "Multi-institutional randomized phase II trial of gefitinib for previously treated patients with advanced non-small-cell lung cancer (The IDEAL 1 Trial) [corrected]." J Clin Oncol **21**(12): 2237-2246.
Garcia-Echeverria, C. (2010). "Allosteric and ATP-competitive kinase inhibitors of mTOR for cancer treatment." Bioorg Med Chem Lett **20**(15): 4308-4312.
Gladden, A. B., A. M. Hebert, et al. (2010). "The NF2 tumor suppressor, Merlin, regulates epidermal development through the establishment of a junctional polarity complex." Dev Cell **19**(5): 727-739.
Graus-Porta, D., R. R. Beerli, et al. (1997). "ErbB-2, the preferred heterodimerization partner of all ErbB receptors, is a mediator of lateral signaling." EMBO J **16**(7): 1647-1655.
Gronholm, M., M. Sainio, et al. (1999). "Homotypic and heterotypic interaction of the neurofibromatosis 2 tumor suppressor protein merlin and the ERM protein ezrin." J Cell Sci **112 (Pt 6)**: 895-904.
Gronholm, M., L. Vossebein, et al. (2003). "Merlin links to the cAMP neuronal signaling pathway by anchoring the RIbeta subunit of protein kinase A." J Biol Chem **278**(42): 41167-41172.
Haase, V. H., J. A. Trofatter, et al. (1994). "The murine NF2 homologue encodes a highly conserved merlin protein with alternative forms." Hum Mol Genet **3**(3): 407-411.

Hall, R. A., L. S. Ostedgaard, et al. (1998). "A C-terminal motif found in the beta2-adrenergic receptor, P2Y1 receptor and cystic fibrosis transmembrane conductance regulator determines binding to the Na+/H+ exchanger regulatory factor family of PDZ proteins." Proc Natl Acad Sci U S A **95**(15): 8496-8501.
Hidalgo, M., L. L. Siu, et al. (2001). "Phase I and pharmacologic study of OSI-774, an epidermal growth factor receptor tyrosine kinase inhibitor, in patients with advanced solid malignancies." J Clin Oncol **19**(13): 3267-3279.
Honegger, A. M., T. J. Dull, et al. (1987). "Point mutation at the ATP binding site of EGF receptor abolishes protein-tyrosine kinase activity and alters cellular routing." Cell **51**(2): 199-209.
Huse, M. and J. Kuriyan (2002). "The conformational plasticity of protein kinases." Cell **109**(3): 275-282.
Jackman, D., W. Pao, et al. (2010). "Clinical definition of acquired resistance to epidermal growth factor receptor tyrosine kinase inhibitors in non-small-cell lung cancer." J Clin Oncol **28**(2): 357-360.
James, M. F., S. Han, et al. (2009). "NF2/merlin is a novel negative regulator of mTOR complex 1, and activation of mTORC1 is associated with meningioma and schwannoma growth." Mol Cell Biol **29**(15): 4250-4261.
Janjigian, Y. Y., E. F. Smit, et al. (2012). "Activity of afatinib/cetuximab in patients with EGFR mutant non-small cell lung cancer and acquired resistance to EGFR inhibitors. ." Annals of Oncology **23**(Supplement 9).
Jannatipour, M., P. Dion, et al. (2001). "Schwannomin isoform-1 interacts with syntenin via PDZ domains." J Biol Chem **276**(35): 33093-33100.
Janne, P. A., X. Wang, et al. (2012). "Randomized phase II trial of erlotinib alone or with carboplatin and paclitaxel in patients who were never or light former smokers with advanced lung adenocarcinoma: CALGB 30406 trial." J Clin Oncol **30**(17): 2063-2069.
Jeselsohn, R., R. Yelensky, et al. (2014). "Emergence of constitutively active estrogen receptor-alpha mutations in pretreated advanced estrogen receptor positive breast cancer." Clin Cancer Res.
Johnson, K. C., J. L. Kissil, et al. (2002). "Cellular transformation by a FERM domain mutant of the Nf2 tumor suppressor gene." Oncogene **21**(39): 5990-5997.
Johnson, M. L., G. J. Riely, et al. (2011). "Phase II trial of dasatinib for patients with acquired resistance to treatment with the epidermal growth factor receptor tyrosine kinase inhibitors erlotinib or gefitinib." J Thorac Oncol **6**(6): 1128-1131.
Kancha, R. K., N. von Bubnoff, et al. (2009). "Functional analysis of epidermal growth factor receptor (EGFR) mutations and potential implications for EGFR targeted therapy." Clin Cancer Res **15**(2): 460-467.
Katakami, N., S. Atagi, et al. (2013). "LUX-Lung 4: a phase II trial of afatinib in patients with advanced non-small-cell lung cancer who progressed during prior treatment with erlotinib, gefitinib, or both." J Clin Oncol **31**(27): 3335-3341.
Kawabata, S., J. R. Mercado-Matos, et al. (2014). "Rapamycin Prevents the Development and Progression of Mutant Epidermal Growth Factor Receptor Lung Tumors with the Acquired Resistance Mutation T790M." Cell Rep **7**(6): 1824-1832.

Kim, Y., J. Ko, et al. (2012). "The EGFR T790M mutation in acquired resistance to an irreversible second-generation EGFR inhibitor." Mol Cancer Ther **11**(3): 784-791.
Kissil, J. L., K. C. Johnson, et al. (2002). "Merlin phosphorylation by p21-activated kinase 2 and effects of phosphorylation on merlin localization." J Biol Chem **277**(12): 10394-10399.
Kobayashi, S., T. J. Boggon, et al. (2005). "EGFR mutation and resistance of non-small-cell lung cancer to gefitinib." N Engl J Med **352**(8): 786-792.
Kris, M. G., R. B. Natale, et al. (2003). "Efficacy of gefitinib, an inhibitor of the epidermal growth factor receptor tyrosine kinase, in symptomatic patients with non-small cell lung cancer: a randomized trial." JAMA **290**(16): 2149-2158.
Kwak, E. L., R. Sordella, et al. (2005). "Irreversible inhibitors of the EGF receptor may circumvent acquired resistance to gefitinib." Proc Natl Acad Sci U S A **102**(21): 7665-7670.
Ladanyi, M., M. G. Zauderer, et al. (2012). "New strategies in pleural mesothelioma: BAP1 and NF2 as novel targets for therapeutic development and risk assessment." Clin Cancer Res **18**(17): 4485-4490.
Lallemand, D., M. Curto, et al. (2003). "NF2 deficiency promotes tumorigenesis and metastasis by destabilizing adherens junctions." Genes Dev **17**(9): 1090-1100.
Lamszus, K., L. Lachenmayer, et al. (2001). "Molecular genetic alterations on chromosomes 11 and 22 in ependymomas." Int J Cancer **91**(6): 803-808.
Laplante, M. and D. M. Sabatini (2012). "mTOR Signaling." Cold Spring Harb Perspect Biol **4**(2).
Laulajainen, M., M. Melikova, et al. (2012). "Distinct overlapping sequences at the carboxy-terminus of merlin regulate its tumour suppressor and morphogenic activity." J Cell Mol Med **16**(9): 2161-2175.
Laulajainen, M., T. Muranen, et al. (2011). "Multistep phosphorylation by oncogenic kinases enhances the degradation of the NF2 tumor suppressor merlin." Neoplasia **13**(7): 643-652.
Lazar, C. S., C. M. Cresson, et al. (2004). "The Na+/H+ exchanger regulatory factor stabilizes epidermal growth factor receptors at the cell surface." Mol Biol Cell **15**(12): 5470-5480.
Lee, Y. J., B. C. Cho, et al. (2010). "Impact of environmental tobacco smoke on the incidence of mutations in epidermal growth factor receptor gene in never-smoker patients with non-small-cell lung cancer." J Clin Oncol **28**(3): 487-492.
Li, D., L. Ambrogio, et al. (2008). "BIBW2992, an irreversible EGFR/HER2 inhibitor highly effective in preclinical lung cancer models." Oncogene **27**(34): 4702-4711.
Li, D., T. Shimamura, et al. (2007). "Bronchial and peripheral murine lung carcinomas induced by T790M-L858R mutant EGFR respond to HKI-272 and rapamycin combination therapy." Cancer Cell **12**(1): 81-93.
Liu, Y., K. Shah, et al. (1998). "A molecular gate which controls unnatural ATP analogue recognition by the tyrosine kinase v-Src." Bioorg Med Chem **6**(8): 1219-1226.
Lopez-Lago, M. A., T. Okada, et al. (2009). "Loss of the tumor suppressor gene NF2, encoding merlin, constitutively activates integrin-dependent mTORC1 signaling." Mol Cell Biol **29**(15): 4235-4249.
Lovly, C. M. and A. T. Shaw (2014). "Molecular pathways: resistance to kinase inhibitors and implications for therapeutic strategies." Clin Cancer Res **20**(9): 2249-2256.

Lynch, T. J., D. W. Bell, et al. (2004). "Activating mutations in the epidermal growth factor receptor underlying responsiveness of non-small-cell lung cancer to gefitinib." N Engl J Med **350**(21): 2129-2139.
Maeda, M., T. Matsui, et al. (1999). "Expression level, subcellular distribution and rho-GDI binding affinity of merlin in comparison with Ezrin/Radixin/Moesin proteins." Oncogene **18**(34): 4788-4797.
Maemondo, M., A. Inoue, et al. (2010). "Gefitinib or chemotherapy for non-small-cell lung cancer with mutated EGFR." N Engl J Med **362**(25): 2380-2388.
Majewski, I. J., L. Mittempergher, et al. (2013). "Identification of recurrent FGFR3 fusion genes in lung cancer through kinome-centred RNA sequencing." J Pathol **230**(3): 270-276.
Manchanda, N., A. Lyubimova, et al. (2005). "The NF2 tumor suppressor Merlin and the ERM proteins interact with N-WASP and regulate its actin polymerization function." J Biol Chem **280**(13): 12517-12522.
McKillop, D., M. Hutchison, et al. (2004). "Metabolic disposition of gefitinib, an epidermal growth factor receptor tyrosine kinase inhibitor, in rat, dog and man." Xenobiotica **34**(10): 917-934.
Merlino, G. T., Y. H. Xu, et al. (1984). "Amplification and enhanced expression of the epidermal growth factor receptor gene in A431 human carcinoma cells." Science **224**(4647): 417-419.
Miller, V. A., V. Hirsh, et al. (2012). "Afatinib versus placebo for patients with advanced, metastatic non-small-cell lung cancer after failure of erlotinib, gefitinib, or both, and one or two lines of chemotherapy (LUX-Lung 1): a phase 2b/3 randomised trial." Lancet Oncol **13**(5): 528-538.
Milton, D. T., G. J. Riely, et al. (2007). "Phase 1 trial of everolimus and gefitinib in patients with advanced nonsmall-cell lung cancer." Cancer **110**(3): 599-605.
Mitsudomi, T., S. Morita, et al. (2010). "Gefitinib versus cisplatin plus docetaxel in patients with non-small-cell lung cancer harbouring mutations of the epidermal growth factor receptor (WJTOG3405): an open label, randomised phase 3 trial." Lancet Oncol **11**(2): 121-128.
Mitsudomi, T. and Y. Yatabe (2010). "Epidermal growth factor receptor in relation to tumor development: EGFR gene and cancer." FEBS J **277**(2): 301-308.
Mok, T. S., Y. L. Wu, et al. (2009). "Gefitinib or carboplatin-paclitaxel in pulmonary adenocarcinoma." N Engl J Med **361**(10): 947-957.
Molina, J. R., P. Yang, et al. (2008). "Non-small cell lung cancer: epidemiology, risk factors, treatment, and survivorship." Mayo Clin Proc **83**(5): 584-594.
Morris, Z. S. and A. I. McClatchey (2009). "Aberrant epithelial morphology and persistent epidermal growth factor receptor signaling in a mouse model of renal carcinoma." Proc Natl Acad Sci U S A **106**(24): 9767-9772.
Morrison, H., L. S. Sherman, et al. (2001). "The NF2 tumor suppressor gene product, merlin, mediates contact inhibition of growth through interactions with CD44." Genes Dev **15**(8): 968-980.
Morrow, K. A., S. Das, et al. (2011). "Loss of tumor suppressor Merlin in advanced breast cancer is due to post-translational regulation." J Biol Chem **286**(46): 40376-40385.

Moyer, J. D., E. G. Barbacci, et al. (1997). "Induction of apoptosis and cell cycle arrest by CP-358,774, an inhibitor of epidermal growth factor receptor tyrosine kinase." Cancer Res **57**(21): 4838-4848.
Mu, Z., T. Klinowska, et al. (2014). "AZD8931, an equipotent, reversible inhibitor of signaling by epidermal growth factor receptor (EGFR), HER2, and HER3: preclinical activity in HER2 non-amplified inflammatory breast cancer models." J Exp Clin Cancer Res **33**: 47.
Murthy, A., C. Gonzalez-Agosti, et al. (1998). "NHE-RF, a regulatory cofactor for Na(+)-H+ exchange, is a common interactor for merlin and ERM (MERM) proteins." J Biol Chem **273**(3): 1273-1276.
O'Reilly, K. E., F. Rojo, et al. (2006). "mTOR inhibition induces upstream receptor tyrosine kinase signaling and activates Akt." Cancer Res **66**(3): 1500-1508.
Oda, K., Y. Matsuoka, et al. (2005). "A comprehensive pathway map of epidermal growth factor receptor signaling." Mol Syst Biol **1**: 2005 0010.
Ohashi, K., Y. E. Maruvka, et al. (2013). "Epidermal growth factor receptor tyrosine kinase inhibitor-resistant disease." J Clin Oncol **31**(8): 1070-1080.
Ohashi, K., L. V. Sequist, et al. (2012). "Lung cancers with acquired resistance to EGFR inhibitors occasionally harbor BRAF gene mutations but lack mutations in KRAS, NRAS, or MEK1." Proc Natl Acad Sci U S A **109**(31): E2127-2133.
Ono, M. and M. Kuwano (2006). "Molecular mechanisms of epidermal growth factor receptor (EGFR) activation and response to gefitinib and other EGFR-targeting drugs." Clin Cancer Res **12**(24): 7242-7251.
Oxnard, G. R., M. E. Arcila, et al. (2011). "New strategies in overcoming acquired resistance to epidermal growth factor receptor tyrosine kinase inhibitors in lung cancer." Clin Cancer Res **17**(17): 5530-5537.
Paez, J. G., P. A. Janne, et al. (2004). "EGFR mutations in lung cancer: correlation with clinical response to gefitinib therapy." Science **304**(5676): 1497-1500.
Pao, W. and J. Chmielecki (2010). "Rational, biologically based treatment of EGFR-mutant non-small-cell lung cancer." Nature reviews. Cancer **10**(11): 760-774.
Pao, W. and J. Chmielecki (2010). "Rational, biologically based treatment of EGFR-mutant non-small-cell lung cancer." Nat Rev Cancer **10**(11): 760-774.
Pao, W. and K. E. Hutchinson (2012). "Chipping away at the lung cancer genome." Nat Med **18**(3): 349-351.
Pao, W., V. Miller, et al. (2004). "EGF receptor gene mutations are common in lung cancers from "never smokers" and are associated with sensitivity of tumors to gefitinib and erlotinib." Proc Natl Acad Sci U S A **101**(36): 13306-13311.
Pao, W., V. A. Miller, et al. (2005). "Acquired resistance of lung adenocarcinomas to gefitinib or erlotinib is associated with a second mutation in the EGFR kinase domain." PLoS Med **2**(3): e73.
Perez-Soler, R., A. Chachoua, et al. (2004). "Determinants of tumor response and survival with erlotinib in patients with non--small-cell lung cancer." J Clin Oncol **22**(16): 3238-3247.
Petrilli, A., A. Copik, et al. (2014). "LIM domain kinases as potential therapeutic targets for neurofibromatosis type 2." Oncogene **33**(27): 3571-3582.

Piepkorn, M., M. R. Pittelkow, et al. (1998). "Autocrine regulation of keratinocytes: the emerging role of heparin-binding, epidermal growth factor-related growth factors." J Invest Dermatol **111**(5): 715-721.
Pineau, P., A. Marchio, et al. (2003). "Homozygous deletion scanning in hepatobiliary tumor cell lines reveals alternative pathways for liver carcinogenesis." Hepatology **37**(4): 852-861.
Pirazzoli, V., C. Nebhan, et al. (2014). "Acquired resistance of EGFR-mutant lung adenocarcinomas to afatinib plus cetuximab is associated with activation of mTORC1." Cell Rep **7**(4): 999-1008.
Politi, K., P. D. Fan, et al. (2010). "Erlotinib resistance in mouse models of epidermal growth factor receptor-induced lung adenocarcinoma." Dis Model Mech **3**(1-2): 111-119.
Politi, K., M. F. Zakowski, et al. (2006). "Lung adenocarcinomas induced in mice by mutant EGF receptors found in human lung cancers respond to a tyrosine kinase inhibitor or to down-regulation of the receptors." Genes Dev **20**(11): 1496-1510.
Porta, C., C. Paglino, et al. (2014). "Targeting PI3K/Akt/mTOR Signaling in Cancer." Front Oncol **4**: 64.
Porta, R., J. M. Sanchez-Torres, et al. (2011). "Brain metastases from lung cancer responding to erlotinib: the importance of EGFR mutation." Eur Respir J **37**(3): 624-631.
Pykett, M. J., M. Murphy, et al. (1994). "The neurofibromatosis 2 (NF2) tumor suppressor gene encodes multiple alternatively spliced transcripts." Hum Mol Genet **3**(4): 559-564.
Ramalingam, S. S., F. Blackhall, et al. (2012). "Randomized phase II study of dacomitinib (PF-00299804), an irreversible pan-human epidermal growth factor receptor inhibitor, versus erlotinib in patients with advanced non-small-cell lung cancer." J Clin Oncol **30**(27): 3337-3344.
Rangwala, R., F. Banine, et al. (2005). "Erbin regulates mitogen-activated protein (MAP) kinase activation and MAP kinase-dependent interactions between Merlin and adherens junction protein complexes in Schwann cells." J Biol Chem **280**(12): 11790-11797.
Red Brewer, M., C. H. Yun, et al. (2013). "Mechanism for activation of mutated epidermal growth factor receptors in lung cancer." Proc Natl Acad Sci U S A **110**(38): E3595-3604.
Regales, L., M. N. Balak, et al. (2007). "Development of new mouse lung tumor models expressing EGFR T790M mutants associated with clinical resistance to kinase inhibitors." PLoS One **2**(8): e810.
Regales, L., Y. Gong, et al. (2009). "Dual targeting of EGFR can overcome a major drug resistance mutation in mouse models of EGFR mutant lung cancer." J Clin Invest **119**(10): 3000-3010.
Reynolds, A. B., J. Daniel, et al. (1994). "Identification of a new catenin: the tyrosine kinase substrate p120cas associates with E-cadherin complexes." Mol Cell Biol **14**(12): 8333-8342.
Rodrik-Outmezguine, V. S., S. Chandarlapaty, et al. (2011). "mTOR kinase inhibition causes feedback-dependent biphasic regulation of AKT signaling." Cancer Discov **1**(3): 248-259.

Rolfo, C., E. Giovannetti, et al. (2014). "Novel therapeutic strategies for patients with NSCLC that do not respond to treatment with EGFR inhibitors." Cancer Treat Rev **40**(8): 990-1004.
Rong, R., X. Tang, et al. (2004). "Neurofibromatosis 2 (NF2) tumor suppressor merlin inhibits phosphatidylinositol 3-kinase through binding to PIKE-L." Proc Natl Acad Sci U S A **101**(52): 18200-18205.
Rosell, R., E. Carcereny, et al. (2012). "Erlotinib versus standard chemotherapy as first-line treatment for European patients with advanced EGFR mutation-positive non-small-cell lung cancer (EURTAC): a multicentre, open-label, randomised phase 3 trial." Lancet Oncol **13**(3): 239-246.
Roskoski, R., Jr. (2014). "The ErbB/HER family of protein-tyrosine kinases and cancer." Pharmacol Res **79**: 34-74.
Roskoski, R., Jr. (2014). "ErbB/HER protein-tyrosine kinases: Structures and small molecule inhibitors." Pharmacol Res.
Rossi, E. D., R. Gerhard, et al. (2014). "Detection of Common and Less Frequent EGFR Mutations in Cytological Samples of Lung Cancer." Acta Cytol: 275-280.
Rouleau, G. A., P. Merel, et al. (1993). "Alteration in a new gene encoding a putative membrane-organizing protein causes neuro-fibromatosis type 2." Nature **363**(6429): 515-521.
Ruttledge, M. H., J. Sarrazin, et al. (1994). "Evidence for the complete inactivation of the NF2 gene in the majority of sporadic meningiomas." Nat Genet **6**(2): 180-184.
Ryu, C. H., S. W. Kim, et al. (2005). "The merlin tumor suppressor interacts with Ral guanine nucleotide dissociation stimulator and inhibits its activity." Oncogene **24**(34): 5355-5364.
Sakashita, S., M. Sakashita, et al. (2014). "Genes and pathology of non-small cell lung carcinoma." Semin Oncol **41**(1): 28-39.
Scoles, D. R., D. P. Huynh, et al. (1998). "Neurofibromatosis 2 tumour suppressor schwannomin interacts with betaII-spectrin." Nat Genet **18**(4): 354-359.
Sekido, Y., H. I. Pass, et al. (1995). "Neurofibromatosis type 2 (NF2) gene is somatically mutated in mesothelioma but not in lung cancer." Cancer Res **55**(6): 1227-1231.
Sequist, L. V., B. Besse, et al. (2010). "Neratinib, an irreversible pan-ErbB receptor tyrosine kinase inhibitor: results of a phase II trial in patients with advanced non-small-cell lung cancer." J Clin Oncol **28**(18): 3076-3083.
Sequist, L. V., R. G. Martins, et al. (2008). "First-line gefitinib in patients with advanced non-small-cell lung cancer harboring somatic EGFR mutations." J Clin Oncol **26**(15): 2442-2449.
Sequist, L. V., B. A. Waltman, et al. (2011). "Genotypic and histological evolution of lung cancers acquiring resistance to EGFR inhibitors." Sci Transl Med **3**(75): 75ra26.
Sequist, L. V., J. C. Yang, et al. (2013). "Phase III study of afatinib or cisplatin plus pemetrexed in patients with metastatic lung adenocarcinoma with EGFR mutations." J Clin Oncol **31**(27): 3327-3334.
Shah, N. P., J. M. Nicoll, et al. (2002). "Multiple BCR-ABL kinase domain mutations confer polyclonal resistance to the tyrosine kinase inhibitor imatinib (STI571) in chronic phase and blast crisis chronic myeloid leukemia." Cancer Cell **2**(2): 117-125.

Shalem, O., N. E. Sanjana, et al. (2014). "Genome-scale CRISPR-Cas9 knockout screening in human cells." Science **343**(6166): 84-87.
Shapiro, I. M., V. N. Kolev, et al. (2014). "Merlin deficiency predicts FAK inhibitor sensitivity: a synthetic lethal relationship." Sci Transl Med **6**(237): 237ra268.
Shaw, R. J., J. G. Paez, et al. (2001). "The Nf2 tumor suppressor, merlin, functions in Rac-dependent signaling." Dev Cell **1**(1): 63-72.
Sheikh, H. A., M. Tometsko, et al. (2004). "Molecular genotyping of medullary thyroid carcinoma can predict tumor recurrence." Am J Surg Pathol **28**(1): 101-106.
Shepherd, F. A., J. Rodrigues Pereira, et al. (2005). "Erlotinib in previously treated non-small-cell lung cancer." N Engl J Med **353**(2): 123-132.
Sherman, L., H. M. Xu, et al. (1997). "Interdomain binding mediates tumor growth suppression by the NF2 gene product." Oncogene **15**(20): 2505-2509.
Shibamoto, S., M. Hayakawa, et al. (1995). "Association of p120, a tyrosine kinase substrate, with E-cadherin/catenin complexes." J Cell Biol **128**(5): 949-957.
Shigematsu, H., T. Takahashi, et al. (2005). "Somatic mutations of the HER2 kinase domain in lung adenocarcinomas." Cancer Res **65**(5): 1642-1646.
Shimizu, T., A. Seto, et al. (2002). "Structural basis for neurofibromatosis type 2. Crystal structure of the merlin FERM domain." J Biol Chem **277**(12): 10332-10336.
Shimoyama, Y., A. Nagafuchi, et al. (1992). "Cadherin dysfunction in a human cancer cell line: possible involvement of loss of alpha-catenin expression in reduced cell-cell adhesiveness." Cancer Res **52**(20): 5770-5774.
Smith, A. L., D. B. Friedman, et al. (2011). "ReCLIP (reversible cross-link immuno-precipitation): an efficient method for interrogation of labile protein complexes." PLoS One **6**(1): e16206.
Sos, M. L., H. B. Rode, et al. (2010). "Chemogenomic profiling provides insights into the limited activity of irreversible EGFR Inhibitors in tumor cells expressing the T790M EGFR resistance mutation." Cancer Res **70**(3): 868-874.
Stamos, J., M. X. Sliwkowski, et al. (2002). "Structure of the epidermal growth factor receptor kinase domain alone and in complex with a 4-anilinoquinazoline inhibitor." J Biol Chem **277**(48): 46265-46272.
Stemmer-Rachamimov, A. O., L. Xu, et al. (1997). "Universal absence of merlin, but not other ERM family members, in schwannomas." Am J Pathol **151**(6): 1649-1654.
Stratton, M. R., P. J. Campbell, et al. (2009). "The cancer genome." Nature **458**(7239): 719-724.
Suda, K., H. Mizuuchi, et al. (2014). "CRKL amplification is rare as a mechanism for acquired resistance to kinase inhibitors in lung cancers with epidermal growth factor receptor mutation." Lung Cancer.
Sun, C. X., C. Haipek, et al. (2002). "Functional analysis of the relationship between the neurofibromatosis 2 tumor suppressor and its binding partner, hepatocyte growth factor-regulated tyrosine kinase substrate." Hum Mol Genet **11**(25): 3167-3178.
Sun, Y., Y. Ren, et al. (2010). "Lung adenocarcinoma from East Asian never-smokers is a disease largely defined by targetable oncogenic mutant kinases." J Clin Oncol **28**(30): 4616-4620.
Takeuchi, K., M. Soda, et al. (2012). "RET, ROS1 and ALK fusions in lung cancer." Nat Med **18**(3): 378-381.

Takezawa, K., V. Pirazzoli, et al. (2012). "HER2 amplification: a potential mechanism of acquired resistance to EGFR inhibition in EGFR-mutant lung cancers that lack the second-site EGFRT790M mutation." Cancer Discov **2**(10): 922-933.
Tamborini, E., L. Bonadiman, et al. (2004). "A new mutation in the KIT ATP pocket causes acquired resistance to imatinib in a gastrointestinal stromal tumor patient." Gastroenterology **127**(1): 294-299.
Travis, W. D., E. Brambilla, et al. (2011). "International association for the study of lung cancer/american thoracic society/european respiratory society international multidisciplinary classification of lung adenocarcinoma." J Thorac Oncol **6**(2): 244-285.
Trofatter, J. A., M. M. MacCollin, et al. (1993). "A novel moesin-, ezrin-, radixin-like gene is a candidate for the neurofibromatosis 2 tumor suppressor." Cell **75**(4): 826.
Wakeling, A. E., S. P. Guy, et al. (2002). "ZD1839 (Iressa): an orally active inhibitor of epidermal growth factor signaling with potential for cancer therapy." Cancer Res **62**(20): 5749-5754.
Walter, A. O., R. T. Sjin, et al. (2013). "Discovery of a mutant-selective covalent inhibitor of EGFR that overcomes T790M-mediated resistance in NSCLC." Cancer Discov **3**(12): 1404-1415.
Wang, S. E., A. Narasanna, et al. (2006). "HER2 kinase domain mutation results in constitutive phosphorylation and activation of HER2 and EGFR and resistance to EGFR tyrosine kinase inhibitors." Cancer Cell **10**(1): 25-38.
Ward, R. A., M. J. Anderton, et al. (2013). "Structure- and reactivity-based development of covalent inhibitors of the activating and gatekeeper mutant forms of the epidermal growth factor receptor (EGFR)." J Med Chem **56**(17): 7025-7048.
Ward, W. H., P. N. Cook, et al. (1994). "Epidermal growth factor receptor tyrosine kinase. Investigation of catalytic mechanism, structure-based searching and discovery of a potent inhibitor." Biochem Pharmacol **48**(4): 659-666.
Ware, K. E., M. E. Marshall, et al. (2010). "Rapidly acquired resistance to EGFR tyrosine kinase inhibitors in NSCLC cell lines through de-repression of FGFR2 and FGFR3 expression." PLoS One **5**(11): e14117.
Weinman, E. J., D. Steplock, et al. (1993). "CAMP-mediated inhibition of the renal brush border membrane Na+-H+ exchanger requires a dissociable phosphoprotein cofactor." J Clin Invest **92**(4): 1781-1786.
Weinstein, I. B. (2002). "Cancer. Addiction to oncogenes--the Achilles heal of cancer." Science **297**(5578): 63-64.
Wiederhold, T., M. F. Lee, et al. (2004). "Magicin, a novel cytoskeletal protein associates with the NF2 tumor suppressor merlin and Grb2." Oncogene **23**(54): 8815-8825.
Wong, A. J., J. M. Ruppert, et al. (1992). "Structural alterations of the epidermal growth factor receptor gene in human gliomas." Proc Natl Acad Sci U S A **89**(7): 2965-2969.
Ye, X., Z. Z. Zhu, et al. (2013). "High T790M detection rate in TKI-naive NSCLC with EGFR sensitive mutation: truth or artifact?" J Thorac Oncol **8**(9): 1118-1120.
Yeh, P., H. Chen, et al. (2013). "DNA-Mutation Inventory to Refine and Enhance Cancer Treatment (DIRECT): a catalog of clinically relevant cancer mutations to enable genome-directed anticancer therapy." Clin Cancer Res **19**(7): 1894-1901.

Yoo, N. J., S. W. Park, et al. (2012). "Mutational analysis of tumour suppressor gene NF2 in common solid cancers and acute leukaemias." Pathology **44**(1): 29-32.
Yu, H. A. and W. Pao (2013). "Targeted therapies: Afatinib--new therapy option for EGFR-mutant lung cancer." Nat Rev Clin Oncol **10**(10): 551-552.
Yun, C. H., K. E. Mengwasser, et al. (2008). "The T790M mutation in EGFR kinase causes drug resistance by increasing the affinity for ATP." Proc Natl Acad Sci U S A **105**(6): 2070-2075.
Zakowski, M. F., M. Ladanyi, et al. (2006). "EGFR mutations in small-cell lung cancers in patients who have never smoked." N Engl J Med **355**(2): 213-215.
Zemmoura, I., P. Vourc'h, et al. (2014). "A deletion causing NF2 exon 9 skipping is associated with familial autosomal dominant intramedullary ependymoma." Neuro Oncol **16**(2): 250-255.
Zhang, Z., J. C. Lee, et al. (2012). "Activation of the AXL kinase causes resistance to EGFR-targeted therapy in lung cancer." Nat Genet **44**(8): 852-860.
Zhou, C., Y. L. Wu, et al. (2011). "Erlotinib versus chemotherapy as first-line treatment for patients with advanced EGFR mutation-positive non-small-cell lung cancer (OPTIMAL, CTONG-0802): a multicentre, open-label, randomised, phase 3 study." Lancet Oncol **12**(8): 735-742.
Zhou, W., D. Ercan, et al. (2009). "Novel mutant-selective EGFR kinase inhibitors against EGFR T790M." Nature **462**(7276): 1070-1074.